

Water source, climate, and water chemistry combine to influence DOC concentration and DOM quality in Buffalo Pound Lake, Saskatchewan

A Thesis Submitted to the College of
Graduate and Postdoctoral Studies
In Partial Fulfillment of the Requirements
For the Degree of Master of Environment and Sustainability
With the School of Environment and Sustainability
University of Saskatchewan Saskatoon, Canada

By

ANTHONY ANDREW PHILIP BARON

Permission to use

In presenting this thesis/dissertation in partial fulfillment of the requirements for a Postgraduate degree from the University of Saskatchewan, I agree that the Libraries of this University may make it freely available for inspection. I further agree that permission for copying of this thesis/dissertation in any manner, in whole or in part, for scholarly purposes may be granted by the professor or professors who supervised my thesis/dissertation work or, in their absence, by the Head of the Department or the Dean of the College in which my thesis work was done. It is understood that any copying or publication or use of this thesis/dissertation or parts thereof for financial gain shall not be allowed without my written permission. It is also understood that due recognition shall be given to me and to the University of Saskatchewan in any scholarly use which may be made of any material in my thesis/dissertation.

Disclaimer

Reference in this thesis to any specific commercial products, process, or service by trade name, trademark, manufacturer, or otherwise, does not constitute or imply its endorsement, recommendation, or favoring by the University of Saskatchewan. The views and opinions of the author expressed herein do not state or reflect those of the University of Saskatchewan and shall not be used for advertising or product endorsement purposes.

Requests for permission to copy or to make other uses of materials in this thesis in whole or part should be addressed to:

Director
School of Environment and Sustainability
University of Saskatchewan
117 Science Place, Kirk Hall
Saskatoon, Saskatchewan, S7N 5C8, Canada

OR

Dean
College of Graduate and Postdoctoral Studies
University of Saskatchewan
116 Thorvaldson Building, 110 Science Place
Saskatoon, Saskatchewan S7N 5C9, Canada

Abstract

Freshwater lakes and reservoirs are key components of the global carbon cycle. Dissolved organic matter (DOM) is an important water quality characteristic that regulates physical, chemical, and biological functions in these systems. Elevated DOM quantity, measured as dissolved organic carbon (DOC) concentration, and changes in DOM source and composition (DOM quality), create challenges for water managers already facing deteriorating sourcewater quality due to cultural eutrophication, climate-related uncertainty, and water scarcity. High DOC and variable DOM quality are a concern to drinking water treatment plants owing to their effects on disinfection byproduct formation, added costs for removal, and risks of bacterial regrowth in water distribution systems. In highly managed drinking water reservoirs like Buffalo Pound Lake, Canada, in the Great Plains of North America, understanding the effects of water source, climate, and in-lake water chemistry on DOM quantity and quality is of particular concern. Inflows to this reservoir are dominated by water releases from a large upstream reservoir (Lake Diefenbaker) with episodic influxes of runoff from the local catchment. Sourcewater variability to Buffalo Pound Lake depends on local hydroclimate, which fluctuates through periods of extreme wet and dry conditions. Long-term analyses demonstrated large fluctuations ($> 10 \text{ mg L}^{-1}$) in monthly DOC concentrations over a 30-year period, and revealed the importance of flows from Lake Diefenbaker and the local catchment, and in-lake nutrient (total phosphorus and ammonium) and solute (sulfate) chemistry, on driving DOC in Buffalo Pound Lake. On a shorter timescale, measurements of DOM quantity and quality along the length of the lake, and across four open-water seasons when Lake Diefenbaker was the primary water source, clearly illustrated the role of internal production on altering DOM quantity and quality from lake inflow to outflow. We observed increases in DOC of up to $1\text{--}2 \text{ mg L}^{-1}$ from the Buffalo Pound Lake inflow to outflow in all years, and several DOM quality metrics suggested a shift toward autochthonous DOM production as water transited through the reservoir. In dry years with greater water residence times, these patterns suggest that long, narrow Buffalo Pound Lake may act similar to a slow-moving river with respect to internal DOM production and processing. This work advances efforts to disentangle long-term drivers of DOC and understand DOM quality dynamics in this shallow eutrophic reservoir and across freshwater systems globally. Our results provide a foundation for DOM quantity and quality forecasting in Buffalo Pound Lake and will inform the design of an ongoing \$325M upgrade to the Buffalo Pound Water Treatment Plant.

Dedication

To my dad, who taught me the importance of a job well done, and gave me an appreciation for the satisfaction of paying attention to the fine details. And to my mom, who is my biggest role model and a dear friend.

Acknowledgements

Looking back there were countless time I needed help to get this thesis finished, and along the way there were always people there to offer their time, advice, or expertise. The SaskWatChe and Bigfoot lab groups are at the top of the list when I think of unwavering support and encouragement. From past to present members—Richard Helmle, Cameron Hoggarth, Katy Nugent, Danielle Spence, Don Selby, Laura McFarlan, Amy Hergott, Lauren Dyck, Jian Liu, Ayden Draude, Mauro de Toledo, Emily Cavaliere, Michelle Wauchope-Thompson, Shanta Sharma, Esther McAleer, Carlie Elliot, Jared Wolfe, Kristin Painter, Aram Jalali Bouraban, Shakhil Ahmed, Anita María Alvarez, Alasdair Morrison, Lana Vuleta—I'm grateful to have you as peers. I also want to thank Blair Kardash from the Buffalo Pound Water Treatment Plant for his cooperation and excitement about this work. Thanks are also owed to Paul Whitfield, Dr. Jonathan Walker, and Dr. Lawrence Sheppard for offering their help with statistical obstacles, and to Dr. Dolly Kothawala for her positive feedback during a lonely online conference in the early stages of this project.

This thesis would not be what it is without the critical feedback from my committee, Drs. John-Mark Davies and Clayton Williams, who have been integral to this project, providing data and their expertise at each stage. This thesis would not have been written without the unconditional support from my supervisors, Drs. Colin Whitfield and Helen Baulch, who have been my rocks from the onset of this endeavour; I will cherish what I've gained, personally and professionally, from working with such great mentors and scientists.

Finally, I want to thank my family and friends, who may not always understand what I'm working on but never fail to instill confidence in myself. And most importantly, I need to thank my partner, Mariana, who is my motivator and always inspires me to keep going.

Table of contents

Permission to use	ii
Disclaimer	ii
Abstract	iii
Dedication	iv
Acknowledgements	v
Table of contents	vi
List of tables	x
List of figures	xii
List of abbreviations	xvii
1.0 Introduction	1
1.1 The role of DOC in lakes and reservoirs	2
1.1.1 Dissolved organic carbon: A master variable	2
1.1.2 Characterization of organic matter in lakes and reservoirs	3
1.1.3 Properties of DOC	4
1.2 Controls of DOC amount in lakes and reservoirs	5
1.2.1 Catchment controls on concentration	5
1.2.2 Temporal variation in DOC concentration	6
1.2.3 Long-term trends in DOC concentration	6
1.3 Drinking water treatability and DOC	8
1.4 Lake DOC in the Great Plains of North America	10
1.5 Significance and research rationale	12
1.6 Thesis structure and research objectives	13
Chapter 2: The importance of autochthonous DOM production in Buffalo Pound Lake, Saskatchewan across a series of dry years	15
2.0 Abstract	15
2.1 Introduction	16

2.2 Methods.....	18
2.2.1 Study site.....	18
2.2.2 Field sampling and laboratory analyses	22
2.2.3 Calculations and data analysis	24
2.2.3.1 Fluorescence spectroscopy.....	24
2.2.4 Statistical analyses	28
2.3 Results.....	29
2.3.1 Sourcewater variability	29
2.3.2 Water quality and DOC concentration.....	31
2.3.2.1 Water quality.....	31
2.3.2.2 TDN and DOC concentrations.....	31
2.3.3 DOM compositional parameters	35
2.3.3.1 Absorbance	35
2.3.3.2 Fluorescence	35
2.3.4 In-lake DOM patterns	37
2.4 Discussion.....	40
2.4.1 Seasonal variation in water quality and DOM quantity and quality	40
2.4.2 Spatial variability in DOM quantity and quality.....	41
2.4.3 Implications for drinking water treatment	44
2.5 Conclusions.....	44
2.6 Acknowledgements.....	45
2.7 Author contributions	45
Segue between Chapter 2 and 3	46
Chapter 3: Extreme variation in DOC and the importance of climate and flow source for Buffalo Pound Lake, Saskatchewan.....	47
3.0 Abstract.....	47
3.1 Introduction.....	48
3.2 Methods.....	50
3.2.1 Study site.....	50

3.2.2.1 Water chemistry	53
3.2.2.2 Streamflow measurements	54
3.2.3 Hydrological calculations	56
3.2.4 Statistical analyses	57
3.2.4.1 Wavelet coherence and phase	58
3.2.4.2 Generalized additive models	60
3.3 Results.....	61
3.3.1 Time series of DOC and environmental predictors	61
3.3.2 Wavelet coherence and phase	65
3.3.3 Generalized additive modeling	69
3.4 Discussion.....	71
3.4.1 Variability in DOC concentration and flow conditions	71
3.4.2 DOC–predictor relationships	73
3.4.3 Flow management and effective water treatment	77
3.5 Conclusions.....	79
3.6 Acknowledgements.....	79
3.7 Author contributions	80
Chapter 4: General conclusions	81
4.0 Summary	81
4.1 Implications for watershed management and forecasting lake and reservoir DOC concentrations	84
4.2 Impact and opportunities for future work	84
References.....	86
Appendix A: Supplementary information Chapter 2 (The importance of autochthonous DOM production in Buffalo Pound Lake, Saskatchewan across a series of dry years).....	110
A.1 Sampling and site information, and summary statistics.....	111
A.1.1 Testing for site similarities with ANOVA and Student’s t-test	112
A.2 Additional DOM absorbance and fluorescence metrics	117
A.3 Linear modelling	122

Appendix B: Supplementary information Chapter 3 (Extreme variation in DOC and the importance of climate and flow source for Buffalo Pound Lake, Saskatchewan) 124

List of tables

Table 2.1. Sampling locations, geographic coordinates, and distances along Buffalo Pound Lake relative to the approximate downstream location of the lake inflow. See also Figure 2.2	21
Table 2.2. Common absorbance fluorescence optical measurements used to characterize DOM composition and used in this study. Table adapted from Hansen et al. (2016, 2018) and references therein.	26
Table 3.1. Analytical methods (APHA, 2012) used at the BPWTP ISO/IEC 17025 accredited laboratory, and sampling frequency and duration. Analytical instruments reported here correspond to current methods used by the BPWTP. All instrument changes between 1990 and 2019 were cross validated and subjected to testing requirements associated with accreditation (B. Kardash pers. comm.). MM refers to the plant’s Methods Manual procedures, with these methods based on APHA (2012) methods.	55
Table 3.2. Coherence and phase relationships between DOC and environmental predictors that had significant coherence ($\alpha = 0.05$) at short (< 18 -month) and long (> 18 -month) timescales. Mean coherence p -values are calculated over the reported timescale band for each significant relationship. $\cos(\phi)$ and $\sin(\phi)$ are transformations of the average phase ϕ over the reported timescale band where $\cos(\phi)$ describes how close the relationship between DOC and each parameter is to being in-phase and $\sin(\phi)$ focuses on whether the time-lagged relationship between DOC and each predictor tends to be positive or negative. Because phases are angular measurements, ϕ ranges between $-\pi$ and π , and $\cos(\phi)$ and $\sin(\phi)$ range between -1 and 1 . Relationships are identified as in-phase when $\cos(\phi) \approx 1$, anti-phase when $\cos(\phi) \approx -1$, and quarter-phase when $\cos(\phi) \approx 0$. When $\sin(\phi) \approx -1$ the relationship is time-lagged positive (i.e., a change in DOC precedes a change in the predictor), whereas when $\sin(\phi) \approx 1$ the relationship is time-lagged negative (DOC lags behind the predictor). When relationships are perfectly in-phase or anti-phase (i.e., not time-lagged), $\sin(\phi) = 0$	68
Table A.1. Field sampling dates and complete sampling days from 2016–2019 at locations along the length of Buffalo Pound Lake during the open water seasons from 2016–2019. Note that the locations reported in this table are compressed from 11 <i>sites</i> to a maximum of 8 <i>locations</i> based on findings of homogeneity as described below and in Table A.2 and Figures A.1 and A.2). ..	111
Table A.2. Results from ANOVA and Student’s t-test runs for each parameter and site grouping. Test runs that used log-transformed data are not shown; instead p -values for untransformed data are reported (consistent with results below, log-transformation did not produce a significant test result in any case).	113
Table A.3. Summary statistics for water quality, DOC concentration, and DOM absorbance and fluorescence parameters. Abbreviations: Q1 – first quartile; Q3 – third quartile.	116

Table A.4. Equations, R^2 , and false discovery rate adjusted (Benjamini and Hochberg, 1995) p-values between DOM quantity and quality parameters and distance along Buffalo Pound Lake for individual years shown in Figure A.8. 123

Table B.1. Site names, abbreviations, Water Security Agency gauging station numbers, geographic coordinates, and gauged and estimated flow records for five contributing streams and areas above Buffalo Pound Lake. 124

Table B.2. Summary statistics for DOC concentration and eight environmental predictors (1990–2019). The real number of observed values N is reported here; where $N < 360$ missing values were imputed using $k = 1$ nearest neighbour regression (Altman, 1992; Fix and Hodges, 1951). Abbreviations: Q1 – first quartile; Q3 – third quartile; LOQ – limit of quantification. 127

Table B.3. Coherences between DOC concentration and nine environmental predictors at short (2- to 18-month timescales) and long (19- to 120-month) timescales. Significant relationships are bolded and denoted by *** ($p < 0.001$), ** ($p < 0.01$), and * ($p < 0.05$). Relationships marginally non-significant ($p < 0.1$) are italicized and denoted by †. 129

List of figures

Figure 2.1. Map of Buffalo Pound Lake, Saskatchewan, Canada, highlighting its gross (grey) and effective (green) drainage areas, including upstream Lake Diefenbaker and the Qu’Appelle River. The middle of the lake is located at 50.65127° N, 105.508225° W. Red diamonds denote Water Survey of Canada streamflow gauging stations in the Buffalo Pound Lake watershed with complete or reconstructed records over the study period (see Section 2.4.1 and Table B.1). The inset map of Canada was plotted using the R package mapcan (McCormack and Erlich, 2019). Gross and effective drainage area shapefiles were obtained from the Prairie Farm Rehabilitation Administration (PFRA). Lake and river geospatial data were retrieved through the Government of Canada’s Open Government License (Statistics Canada, 2006, 2011). 19

Figure 2.2. Map of Buffalo Pound Lake including parts of its gross (grey) and effective (green) drainage areas. Diamond symbols represent 8 locations along the length of the reservoir sampled by WSA in this study. Site geographic information is presented in Table 2.1. 20

Figure 2.3. Flows from Lake Diefenbaker outflow (black), the local catchment (green), and Buffalo Pound Lake inflow (blue) from 2016–2019. Upper and lower grey lines are the 95th and 5th percentile of flows from 1990–2019 respectively. Red Xs are open water season sampling dates where DOM quantity and quality were measured. Note that the y-axis scales vary by column. Note also that estimated ungauged flows (Q_U) to Buffalo Pound Lake make up the difference shown between Q_{BP} and that shown from Q_{LD} and Q_{LC} , and that in any given year not all Q_{LD} and Q_{LC} contribute to Q_{BP} (Chapter 3) 30

Figure 2.4. (a) Turbidity, (b) photosynthetically-available radiation (PAR) extinction coefficient (k_T), (c) Secchi depth (Z_{SD}), and (d) chlorophyll *a* concentration measured at 8 locations along Buffalo Pound Lake from 2016–2019. 33

Figure 2.5. (a) Total dissolved nitrogen and (b) DOC concentrations measured at 8 locations along Buffalo Pound Lake from 2016–2019. Points are mean values and error bars represent the standard deviation of mean values ($N = 3–6$). TDN was not monitored in 2016 and 2019. 34

Figure 2.6. (a) $SUVA_{254}$, (b) $S_{275–295}$, (c) FI, (d) HIX, and (e) $\beta:\alpha$ measured at 8 locations along Buffalo Pound Lake from 2016–2019. Points are mean values and error bars represent the standard deviation of mean values ($N = 3–6$). 36

Figure 2.7. (a) Dissolved organic carbon concentration, (b) TDN concentration, (c) $SUVA_{254}$, (d) $S_{275–295}$, (e) FI, (f) HIX, and (g) $\beta:\alpha$ measured at 8 locations along Buffalo Pound Lake from 2016–2019. Points are mean values and error bars represent the standard deviation of mean values ($N = 10–22$). Lines are fitted linear model trend lines ($R^2 = 0.87–0.98$, $p < 0.0001$). 39

Figure 3.1. Map of Buffalo Pound Lake, Saskatchewan, Canada, highlighting its gross (grey) and effective (green) drainage areas, including upstream Lake Diefenbaker and the Qu’Appelle

River. The middle of Buffalo Pound Lake is located at 50.65127° N, 105.508225° W. Red diamonds denote Water Survey of Canada (WSC) streamflow gauging stations in the Buffalo Pound Lake watershed with complete or reconstructed records over the study period (see Section 3.2.3 and Table B.1). The inset map of Canada was plotted using the R package mapcan (McCormack and Erlich, 2019). Gross and effective drainage area shapefiles were obtained from the Prairie Farm Rehabilitation Administration (PFRA). Lake and river geospatial data were retrieved through the Government of Canada’s Open Government License (Statistics Canada, 2006, 2011). 52

Figure 3.2. Monthly Buffalo Pound Lake DOC concentrations from 1990–2019 by (a) year, showing the pattern in DOC concentration over the full time series, and (b) day of year, showing the intraannual variation in DOC concentration. 63

Figure 3.3 (a–i) Monthly time series of flows from Q_{LD} , Q_{BP} , Q_{LC} , and SO_4^{2-} , TP, SRP, Chl a , NO_3^- , and NH_4^+ , concentrations from 1990–2019..... 64

Figure 3.4. (a–i) Wavelet coherence using the wavelet mean field (Sheppard et al., 2016) for nine DOC–environmental predictor pairs. Coherence magnitude (y -axis, range 0–1) represents the sum of the mean squared magnitude of the wavelet mean field over all timescales. The x -axis (log scale, reversed) depicts the range of timescales (2 to 120 months) for which coherence can be reliably investigated for each time series (1/3 of the total length of the original time series). The blue solid line is coherence. The solid black line is the 95th quantile of coherences of surrogate data sets ($n = 10,000$ surrogates). Coherence is significant ($\alpha = 0.05$) for timescales in which the red dashed line is above the black line. Bars above the coherence line are timescales over which coherence was tested for significance. Timescales are defined as short (≤ 18 months) and long (> 18 months). 66

Figure 3.5. Distributions of phase differences at (a) short (< 18 -month) and (b) long (> 18 -month) timescales for environmental predictors that were significantly coherent with DOC concentration. Radius length is proportional to the frequency of each type of relationship observed (lagged, in-phase, anti-phase), where longer radii indicate higher frequency (as in (a)). Lagged negative refers to fluctuations in DOC leading ahead of fluctuations in a predictor; lagged positive refers to fluctuations in DOC lagging behind fluctuations in a predictor (e.g., SO_4^{2-} in (a) and Q_{LD} in (b)). In-phase relationships are analogous to positive correlation, whereas anti-phase relationships are analogous to negative correlation. See Table 3.2 for details..... 67

Figure 3.6. Partial effects of (a) Chl a , (b) Q_{LD} , (c) NH_4^+ , (d) SO_4^{2-} , and (e) TP for the GAM fitted to the DOC time series with significantly coherent environmental predictor covariates. The x -axes show observed values for each environmental predictor. The y -axes show the partial effects of thin plate regression spline smooths (black lines) for each environmental predictor. Grey shaded regions are the 95% confidence interval. The rug (inset on x -axis) displays the distribution of observed values. Chlorophyll a was the only non-significant covariate ($p = 0.15$); all other environmental predictors were significant at $p < 0.001$ 70

Figure 3.7. Raw DOC concentration time series (black points) overlain with the GAM fit with SO_4^{2-} , TP, Chl *a*, NH_4^+ , and Q_{LD} (blue line). The shaded blue area is the 95% confidence interval of the GAM model fit using 10,000 samples drawn from the posterior multivariate normal distribution. This model explained 56% of the deviance in DOC concentration with an R^2_{adj} of 0.50..... 71

Figure A.1. Sites near the Buffalo Pound Lake inflow that were tested for similarities in (a) DOC concentration, (b) an absorbance metric (SUVA_{254}), and (c–d) fluorescence indexes ($\beta:\alpha$ and HIX). Coloured points are individual samples collected during sampling events from 2016–2019..... 114

Figure A.2. Sites upstream of the causeway on Buffalo Pound Lake that were tested for similarities in (a) DOC concentration, (b) an absorbance metric (SUVA_{254}), and (c–d) fluorescence indexes ($\beta:\alpha$ and HIX). Coloured points are individual samples collected during sampling events from 2016–2019..... 115

Figure A.3. (a–d) Absorbance (m^{-1}) of bulk water samples at 254, 280, 350, and 440 nm wavelengths measured at 8 locations along Buffalo Pound Lake from 2016–2019. Points are mean values and error bars represent the standard deviation of replicate measures ($N = 3-6$). Samples from the lake had high absorbance in the lower UV range (a, b) and much lower absorbance at near-visible and visible wavelengths (c, d)..... 117

Figure A.4. (a) Spectral slope $S_{350-400}$ and (b) slope ratio S_{R} ($S_{275-295}:S_{350-400}$) measured at 8 locations along Buffalo Pound Lake from 2016–2019. Points are mean values and error bars represent the standard deviation of replicate measures ($N = 3-6$). Less intense absorbance near-visible wavelengths (Figure A.3) affected $S_{350-400}$ measurements, as evidenced by the large range in mean \pm one standard deviation values (a). 118

Figure A.5. (a–d) Spectral peak ratios (C:T, A:T, C:A, and C:M) measured at 8 locations along Buffalo Pound Lake from 2016–2019. Points are mean values and error bars represent the standard deviation of replicate measures ($N = 3-6$)..... 119

Figure A.6. (a–e) DOC-normalized (specific) humic-like fluorescence peaks (spA, spC, spM, spD, and spE) measured at 8 locations along Buffalo Pound Lake from 2016–2019. Units are in RU L mg-C^{-1} . Points are mean values and error bars represent the standard deviation of replicate measures ($N = 3-6$). Humic-like peaks were strongly correlated with one another ($R^2 = 0.89-0.99$, $p < 0.00001$ for 10 pairs correlation pairs). In y-axis labels ex refers to excitation wavelength and em refers to emission wavelength..... 120

Figure A.7. (a–c) DOC-normalized (specific) fresh-like fluorescence peaks (spB, spT, and spN) measured at 8 locations along Buffalo Pound Lake from 2016–2019. Units are in RU L mg-C^{-1} . Points are mean values and error bars represent the standard deviation of replicate measures ($N = 3-6$). Fresh-like specific peaks had weak to strong correlations. Peaks spN and spN were weakly

correlated ($R^2 = 0.33$, $p = 3.3 \times 10^{-4}$), whereas correlations were stronger between spT and spB ($R^2 = 0.64$, $p = 2.5 \times 10^{-8}$), and spT and spN ($R^2 = 0.72$, $p = 6.7 \times 10^{-10}$). In y-axis labels ex refers to excitation wavelength and em refers to emission wavelength. 121

Figure A.8. (a) Dissolved organic carbon concentration, (b) TDN concentration, (c) SUVA₂₅₄, (d) $S_{275-295}$, (e) FI, (f) HIX, and (g) $\beta:\alpha$ measured at 8 locations along Buffalo Pound Lake from 2016–2019. Points are mean values at each site in an individual year ($N = 3-6$). Lines are fitted linear model trend lines ($R^2 = 0.16-0.97$, $p < 0.0001$). 122

Figure B.1. A hypothetical time series (a) and its wavelet transform as a function of time and timescale (b), adapted from Reuman et al. (2021). The time series in (a) is constructed from three components: 1) a sine wave of amplitude 1 and period 15 that operates for time $t = 1, \dots, T$ but disappears at $t > 100$; 2) a sine wave of amplitude 1 and period 8 that operates for $t = 101, \dots, 200$ but is absent for $t < 100$; and 3) normally distributed white noise of mean 0 and standard deviation 0.5. The wavelet transform (b) is a complex-valued function of time $t = 1, \dots, 200$ and timescale σ . The magnitude of the wavelet transform $|W_\sigma(t)|$, presented as the z-axis in (b), is an estimate of the strength of the oscillations in $x(t)$ at time t occurring at timescale σ (Addison, 2002; Reuman et al., 2021). The wavelet transform is based on a convolution of a wavelet function with the time series Reuman et al. (2021). Because of this, times and timescales where the overlap of the wavelet transform with the time series is insufficient and unreliable are omitted. The ‘rocket ship nose cone’ plot results from omission of these regions (i.e., at times closer the edges of the time series). At long timescales more values are omitted because long-timescale wavelets extend over the end of the time series further in the convolution computation. 125

Figure B.2. Illustration adapted from Walter et al. (2021) of timescale-specific relationships between two variables (a) and different phase relationships (b–d). In (a) the two variables are perfectly positively correlated on short timescales and perfectly negatively related at long timescales, a relationship masked through standard correlation methods. In (b) fluctuations are in-phase ($\phi = 0$), corresponding to positive correlation. In (c) fluctuations are temporally lagged positive, with the pink signal peaking ahead of the blue signal ($\phi = \pi/2$); a time-lagged negative relationship would show the blue signal peaking ahead of the pink signal ($\phi = -\pi/2$). In (d) fluctuations are anti-phase ($\phi = \pi$), corresponding to negative correlation. 126

Figure B.3. (a–j) Wavelet transforms of DOC, TP, SRP, SO_4^{2-} , Chl *a*, NO_3^- , NH_4^+ , Q_{LD} , Q_{LC} , and Q_{BP} showing the magnitude of the transform (z-axis, colour bar) against time (x-axis) and timescale (y-axis). Note the y-axis is log-transformed. The wavelet transform is based on a convolution of a wavelet function with the time series (Reuman et al., 2021). Because of this, times and timescales where the overlap of the wavelet transform with the time series is insufficient and unreliable are omitted. The ‘rocket ship nose cone’ plot results from omission of these regions (i.e., at times closer to the edges of the time series). At long timescales more values

are omitted because long-timescale wavelets extend over the end of the time series further in the convolution computation. 128

Figure B.4. Distributions of phase differences at (a) short (< 18-month) and (b) long (> 18-month) timescales for all environmental predictors and DOC concentration. Note: Figure 3.5 in the main text presents only the environmental predictors that were significantly coherent with DOC. Radius length is proportional to the frequency of each type of relationship observed (lagged, in-phase, anti-phase), where longer radii indicate higher frequency (as in (a)). Lagged negative refers to peaks in DOC leading ahead of peaks in a predictor; lagged positive refers to peaks in DOC lagging behind peaks in a predictor. In-phase relationships are analogous to positive correlation, whereas anti-phase relationships are analogous to negative correlation. .. 129

Figure B.5. Model diagnostics of the GAM of DOC concentration with SO_4^{2-} , TP, Chl *a*, NH_4^+ , and Q_{LD} (Figure 3.7 in main text). (a) QQ plot of residuals showing some deviation from normality, which is likely affected by the few extreme high and low DOC concentrations in the 30-year record. (b) Residuals vs linear predictor plot. While there is not a strong pattern in this plot (evidence of relatively good fit), there are several point at the tails of ‘Linear predictor’ and the higher end of ‘Deviance residuals’ that suggest relatively high and low DOC concentrations were poorly estimated by this model. (c) Histogram of residuals. Residuals are approximately normally distributed with a few extreme values at the tails. (d). Observed vs fitted values showing the fit between measured (*y*-axis) and modeled (*x*-axis) DOC concentrations. At DOC concentrations < ~8 mg L⁻¹ the GAM provides a good fit to the data; however at concentrations > ~8 mg L⁻¹ there is considerable variation between observed and estimated DOC concentrations. At these higher concentrations the coherent environmental predictor covariates struggled to explain variation in DOC. 130

Figure B.6. Intraannual variation in DOC:DON at Buffalo Pound Lake between 1990 and 2019. 131

Figure B.7. Buffalo Pound Lake ultraviolet absorbance at 254 nm (UV_{254}) normalized to DOC concentration (SUVA_{254}) from 1990 to early 1991 and late 1997 to 2019, calculated as UV_{254} divided by DOC concentration. 131

List of abbreviations

$\beta:\alpha$	freshness index
$^{\circ}\text{C}$	degrees Celsius
$\mu\text{g L}^{-1}$	micrograms per litre
μm	micrometre
$A_{254}, A_{280}, A_{350}, A_{440}$	ultraviolet absorbances at 254, 280, 350, and 440 nanometres
$A_{\text{BP}}, A_{\text{IC}}, A_{\text{RC}}$	effective drainage areas of Buffalo Pound Lake, Iskwao Creek, and Ridge Creek
APHA	American Public Health Association
AU cm^{-1}	absorbance units per centimetre
B1.7	Lake Inflow
B3.8	Upstream Causeway
B5.2	Below Causeway
B9.0	South Lake
B13.0	Sun Valley
B19.8	Parkview
B25.2	Water Treatment Plant
B29.1	Above Outlet
BPWTP	Buffalo Pound Water Treatment Plant
C	carbon
Chl <i>a</i>	chlorophyll <i>a</i>
CI	95% confidence interval
CO_2	carbon dioxide
<i>d</i>	Cohen's <i>d</i> (effect size)
DBP	disinfectant byproduct
DIC	dissolved inorganic carbon
DOC	dissolved organic carbon
DOM	dissolved organic matter
DON	dissolved organic nitrogen
DOP	dissolved organic phosphorus
EEM	excitation-emission matrix
em	emission
ex	excitation

FI	fluorescence index
GAM	generalized additive model
GE	General Electric
HAA	haloacetic acid
HIX	humification index
IC	inorganic carbon
ISO/IEC 17025	International Organization for Standardization general requirements for the competence of testing and calibration laboratories
km	kilometre
km ²	square kilometres
k _T	photosynthetically-available radiation extinction coefficient
L mg ⁻¹ m ⁻¹	litres per milligram-metre
L mg-C ⁻¹ m ⁻¹	litres per milligram carbon-metre
LOQ	limit of quantification
m	metre
m ³	cubic metre
m ³ s ⁻¹	cubic metre per second
MAC	maximum acceptable concentration
mm	millimetre
mg L ⁻¹	milligrams per litre
MW	molecular weight
N	nitrogen
NH ₄ ⁺ -N	total ammonium-nitrogen
nm	nanometre
NO ₃ ⁻ -N	nitrate-nitrogen
NOM	natural organic matter
NTU	nephelometric turbidity units
OM	organic matter
P	phosphorus
PAR	photosynthetically-available radiation
PFRA	Prairie Farm Rehabilitation Administration
POC	particulate organic carbon

Q1	first quartile
Q3	third quartile
Q_{BP}	streamflow at gauging station above the inflow to Buffalo Pound Lake
Q_{IC}	streamflow measured at Iskwao Creek gauging station
Q_{LC}	streamflow from the local watershed (Ridge Creek and Iskwao Creek) contributing to Buffalo Pound Lake, and scaled to the lake's effective drainage area
Q_{LD}	streamflow below the Qu'Appelle River Dam at the outflow of Lake Diefenbaker
Q_{RC}	streamflow measured at Ridge Creek gauging station
Q_U	streamflow estimated for the ungauged areas of the Buffalo Pound Lake catchment
RRPL	Roy Romanow Provincial Lab
RU	Ramen units
$RU\ L\ mg-C^{-1}$	Ramen units-litre per milligrams carbon
S	sulfur
$S_{275-295}$	spectral slope from 275 to 295 nanometres
$S_{350-400}$	spectral slope from 350 to 400 nanometres
SO_4^{2-}	sulfate ion
spA, spB, spC, spD, spE, spM, spN, spP, spT	specific fluorescence at various peaks of excitation-emission pairs normalized to dissolved organic carbon concentration
S_R	spectral slope ratio ($S_{275-295}:S_{350-400}$)
SRP	soluble reactive phosphorus
SUVA	dissolved organic carbon-specific ultraviolet absorbance
$SUVA_{254}$	dissolved organic carbon-specific ultraviolet absorbance at 254 nanometres
TC	total carbon
TDN	total dissolved nitrogen
THM	trihalomethane
TOC	total organic carbon
TP	total phosphorus
UV	ultraviolet
UV-A	ultraviolet region of the electromagnetic spectrum spanning 320–400 nm
UV-B	ultraviolet region of the electromagnetic spectrum spanning 280–320 nm
Vis	visible

WSA

Saskatchewan Water Security Agency

Z_{SD}

Secchi disc depth

Chapter 1: General introduction

1.0 Introduction

Dissolved organic matter (DOM), often measured as dissolved organic carbon (DOC), is an important water quality characteristic that regulates the structure and function of lake and reservoir ecosystems (Prairie, 2008). Organic matter (OM), predominantly formed via photosynthesis either within a water body (autochthonous) or on land and transported to a water body (allochthonous), is a critical energy source in lake ecosystems and fundamental to lake productivity and metabolism of aquatic organisms (Wetzel, 2001a). In addition, the light-absorbing properties of dissolved organic compounds trap and re-emit solar energy within the water column of lakes, affecting thermal structure, stratification, and mixing patterns, which in turn influence nutrient cycling and the distributions of dissolved gases and aquatic plants, animals, and microorganisms (Wetzel, 2001a).

In lakes and reservoirs used as drinking water sources, elevated DOM concentrations (i.e., DOM quantity) and changes in DOM colour and composition (i.e., DOM quality) can be problematic, and are a major concern for drinking water treatment plants. At high DOM levels, water treatment is more challenging, necessitating costly DOM removal during pre-treatment (Cooke and Kennedy, 2001) and other actions to limit harmful disinfection byproduct (DBP) formation (Williams et al., 2019) and bacterial regrowth in water distribution systems (LeChevallier et al., 1996). Managing DBPs in drinking water supplies and designing effective water treatment facilities requires understanding the range and nature of both catchment and in-lake DOM quantity and quality.

Multiple factors influence DOM quantity and quality at broad spatial and temporal scales, including limnology, climate, hydrology, land cover, and land-use. Widespread changes in DOM in lakes in the Northern Hemisphere have led to a search for common drivers of these changes (e.g., Pagano et al., 2014; Temnerud et al., 2014; Winterdahl et al., 2014). Instead of common drivers, these studies have revealed a complexity of contributing factors, including climate change, and altered hydrochemistry coupled with changes in land-use and acid deposition history. This research will show, for the first time in the Canadian Prairies, that a suite of hydroclimatic and water quality observations can be used to characterize long-term and spatial variation of DOM quantity and quality in a eutrophic prairie reservoir (Buffalo Pound Lake, SK, the drinking water source for one quarter of the province's residents). I will use water quality

data from the Buffalo Pound Water Treatment Plant (BPWTP), and flow data and four years of open-water season DOM spatial surveying by the SK Water Security Agency (WSA). Detailed characterization of DOM quantity and quality through long-term and spatial analyses will inform reservoir management and treatment plant design, provide a basis for DOM prediction in the Buffalo Pound Lake watershed, and contribute to a deeper understanding of DOM dynamics and changes in sourcewater quality in freshwater lakes of the Canadian Prairies. This work is codesigned with the BPWTP and will help inform design of a planned \$325M plant upgrade with a goal of ensuring treatment is robust to anticipated future DOM variability.

This introductory chapter reviews the connections between lakes and reservoirs and their watersheds, DOM quantity and quality, water treatability, and long-term DOM change. The chapter begins with a discussion of the importance of DOC in supporting the function of freshwater lakes and reservoirs. Next, DOM sources in terrestrial and aquatic environments, and DOM composition from these sources is reviewed. Then, the various spatial and temporal controls on DOM entering lakes and reservoirs and the environmental drivers of long-term trends in DOC concentration are detailed. Following this, the role of DOM in drinking water treatment is discussed. Canadian Prairie lake DOM quantity and quality with a focus on Buffalo Pound Lake is also described. The chapter ends with the significance and rationale of this research, and the objectives of the two manuscript-style data chapters that comprise this work.

1.1 The role of DOC in lakes and reservoirs

1.1.1 Dissolved organic carbon: A master variable

Lakes and reservoirs occupy a small fraction of Earth's surface but serve a disproportionately large role in the global carbon (C) cycle. Inland waters, including lakes and reservoirs, cover ~3% of Earth's continental land area (Downing et al., 2006) but the extent of C transformations in these systems is similar in magnitude to that of terrestrial and marine ecosystems. Inland waters receive C from terrestrial environments and actively transform, transport, or store it (Tranvik et al., 2009), while also fixing C from the atmosphere directly. Carbon emissions to the atmosphere from inland waters are proportional to global terrestrial net ecosystem production, and the rate of organic C burial in lake and reservoir sediments exceeds that of the ocean floor on a per area basis (Tranvik et al., 2009). Aside from C buried in sediments over millennia, DOC in the water column represents the largest organic C store of lakes and is integral to the physical, chemical, and biological properties that govern aquatic

ecosystems (Prairie, 2008). In this way, DOC is considered a master variable; it dictates the quantity and spectral properties of light reaching aquatic organisms, affects lake thermal regime and physical structure, influences the metabolic activity of aquatic organisms and ecosystems, impacts the fate of nutrients, and affects mobility, reactivity, and bioavailability of metals and organic contaminants (Prairie, 2008).

1.1.2 Characterization of organic matter in lakes and reservoirs

Organic matter in lake ecosystems is derived from allochthonous (produced in the catchment) and autochthonous (produced in the lake) sources. This OM is typically divided into dissolved and particulate fractions based on particle size. Dissolved organic matter is a complex mixture of organic compounds (including nitrogen, i.e., dissolved organic nitrogen (DON), phosphorus (DOP), and other elements) that pass through filters, with a 0.45 μm filter commonly used to operationally differentiate dissolved from particulate OM. Similar to DOM, the particulate fraction of OM is chemically complex, but dominated by C (POC). On the whole, the total OM pool is typically comprised of at least ~50% C by mass (Pagano et al., 2014) hence DOC is the dominant component of OM reaching most natural surface waters (Thurman, 1985; Weishaar et al., 2003). Ratios of DOC to POC in eutrophic lakes and reservoirs are typically in the range of 5:1 to 6:1 but fluctuate with season and depth (Wetzel, 2001b). Total organic C (TOC, the sum of DOC and POC) is the combined pool, accounting for all organic C forms found in the water column.

Leaching of degraded OM from the terrestrial landscape is the major source of allochthonous DOC in freshwaters (Pagano et al., 2014). Organic C that is not stored in soil and living plant and animal cells or respired from terrestrial environments is exported via overland flow, streamflow, or groundwater flow as DOC (or POC) to receiving water bodies (Aitkenhead-Peterson et al., 2003; Schlesinger and Bernhardt, 2013). Allochthonous DOC inputs often dominate the DOC pool of lakes (Aitkenhead-Peterson et al., 2003) and drive aquatic ecosystem metabolism (Schlesinger and Bernhardt, 2013).

Autochthonous DOM, produced internally via photosynthesis within freshwater ecosystems, can also be an important DOM source. Together, phytoplankton and macrophytes are the major contributors of autochthonous DOM in freshwater systems (Bertilsson and Jones, 2003). This autochthonous DOM is an important reduced or labile C source, available as an

energy source to heterotrophs (Bertilsson and Jones, 2003). When algae die, organic substances are released into the water column as dissolved compounds or particulate detritus, an important secondary source of DOM. Herbivore grazing of phytoplankton can also be a significant source of secondary DOM within the water column (Lampert, 1978). Finally, actively growing phytoplankton cells also contribute DOM to the water column in lakes and reservoirs through extracellular release of these compounds. In all cases, DOM of phytoplanktonic origin is either directly available as an energy source for heterotrophic microorganisms, or available for biotic and abiotic transformations (Bertilsson and Jones, 2003). While algae are typically the dominant autochthonous DOM source, in productive lakes with large littoral zones, macrophytes can be important, potentially being the dominant autochthonous DOM source (Bertilsson and Jones, 2003).

1.1.3 Properties of DOC

Dissolved organic C is a complex mixture of aromatic (low C to hydrogen (H) ratio) and aliphatic (high C:H) compounds (Pagano et al., 2014). The composition of DOC is largely a function of its source in the environment. Allochthonous DOC is often comprised of high molecular weight (MW), aromatic, coloured humic and fulvic acids exported from upstream soils and wetlands, whereas autochthonous DOC of microbial or planktonic origin is generally low MW, protein-like, and contains more degradable materials (i.e., is less coloured with more non-humic, aliphatic compounds; Aitkenhead-Peterson et al., 2003; Schlesinger and Bernhardt, 2013). Humic substances are typically high MW, refractory aromatic compounds containing amide, carboxyl, ketone, hydroxyl/phenolic, and other functional groups that are relatively resistant to decay. Humins and humic acids make up the bulk of humic substances and can be categorized by MW, solubility, and structure. Fulvic acids are the lowest MW organic acids of the DOM pool, typically made up of carboxylic and phenolic groups and soluble at all pH levels. Humic acids are larger than fulvic acids, soluble at $\text{pH} > 2$, and contain more phenolic and aromatic groups with long aliphatic chains. Humins, the largest class of humic substances, are insoluble across the pH spectrum. Non-humic substances (carbohydrates, proteins, lipids, pigments) are generally low MW, labile, highly soluble, and non-structural molecules and make up a small portion of the DOC pool in lakes because they are consumed rapidly by fungi and microbes prior to hydrological export.

The molecular properties of DOC regulate its interactions with other chemicals in the environment. For example, the chemical properties of DOC (i.e., its quality) influence the solubility and mobility of toxic metals, including mercury (Ravichandran, 2004), copper (Ashworth and Alloway, 2007), and lead (Klaminder et al., 2006). These same properties permit DOC removal during water treatment using coagulants like Al^{3+} (Exall and Vanloon, 2000) and have important implications for the formation and effective removal of harmful disinfection byproducts during water treatment (Williams et al., 2019).

1.2 Controls of DOC amount in lakes and reservoirs

1.2.1 Catchment controls on concentration

The range in DOC concentrations of inland waters is hierarchically regulated. In a study of 7,514 lakes across 6 continents, Sobek et al. (2007) found that climatic and topographic characteristics determine the possible range of DOC concentrations at regional scales, whereas catchment and lake properties dictate DOC concentrations in individual lakes. Regional climate characteristics like mean annual temperature have been linked to DOC concentrations in boreal streams (Laudon et al., 2011) and lakes (Weyhenmeyer and Karlsson, 2009). Catchment DOC inputs to lakes are highly correlated with precipitation and annual runoff, thus DOC loading (the sum of all DOC export to a lake) is regulated by local hydrology, climate, and landscape features (Pace and Cole, 2002; Porcal et al., 2009). At the landscape scale, allochthonous DOC leached from terrestrial soils is transported to streams and lakes, and the amount of DOC leached from soils is determined by soil moisture, production of soil organic C, and flow path from soil to stream or lake (Clark et al., 2010; Sobek et al., 2007).

Several physiographic properties of a watershed influence lake DOC concentration, including watershed slope and topography (Sobek et al., 2007; Xenopoulos et al., 2003), land-use (Williams et al., 2010; Wilson and Xenopoulos, 2009), hydrological connectivity and wetland area (Dillon and Molot, 1997; Kortelainen, 1993; Laudon et al., 2011; Schiff et al., 1997), and drainage ratio (catchment:lake area). Within lakes, allochthonous DOC inputs and autochthonous DOC production contribute to the DOC pool. Lake area, morphometry, and water residence time as well as internal loss and transformation (e.g., mineralization to CO_2 and sedimentation) processes also influence and dictate DOC concentration (Algesten et al., 2004; Casas-Ruiz et al., 2021; Cole et al., 2007; Finlay et al., 2010).

1.2.2 Temporal variation in DOC concentration

Seasonal cycles influence DOC concentrations in many freshwater systems, and are often linked to changes in biological DOC production and hydrological export (Clark et al., 2010). The largest source of DOC variation in some lakes in cold regions occurs intra-annually, with DOC inputs peaking during spring snowmelt despite biological DOC production peaking in summer (Buffam et al., 2007; Clark et al., 2010; Laudon et al., 2004). High precipitation storm events can also affect DOC fluxes to lakes. In organo-mineral soils during high precipitation events and during snowmelt, for example, DOC is mobilized as its flow path shifts from baseflow through the mineral soil layer (where DOC is retained) to stormflow conditions through the organic soil and litter layers (where DOC is produced), resulting in greater DOC flux during storm discharge (Clark et al., 2010). However, lake DOC concentrations do not always increase with high DOC loading events if dilution effects are greater than the amount of DOC exported (Clark et al., 2007). Inter-annual variations in rainfall can also account for much among-year DOC variability by heightening seasonal differences between wet and dry years (Clark et al., 2010). The seasonal and inter-annual variation in lake DOC concentrations is often one to two orders of magnitude greater than the long-term change in DOC at decadal time scales (Clark et al., 2010).

1.2.3 Long-term trends in DOC concentration

Rising DOC concentrations, beginning in the late 1980s, have been observed in many lakes and streams of Europe and eastern North America. Much of the debate about the rise in DOC in these systems has focused on climatic factors, including rising atmospheric temperature and CO₂ concentrations, as well as shifts in precipitation patterns and frequency of extreme storm events. For example, rising temperatures and atmospheric CO₂ concentrations can promote greater primary production, resulting in the accumulation of degrading biomass and an increase in the DOC pool of an ecosystem (Pagano et al., 2014). Variable precipitation patterns and associated changes in wet/dry periods can also affect DOC concentrations by altering the water balance of a region (Jane et al., 2017). Changes in precipitation patterns, frequency of extreme precipitation events, and annual streamflow variability have also been reported as drivers of increasing DOC trends (Eimers et al., 2008b). Others have argued that declining anthropogenic sulphur (S) emissions beginning in the 1980s have been the cause for rising DOC concentrations in streams and lakes of Europe and North America (Monteith et al., 2007). More stringent

international air quality regulations have led to reduced sulfate (SO_4^{2-}) acidification of terrestrial systems and freshwaters across eastern North America, and central and northern Europe. Observational and experimental evidence from lakes, streams, and peat soils in the United Kingdom (UK) suggests a strong link between increased DOC solubility in freshwaters with declining soil water acidity and ionic strength (Evans et al., 2006). Most of the variance in lake and stream DOC concentrations in these systems was explained by concomitant declining trends in anthropogenic S emissions and sea-salt loading from the late 1980s to early 2000s, while the effects of trends in precipitation and atmospheric temperature and CO_2 were less apparent. Conversely, SO_4^{2-} deposition rates were not related to annual DOC concentrations over a 21-year (1978–1998) period in nine softwater oligotrophic boreal lakes in Ontario, Canada (Hudson et al., 2003). Unlike the UK streams and lakes described in Evans et al. (2006), these lakes showed little evidence of an increasing or decreasing trend in DOC concentrations despite declining SO_4^{2-} deposition over the study period. Variation in DOC concentrations in these lakes was instead attributed to patterns in solar radiation (mean daily ice-free total photosynthetically available radiation: PAR) and winter (December to March) precipitation. Clark et al. (2010) argue that such discrepancies between studies can be attributed to regional differences in acid deposition loading and catchment characteristics that affect sensitivity to changes in acidity and therefore the magnitude of DOC change with declining S deposition. Likewise, a large-scale study of 522 acid-affected lakes and streams in North America and Europe provided multiple lines of evidence for declining S deposition as the dominant driver of rising DOC concentrations in these systems between 1990 and 2004 (Monteith et al., 2007). Over this period DOC concentration trends could not be explained by trends, or lack thereof, in seasonal and annual stream hydrology or air temperature, or atmospheric nitrogen deposition (measured as stream or lake nitrate (NO_3^-) concentration). Monteith et al. (2007) further argue that rising CO_2 concentration cannot explain simultaneous increasing and decreasing DOC trends in different regions. Instead, declining S deposition in acidified regions increases DOC concentration through two possible mechanisms: 1) by increasing soil pH, which increases soil OM solubility and thus export as DOC and 2) by reducing the ionic strength of soil solution, which lowers the concentrations of SO_4^{2-} , Ca^{2+} , Mg^{2+} , and Al^{3+} ions that work to suppress DOC flux from soils (Monteith et al., 2007). It is thus differences in buffering capacity of soils (catchment sensitivity to acid deposition) that likely accounts for the variation in DOC trends across regions with

similar patterns of deposition. While DOC concentration trends are widespread, this does not always amount to changes in DOC flux over the same period and at finer regional scales, suggesting that hydrology also plays a key role in regions with a history of ecosystem acidification (Eimers et al., 2008b).

Long-term DOC trends are also being observed in regions with no history of anthropogenic acidification. Instead, climate change may be driving shifts in lake DOC concentrations at broad regional scales. As noted above, inter-annual variation in DOC concentrations is typically much greater than long-term changes in DOC. However, long-term trends in DOC concentration that are lower in magnitude than seasonal or inter-annual variation may still be associated with important changes in DOM quality. Higher precipitation in boreal regions is expected to increase allochthonous DOM inputs to streams and lakes through increases in runoff (Eimers et al., 2008a). Rising annual temperatures in the Canadian Arctic are melting permafrost, altering vegetation distributions, and, consequently, flow paths, soil residence times, and terrestrial carbon cycling in the Yukon River basin (Striegl et al., 2005). The result has been declines in DOC export to lakes because a larger fraction of DOC has begun infiltrating and decomposing in the active soil layer as permafrost soils melt, rather than more rapid transport to streams and lakes. For hardwater lakes of the Great Plains in Canada and the United States, where water levels are often maintained by meltwater from winter precipitation, declining winter snow packs may reduce allochthonous DOM influxes (Finlay et al., 2010). Given the widespread occurrence of changing DOC quantity, and the importance of DOC quality to its behaviours, changing sources of DOC that regulate concentrations may also influence the chemical nature of freshwater DOC.

1.3 Drinking water treatability and DOC

Lakes and reservoirs are used as drinking water and municipal water supplies in many parts of the world. Elevated DOC concentrations and changes in DOC colour and quality can be problematic and pose challenges for drinking water treatment (Williamson et al., 2016). Water must be treated for human consumption to remove contaminants and toxic substances and manage microbes. At high DOC levels water treatment is impaired by costly increases in coagulant loads required for pre-treatment DOM removal (Cooke and Kennedy, 2001) and coliform regrowth in distribution systems (LeChevallier et al., 1996). Untreated DOC can also

contribute to poor taste and odour problems (Matilainen et al., 2011). When chlorine reacts with DOC during water treatment, the compounds that comprise DOC can act as precursors for a suite of harmful DBPs with potentially carcinogenic and mutagenic properties (Chow et al., 2003). Disinfection byproduct formation is a major concern for drinking water utilities and a threat to human health (Williams et al., 2019). Prolonged exposure to DBPs in chlorinated drinking water supplies may be linked to increased risk of bladder cancer, miscarriage, and genetic polymorphism (Hrudey and Fawell, 2015; Li and Mitch, 2018; Wagner and Plewa, 2017). During water treatment, DBPs form when chemical disinfectants, such as chlorine or ozone, used to kill pathogens, react with source water DOC (Deborde and von Gunten, 2008; Lavonen et al., 2013; Li and Mitch, 2018). In chlorinated drinking water supplies, trihalomethanes (THMs) and haloacetic acids (HAAs) are two of the most common DBP classes, though over 700 DBPs have been identified (Lavonen et al., 2013). Bromide present in source waters can also be incorporated into DBPs, forming brominated THMs (Deborde and von Gunten, 2008; Heeb et al., 2014). In Canada, four THM and five HAA compounds are federally regulated, with total THM and HAA maximum acceptable concentrations (MAC) set at 100 and 80 $\mu\text{g L}^{-1}$, respectively (Health Canada, 2006, 2008). To mitigate potentially harmful THM and HAA formation in drinking water supplies, drinking water utilities often add pre-treatment steps to reduce DOC concentrations, including alum additions to promote coagulation and flocculation, making treatment more expensive (Cooke and Kennedy, 2001; Pagano et al., 2014).

Understanding the DOM molecular components that contribute to THM and HAA formation is critical to safe and effective water treatment. Inexpensive approaches for estimating required pre-treatment DOC removal include absorbance metrics like specific DOC absorbance at 254 nm (SUVA_{254}), an average absorptivity measure for the suite of molecules comprising DOM in a water sample that is often used as a surrogate measurement for DOC aromaticity (Traina et al., 1990; Weishaar et al., 2003). This metric is known to be useful for estimating coagulant loads needed for DOC removal because it is an effective indicator of humic DOC (Randtke, 1999), but is less adept at predicting DOC reactivity with common disinfectants like chlorine (Li et al., 2000; Reckhow et al., 1990) and ozone (Westerhoff et al., 1999). Predicting DOM chemical reactivity is made difficult by the intrinsic complexity of the organic compounds that comprise DOM (Weishaar et al., 2003). Measurements from more than 100 surface waters in the conterminous United States showed that SUVA_{254} is a weak universal indicator of THM

formation potential for whole water samples, but can still be a useful proxy for waters where DOC is known to be comprised mainly of humic substances (Fram et al., 1999; Weishaar et al., 2003). Results from these studies suggest that non-aromatic compounds that are not UV absorbent can contribute to THM formation and that some compounds that contribute to overall absorbance are inert with respect to THM formation. While allochthonous DOC is generally associated with THM and HAA formation (Golea et al., 2017; Lavonen et al., 2013; Wang et al., 2017; Yang et al., 2015), autochthonous DOC, particularly that derived from algal blooms, can also produce high levels of these DBPs (Chen et al., 2008; Liao et al., 2017). Understanding finer scale changes in DOM composition and how they link to specific DBP formation is critical for drinking water treatment (Williams et al., 2019). To achieve this, more advanced techniques to characterize the DOM pool, including DOM absorbance and fluorescence excitation and emission (EEM) scans, have been developed with the intent, in part, to determine ideal timing for chlorination during water treatment where the availability of DOM precursors is reduced to a point of minimal DBP formation (Williams et al., 2019). In the Canadian Prairies where water quality is (often naturally) poor in multiple regions, including Buffalo Pound Lake, water treatment plants face multiple challenges of local changes to DOM (e.g., eutrophication and algal blooms, cyanobacterial toxins, waterborne pathogens; Schindler and Donahue (2006)) in addition to considerable variation in sourcewater DOM quantity and quality. Optimizing treatment operations to effectively remove DOM and limit DBP formation is a pressing issue for water managers in the region and is a major focus in plans for an ongoing \$325M upgrade to the water treatment plant at Buffalo Pound Lake. In Buffalo Pound Lake, THM and HAA formation has been linked to specific portions of the DOM pool (Williams et al., 2019). Further study of Buffalo Pound Lake DOM quantity and quality can help the BPWTP target and remove portions of the DOM pool that are linked to specific chlorinated and brominated DBPs.

1.4 Lake DOC in the Great Plains of North America

In the Canadian prairies, DOM/DOC research has largely focussed on saline lakes where DOC concentrations can exceed 150 mg L^{-1} (e.g., Arts et al. 2000; Osburn et al. 2011; Waiser and Robarts 2000) with less attention given to freshwater lakes (Arts et al., 2000). In a study of 20 saline and 24 freshwater lakes and wetlands in Saskatchewan, Arts et al. (2000) found that for systems with similar DOC concentrations, light tended to penetrate deeper in saline lakes and

wetlands than in freshwater systems in both the ultraviolet-A (UV-A; 320–400 nm) and UV-B (280–320 nm) regions of the electromagnetic spectrum. This contrast was attributed to differences in DOM composition between saline and freshwater lakes, particularly in its chromophoric properties. Endorheic saline lake DOC was highly bleached, degraded, and old, resulting in relatively clear waters despite high DOC concentrations, whereas freshwater DOM was younger, more humic, and less degraded. A case study of one of these systems, saline Redberry Lake and its major freshwater inflow Oscar Creek, found a similar relationship between DOC concentration and DOM quality (Waiser and Robarts, 2000). Seasonal DOC concentrations in Oscar Creek were much lower (14.9 mg L^{-1}) than Redberry Lake (35 mg L^{-1}) but lake water was clear despite allochthonous DOM inputs from highly coloured Oscar Creek being the dominant DOM source. Compositional differences between inflow and lake DOM were also evident. Water from Oscar Creek had more aromatic, coloured DOM, whereas Redberry Lake water had lower molecular weight, less coloured DOM signatures resembling autochthonous production despite chlorophyll *a* (Chl *a*) concentrations of $0.7 \text{ } \mu\text{g L}^{-1}$ over the study period. Water residence time in this endorheic lake is long (20 years) and ^{14}C dating confirmed that a portion of the lake DOC was at least 700 years old. Waiser and Robarts (2000) thus concluded that differences in DOM composition between lake water and water from the inflow were a product of increased light attenuation and photobleaching in Redberry Lake caused by prolonged processing compared to Oscar Creek, resulting in clear lake water and DOM that resembles that of autochthonous origin.

There is a need to better understand the relative importance of fluvial DOC sources for both DOC quantity and quality in Buffalo Pound Lake, the drinking water source for one quarter of the population of Saskatchewan, Canada. Water levels in the reservoir are maintained by water releases from upstream Lake Diefenbaker, with this source water representing the dominant water input to Buffalo Pound Lake. Catchment flows are comparatively small and intermittent, yet terrestrial DOM has been shown to dominate the DOM pool in Buffalo Pound Lake (Williams et al., 2019). Previous work to quantify catchment DOC inputs to Buffalo Pound Lake was constrained by lack of DOC concentrations in inflowing rivers and estimates of overland flow and groundwater influx (Finlay et al., 2010). In addition to water source, long-term changes and variation in DOM quantity and quality in Buffalo Pound Lake have yet to be characterized and require further study of both catchment and in-lake drivers of change over

multi-year time scales. Moreover, while DOM both entering and within lakes in Saskatchewan has been shown to be of the more allochthonous coloured, aromatic, humic, refractory type (Arts et al., 2000; Waiser and Robarts, 2000), seasonal and inter-annual variation in DOM quantity and quality in the Buffalo Pound Lake watershed have not been studied extensively. A deeper look into DOM signatures spanning multiple open-water seasons will enhance our understanding of DOM sources, and processing of terrestrial and in-lake derived DOM. Detailed study of long-term change and considerable inter-annual variability in DOM quantity and quality in Buffalo Pound Lake will enhance our understanding of dynamics in this watershed heavily impacted by agricultural activity and support effective drinking water treatment by the BPWTP.

1.5 Significance and research rationale

The factors that drive surface water DOC concentration and DOM quality in the Canadian prairies is a major knowledge gap. Few studies have assessed long-term change in freshwater DOC concentrations in the region (e.g., Finlay et al., 2010), or investigated the climatic, hydrological, or in-lake drivers of this change. Research that assesses freshwater DOM quality over multiple open-water seasons is likewise sparse in this region. The investigations presented in this study aim to address each of these knowledge gaps by looking at the drivers of change in DOC concentration over a 30-year period, and by assessing patterns in whole-lake DOM quality over four open-water seasons. Buffalo Pound Lake is a highly managed system with tightly controlled water levels and variable flow sources (the local catchment and upstream mesotrophic Lake Diefenbaker), each likely to have unique DOM quality signatures. Flows into Buffalo Pound are a product of management and climate, and also dependent on climatic change; cycles of extreme drought and years with abundant precipitation drastically change the hydrology of the region and in turn can impact water quality (McGowan et al., 2005; Painter et al., 2022a). Measurements of DOC concentration and in-lake water chemistry from 1990–2019 collected by the BPWTP, and records of streamflow from Lake Diefenbaker, the local catchment, and the inflow to Buffalo Pound Lake over this period, offer an excellent opportunity to assess variation in DOC concentration and uncover the relationship between DOC concentration, in-lake water chemistry, and the effects of flow management in this system. Longitudinal DOM quality measurements collected by the WSA over four open-water seasons

likewise invite a deeper look into the sources, transformations, and cycling of DOM in Buffalo Pound Lake.

Collectively, studying the dynamics of DOC concentration and DOM quality in the Canadian prairies will 1) enhance our understanding of the drivers and mechanisms of change in DOM in a region not impacted by SO_4^{2-} deposition or previously studied in-depth, thus adding a unique perspective to the literature on long-term DOC change; 2) broaden our understanding of the way DOM is cycled in shallow eutrophic reservoirs; and 3) benefit water managers in the region, particularly the BPWTP, by unraveling the impacts that flow management can have on water quality, and ultimately aid in optimizing water treatment operations, present and future watershed planning, and inform flow management decision-making.

1.6 Thesis structure and research objectives

This introduction is followed by two manuscript chapters (Chapters 2 and 3), each with several objectives. These manuscript chapters are followed by a general discussion and conclusions chapter (Chapter 4), which summarises the main findings of each chapter and their connections, describes some of the limitations of this work, discusses opportunities for future research on this topic, and provides an overview of some of the broader impacts of this work. Following this section is a list of references. Supporting information for each manuscript chapter follows in Appendices A and B. Here, the objectives of Chapters 2 and 3 and their respective titles are presented.

Chapter 2: The importance of autochthonous DOM production in Buffalo Pound Lake, Saskatchewan across a series of dry years

- Objective 1: Quantify DOC concentration and assess DOM quality at sites spanning from near the inflow to the outflow of Buffalo Pound Lake over four open-water seasons to determine if and how DOM patterns change as water moves through the reservoir
- Objective 2: Investigate the seasonal and interannual variation in DOC concentration, and allochthonous and autochthonous sources, production, and processing of DOM along the length of the lake

Chapter 3: Extreme variation in DOC and the importance of climate and flow source

- Objective 1: Quantify long-term variation in DOC concentration in Buffalo Pound Lake over a 30-year period (1990–2019) encompassing both wet conditions and severe drought

- Objective 2: Investigate predictor–response relationships between DOC concentration, flows from upstream Lake Diefenbaker and the local catchment, and a suite of in-lake water chemistry parameters

Chapter 2: The importance of autochthonous DOM production in Buffalo Pound Lake, Saskatchewan across a series of dry years

Anthony A. P. Baron¹, Colin J. Whitfield^{1,2}, Clayton J. Williams³, John-Mark Davies^{1,4}, Helen M. Baulch^{1,2}

¹School of Environment and Sustainability, University of Saskatchewan, Saskatoon, Saskatchewan, Canada.

²Global Institute for Water Security, University of Saskatchewan, Saskatoon, Saskatchewan, Canada

³Department of Environmental Studies and Science, Saint Michael's College, Colchester, Vermont, USA

⁴Saskatchewan Water Security Agency, Saskatoon, Saskatchewan, Canada

2.0 Abstract

The compositional characteristics (i.e., quality) of dissolved organic matter (DOM) are increasingly recognized as integral to water quality monitoring programs. In addition to dissolved organic carbon (DOC) concentration and its specific absorbance at 254 nm (SUVA₂₅₄), understanding DOM quality dynamics in drinking water reservoirs can inform drinking water treatment by providing insight into disinfection byproduct formation (e.g., Williams 2019). Using linear models, we clearly demonstrate shifts in DOC concentration and DOM quality along the length of Buffalo Pound Lake, Canada, a shallow eutrophic reservoir in the semi-arid Great Plains of North America, over four open-water water seasons (2016–2019). We assessed seasonal differences in DOC concentration, DOM quality, and water quality (chlorophyll *a*, turbidity, photosynthetically-available radiation (PAR) extinction coefficients, and Secchi depth) to understand intra-annual changes in the lake that may be associated with spring snowmelt and summer cyanobacterial blooms, and found no seasonal differences in DOC concentration or DOM quality, despite significant differences in other water quality parameters. Across all years we observed significant trends in DOC concentration, SUVA₂₅₄, and several DOM quality metrics (spectral slope from 275–295 nm [$S_{275-295}$], fluorescence index [FI], humification index [HIX], and freshness index [$\beta:\alpha$]) from the lake inflow to the lake outflow. Most notably, DOC concentrations increased 1–2 mg L⁻¹ along the length of the lake, with concurrent decreases in SUVA₂₅₄ and shifts in $S_{275-295}$, FI, HIX, and $\beta:\alpha$ that suggest a tendency towards increasing

autochthony nearer the lake outflow. Inflows to the lake during our study were primarily from a larger mesotrophic reservoir upstream (Lake Diefenbaker) with minimal runoff from the local catchment. Our findings highlight the important role of in-lake processing of DOM and autochthonous sources as water moves from inlet toward the Buffalo Pound Water Treatment Plant near the lake outlet, which will help the Buffalo Pound Water Treatment Plant continue to provide safe drinking water and inform water treatment operations.

2.1 Introduction

Despite their importance for drinking water supply systems, drinking water reservoirs face multiple threats arising from the ways humans have transformed global water resources. Anthropogenic activities that degrade reservoir water quality include nutrient pollution from urban and agricultural activities, and release of pollutants through industrial or urban effluents, while altered timing and quantity of inflows can have indirect effects. Several studies have demonstrated strong associations between human activity and dissolved organic matter (DOM) composition, particularly in urban areas and agricultural watersheds (Williams et al., 2016; Wilson and Xenopoulos, 2009). Variability in DOM quantity and quality has important implications for lake and reservoir water quality and provision of ecosystem services such as drinking water (Williams et al., 2019; Williamson et al., 2016). In addition to dissolved organic carbon (DOC) concentrations that have traditionally been observed, there is increasing recognition of the need to monitor DOM quality dynamics in systems where drinking water is sourced (Jane et al., 2017; Williams et al., 2019). In particular, changes in DOM source, composition, and reactivity driven by variable water sources (e.g., from an upstream reservoir versus local catchment runoff) can affect the type and quantity of disinfection byproduct formation during water treatment (Croue et al., 1999; Williams et al., 2019), even in the absence of significant changes in DOC concentration (Kraus et al., 2011).

Dissolved organic matter in drinking water reservoirs is divided into two groups based on origin: allochthonous, of terrestrial origin and delivered via riverine inflows or catchment runoff, and autochthonous, or internally-produced DOM. Autochthonous DOM sources include phytoplankton and macrophytes, bacterial DOM production, and DOM released from bottom sediments (Bertilsson and Jones, 2003; Kraus et al., 2011). Allochthonous and autochthonous DOM typically differ in their chemical make-up, which facilitates assessments of DOM source,

composition, and reactivity via optical measurements such as fluorescence spectroscopy. For example, autochthonous DOM contains no lignin, a component inherent in terrestrial plant-derived DOM. Internally-produced DOM also tends to be lower in aromatic content and higher in aliphatic content than allochthonous DOM, and generally has a lower C:N ratio because it is often sourced from phytoplankton (Aiken et al., 1992; Kraus et al., 2011; Mash et al., 2004; Rostad et al., 1997).

Several factors influence variability in DOM quantity and quality in lakes and reservoirs, and at varying timescales (Howard et al., 2021). These include precipitation and runoff patterns (Sedro and Melack 2012), rates of photodegradation (Cory and Kling, 2018; Osburn et al., 2011) and microbial processing (Fasching et al., 2014), seasonal changes in water temperature (Dinsmore et al., 2013; Gudasz et al., 2010) and dissolved oxygen (Bastviken et al., 2004), the balance between DOM uptake and extracellular release by plankton (Romera-Castillo et al., 2010; Tittel and Kamjunke, 2004; Zhang et al., 2009), and other landscape features such as agricultural intensity, water flow paths, and the presence of wetlands in the catchment (Dillon and Molot, 1997; Frost et al., 2006; Larson et al., 2014; McDowell and Likens, 1988; Williams et al., 2016; Wilson and Xenopoulos, 2008; Xenopoulos et al., 2003). Nonetheless, controls on DOM quality have not been investigated to the same extent in arid and semi-arid systems compared to boreal and temperate watersheds. For lakes and reservoirs where allochthonous DOM inputs may vary at interannual scales owing to water management or climate cycles, characterizing within reservoir DOM patterns can help to identify potential system behaviour under different water regimes, and inform drinking water treatment and watershed management.

This study investigates DOM quantity and quality at sites spanning from near the inflow to the outflow of a reservoir on the semi-arid Great Plains of North America (Buffalo Pound Lake, Canada). Our objective was to investigate if and how the amount of DOM and its compositional patterns change as water moves through this long, narrow reservoir. We used four years of DOC concentration and DOM optical spectroscopy measurements to understand variation in DOM amount, and allochthonous and autochthonous sources, production, and processing of DOM throughout Buffalo Pound Lake. We hypothesized that autotrophic production by algae and macrophytes would lead to an increase in DOC concentration nearer the outflow of the lake while also shifting the DOM pool from more aromatic, terrestrial-like signatures to more aliphatic, recently produced autochthonous-like signatures from inflow to

outflow. In addition to longitudinal DOM changes, we also assessed interannual variability, and seasonality by comparing spring (April–June) and summer (July–September) DOM quantity and quality. By examining interannual, seasonal, and longitudinal differences in DOM quantity and quality in Buffalo Pound Lake, we aimed to characterize important sources of DOM and how in-lake influences affect DOM in this reservoir to inform approaches to treatment of drinking water sourced here.

2.2 Methods

2.2.1 Study site

Buffalo Pound Lake is a shallow eutrophic multipurpose drinking water reservoir in southern Saskatchewan, Canada, that services ~25% of the province’s population (Figure 2.1). The middle of the lake is located at approximately 50.65127° N, 105.508225° W, in the semi-arid Great Plains of North America. In addition to providing source drinking water, the lake is also home to a Saskatchewan provincial park and is a popular spot for fishing, boating, swimming, and other recreation. Short, warm summers and long, cold winters define the climate in this region, where annual average temperature is ~3°C (Haig et al., 2021). While mean annual precipitation is 320 mm (McGowan et al., 2005) there is considerable interannual variation, and both wet and dry climatic cycles are common. Buffalo Pound Lake is long and narrow (~29 km by 1 km), with a mean depth of 3 m (max depth 5.6 m). In 1939, this natural lake was impounded to raise water levels by damming the Qu’Appelle River near the confluence with the Moose Jaw River. The lake has a storage capacity of $9 \times 10^7 \text{ m}^3$ (BPWTP, 2021), and an agricultural catchment with nutrient-rich soils drains to the lake (Hammer, 1971). High nutrient influxes and internal loading promote the formation of perennial cyanobacterial blooms, and contribute to poor water quality in the lake (Painter et al., 2022a). Water levels in the lake are tightly controlled, and inflows to the lake are dominated by releases from the Qu’Appelle River Dam from upstream mesotrophic Lake Diefenbaker reservoir. Mean annual water releases from Lake Diefenbaker ranged from $1.8\text{--}4.8 \text{ m}^3 \text{ s}^{-1}$ between 2015–2020 (BPWTP, 2021), and reflect variability in local climate and hydrology. Between Lake Diefenbaker and Buffalo Pound Lake, water transits a 35 km channelized section of the Qu’Appelle River, bypasses a small marshy lake (Eyebrow Lake), then transitions to a more natural, meandering 62 km stretch of the Qu’Appelle River before entering Buffalo Pound Lake (Painter et al., 2022a).

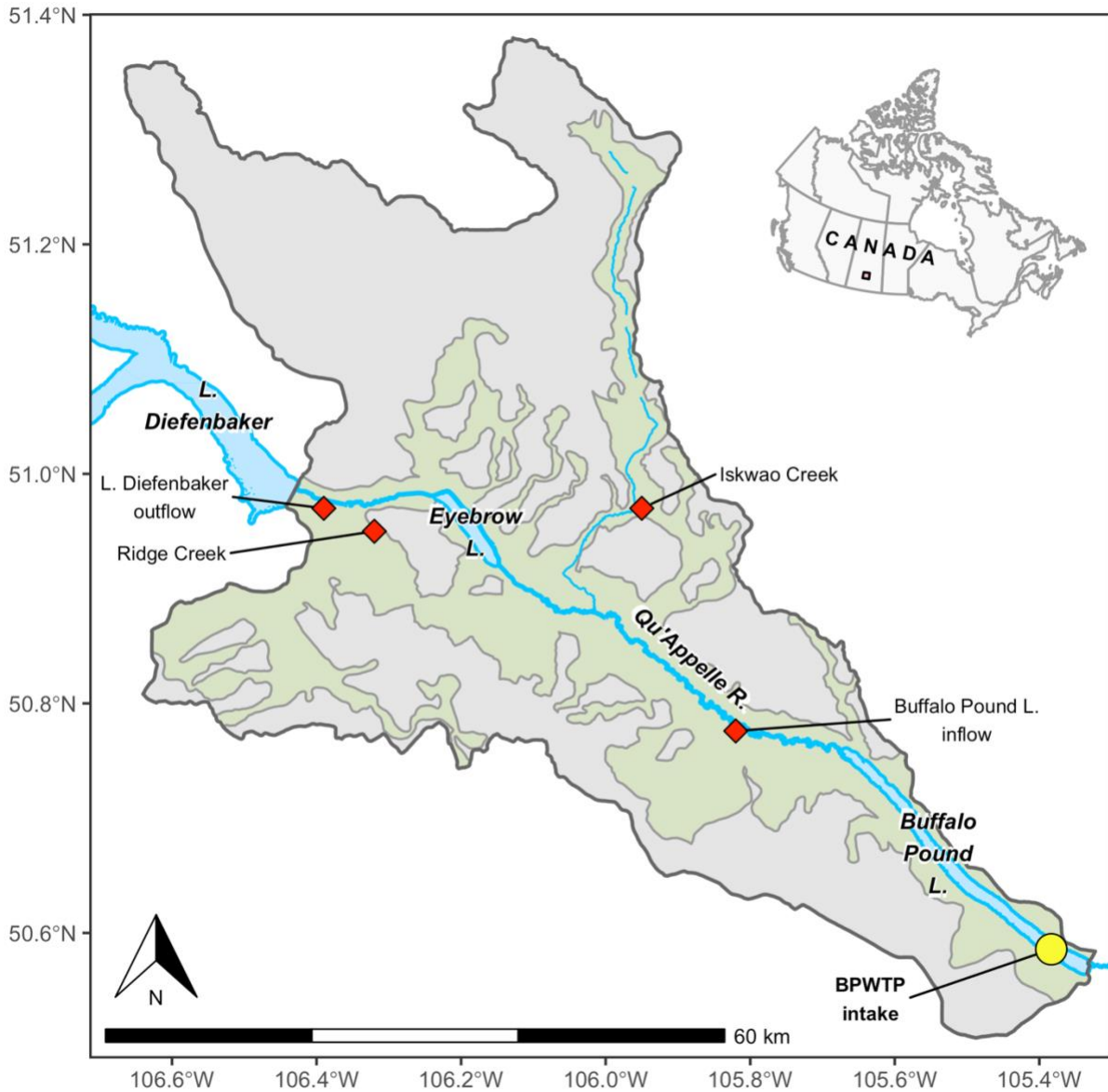


Figure 2.1. Map of Buffalo Pound Lake, Saskatchewan, Canada, highlighting its gross (grey) and effective (green) drainage areas, including upstream Lake Diefenbaker and the Qu'Appelle River. The middle of the lake is located at 50.65127° N, 105.508225° W. Red diamonds denote Water Survey of Canada streamflow gauging stations in the Buffalo Pound Lake watershed with complete or reconstructed records over the study period (see Section 2.4.1 and Table B.1). The inset map of Canada was plotted using the R package mapcan (McCormack and Erlich, 2019). Gross and effective drainage area shapefiles were obtained from the Prairie Farm Rehabilitation Administration (PFRA). Lake and river geospatial data were retrieved through the Government of Canada's Open Government License (Statistics Canada, 2006, 2011).

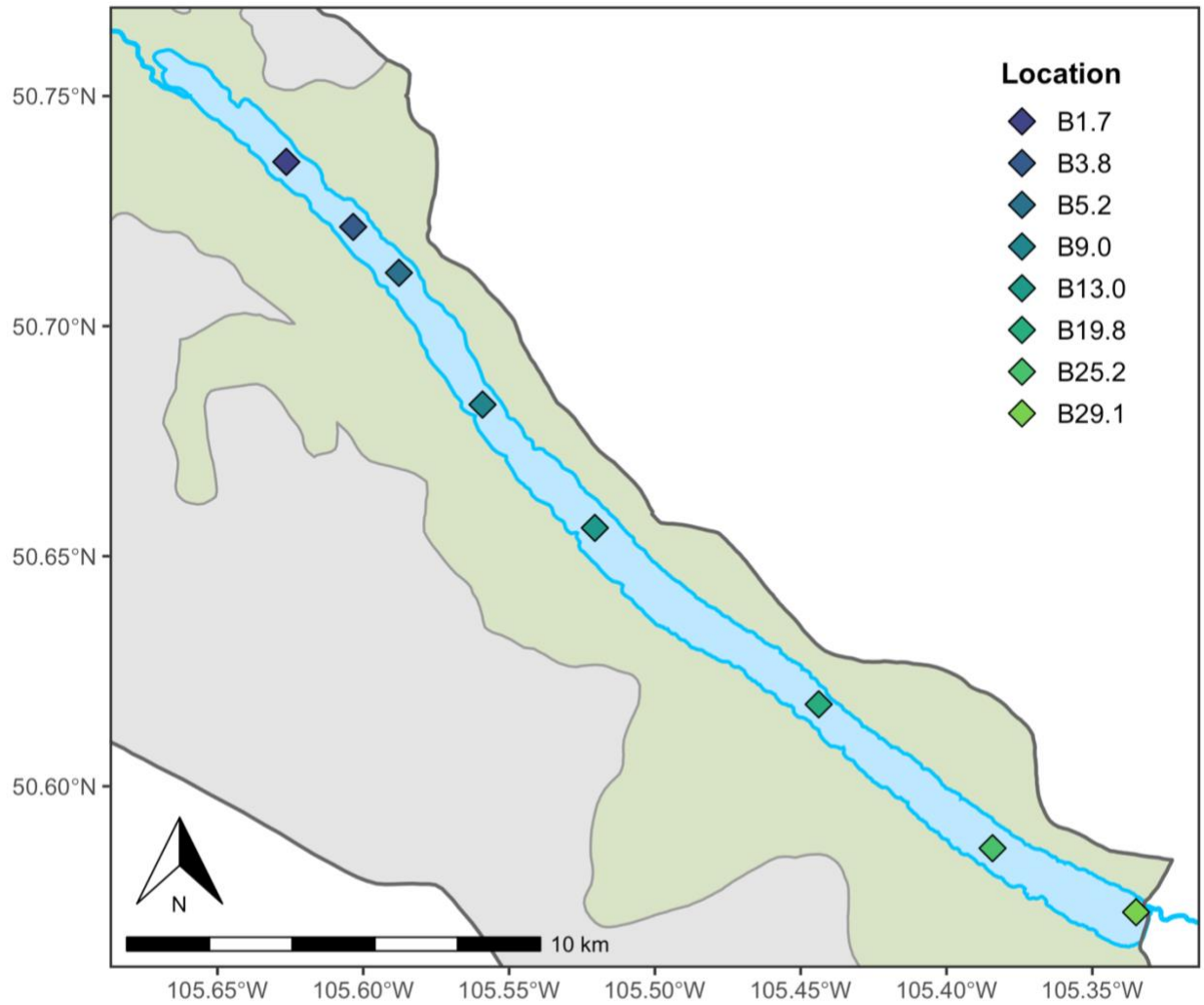


Figure 2.2. Map of Buffalo Pound Lake including parts of its gross (grey) and effective (green) drainage areas. Diamond symbols represent 8 locations along the length of the reservoir sampled by WSA in this study. Site geographic information is presented in Table 2.1.

Table 2.1. Sampling locations, geographic coordinates, and distances along Buffalo Pound Lake relative to the approximate downstream location of the lake inflow. See also Figure 2.2.

Site	Abbreviation	Latitude	Longitude	Distance from approximate lake inflow (km)
Lake Inflow	B1.7	50.7356	-105.6265	1.7
Upstream Causeway	B3.8	50.7219	-105.6014	3.8
Below Causeway	B5.2	50.7116	-106.5878	5.2
Opposite South Lake	B9.0	50.6830	-106.5591	9.0
Opposite Sun Valley	B13.0	50.6562	-106.5206	13.0
Opposite Parkview	B19.8	50.6178	-106.4438	19.8
WTP Intake	B25.2	50.5865	-106.3842	25.2
Above Outlet	B29.1	50.5726	-106.3303	29.1

2.2.2 Field sampling and laboratory analyses

To characterize DOM quantity and quality throughout the length of the system bulk surface water samples were collected at 11 sites stretching from the near the inflow of the lake to the outflow. Each site was sampled approximately monthly during the open water season (March to October; 3 times in 2016 and 6 times in each of 2017, 2018, and 2019). Sites near the inflow to Buffalo Pound Lake and upstream of a causeway on the lake are located close together relative to the width and length of the lake. To reduce overlap between sites near the inflow and causeway we took the average of each parameter and geographic coordinates of three inflow sites and two causeway sites, reducing the number of sites reported hereafter from 11 to 8, and herein we refer to the 8 remaining as “locations” (Table 2.1, Figure 2.2, with more information on rationale in Appendix A).

Water samples were collected using a standard Van Dorn discrete sampler at 1 m depth, unless the lake depth at a given site was < 1.3 m, in which case samples were collected at 0.5 m depth. Once collected, samples were transferred to laboratory-supplied bottles and held in a cooler with blue ice until back at the WSA lab in Regina, Saskatchewan or at the Global Institute for Water Security lab in Saskatoon, Saskatchewan then stored overnight in a fridge (4°C). The following day, samples for chlorophyll *a* (Chl *a*) were sent from the WSA lab to the Roy Romanow Provincial Lab (RRPL, Regina, Saskatchewan) while samples for analysis of DOC and TDN concentrations, and analysis of DOM fluorescence spectroscopy were shipped elsewhere from the Global Institute for Water Security lab in Saskatoon (details follow).

Water samples for analyses of DOC concentration, DOM excitation and emission matrices (EEM), and total dissolved nitrogen (TDN) were filtered through 0.45 µm nylon membrane syringe filters (AMD Manufacturing) into 40 mL amber glass scintillation vials with septa or Teflon lined caps. DOM/TDN samples were acid sparged prior to combustion using a Shimadzu TOC-L analyzer equipped with a TNM-L module (Badr et al., 2003). Samples were analyzed with the inclusion of a 5-point calibration curve with concentrations ranging from 1–10 mg C L⁻¹ from potassium hydrogen phthalate and 0.5–5 mg N L⁻¹ from NO₃⁻. Nicotinic acid was used as a check standard. Ultraviolet–Visible (UV–Vis) fluorescence and absorbance DOM scans were done in-laboratory using a Horiba Aqualog EV–Vis benchtop fluorimeter/spectrophotometer combination. In 2016 and 2017, EEM samples were analyzed at the State University of New York in Brockport, New York, USA. Samples from 2018 and 2019 were

analyzed at the University of Vermont in Burlington, Vermont, USA. The same scanning set up and data processing was used on both machines (in Brockport and Burlington), and all data were instrument- and baseline-corrected to ensure standardization and comparability (Hansen et al., 2018; Jaffé et al., 2008). Dissolved organic matter light absorbance scans were made from 200–800 nm at 3 nm intervals. At the same time, fluorescence excitation (200–800 nm at 3 nm interval) and emission (245.6–825.8 at 2.33 nm interval) matrix scans were made, with both absorbance and fluorescence scans measured at a fixed 5 nm bandpass and 1 s integration time. Minor differences in baseline and turbidity among samples were corrected by blank subtracting absorbance measurements then subtracting the mean absorbance from 700–800 nm. Instrument performance was checked daily by running a Milli-Q water blank. Standard recommendations and order of operations were used to correct sample EEMs for inner filter effects and instrument bias (Cory et al., 2010b; Murphy et al., 2010; Williams et al., 2010). Sample EEMs were normalized to Raman Units (RU) using the area under the Raman peak from the daily Milli-Q blank scan (Lawaetz and Stedmon, 2009). Corrected EEMs and absorbance spectra were linearly interpolated at a 1 nm interval prior to calculating optical DOM indexes. In 2017 and 2018, two samples in each year did not meet QA/QC standards (i.e., showed evidence of contamination) and were excluded from statistical analyses.

In addition to DOM quantity and quality, several other parameters were measured during the study period. Turbidity (in nephelometric turbidity units, NTU) was measured *in situ* using a YSI EXO1 field meter with an optical turbidity sensor. The turbidity sensor was calibrated or checked against standards weekly using 0 and 124 NTU calibration solutions. Secchi disc depth (Z_{SD} , in m) and the photosynthetically-available radiation (PAR) extinction coefficient (k_T , in m^{-1}) were used to measure water transparency. A LI-COR field meter with an LI192 2π sensor mounted to a lowering cage was used to measure PAR. Light profiles were constructed by measuring PAR at half-metre intervals from the lake surface to just above the sediment surface, or to a depth where measured PAR was < 1% of surface PAR. Care was taken to ensure consistent ambient light, and included measuring PAR in the air immediately prior to and immediately after measuring each light profile. Where pre- and post-measurements differed > 10% the PAR profile was remeasured. Extinction coefficients (m^{-1}) were determined using the slope of the linear regression for the relationship between the natural log of PAR versus depth (Kirk, 1994). Chlorophyll *a* concentrations ($\mu g L^{-1}$) were analyzed at the RRPL, accredited for

chlorophyll analysis by the Canadian Association for Laboratory Accreditation. Bulk water samples were filtered using low vacuum through a 0.45 μm nitrocellulose filter. Chlorophyll *a* was analyzed on pigments extracted from the filter with 90% acetone then vortexed to obtain a slurry. To ensure sufficient pigment extraction, slurries were steeped for at least two hours but less than 24 hours. The slurries were transferred to a holmium oxide glass cuvette with 1 cm path length and absorbance was measured at 630, 647, and 750 nm using a Hack DR/4000 UV-VIS spectrophotometer. Chlorophyll *a* concentrations were calculated using the Jeffrey and Humphrey (1975) trichromatic equation.

Streamflow records from gauges at the outflow of Lake Diefenbaker (Q_{LD}), within the local catchment (Q_{LC}), and directly upstream Buffalo Pound Lake (Q_{BP}) were used to understand sourcewater variation between 2016 and 2019. Water levels in this reservoir are tightly managed to maintain depth to within ± 10 cm of seasonal water level targets. In drier years and during winter months water levels are maintained via water releases from upstream mesotrophic Lake Diefenbaker, the dominant water source to Buffalo Pound Lake. In wetter years and during spring snowmelt, runoff from the local catchment can be an important water source. Chapter 3 provides a complete description of these data and methods. Briefly, gauging stations below Lake Diefenbaker, above Buffalo Pound Lake, and at one tributary (Ridge Creek) provided daily-averaged flow ($\text{m}^3 \text{s}^{-1}$) for the full duration of this study (Figure 2.1). A second local catchment tributary, Iskwao Creek, was gauged until 2006, and the 2007–2019 period was estimated using non-linear regression based on a training data set of Ridge Creek flows from 1972–1992. Combined flows from the local catchment (Q_{LC}) represent the sum of flows from Ridge Creek and Iskwao Creek, and their subsequent scaling up to the effective drainage area—the area of the catchment that may entirely contribute runoff during a flood with a two-year return period (Godwin and Martin, 1975)—of Buffalo Pound Lake as an estimate of all gauged and ungauged runoff sources to the lake.

2.2.3 Calculations and data analysis

2.2.3.1 Fluorescence spectroscopy

To make DOC concentration-independent comparisons across sampling locations, carbon-normalized (specific) UV absorbance at 254 nm (SUVA_{254}) was calculated by dividing the absorbance of filtered water samples at 254 nm (A_{254} , in absorbance unit [AU] cm^{-1}) by DOC

concentration. Spectral slopes were calculated for two wavelength ranges ($S_{275-295}$ and $S_{350-400}$), and a spectral slope ratio (S_R) was determined by dividing $S_{275-295}$ by $S_{350-400}$ (Helms et al., 2008).

Eight fluorescence peaks were normalized to DOC concentration [e.g., spA (excitation at 260 nm/emission at 540 nm [e_{x260}/e_{m540}]) and spT (e_{x275}/e_{m340})] and four peak ratios (e.g., Peak A:Peak T and Peak C:Peak M), measured in RU L mg^{-1} , were used as proxies for DOM composition (Table 2.2). Three fluorescent DOM compositional indexes—fluorescence index (FI) (Cory et al., 2010b; Cory and McKnight, 2005; McKnight et al., 2001), humification index (HIX) (Ohno, 2002; Zsolnay et al., 1999), and freshness index ($\beta:\alpha$) (Huguet et al., 2009; Parlanti et al., 2000; Wilson and Xenopoulos, 2009)—were also calculated to investigate DOM composition and source (Table 2.2).

Table 2.2. Common absorbance fluorescence optical measurements used to characterize DOM composition and used in this study. Table adapted from Hansen et al. (2016, 2018) and references therein.

Measurement	Description		
	Calculation	Purpose	Interpretation
Absorbance			
SUVA at 254 nm ($SUVA_{254}$) in $L\ mg^{-1}\ m^{-1}$	Absorption coefficient at 254 nm divided by DOC concentration	Measure of aromaticity	Higher values are typically associated with more aromatic DOC
Spectral slopes ($S_{275-295}$ and $S_{350-400}$) in nm^{-1}	Nonlinear fit of an exponential function to the absorption spectrum over the wavelength range	Indicators of DOM source, reactivity, and molecular weight	Higher S values typically associated with low molecular weight DOM and/or decreasing aromaticity
Spectral slope ratio (S_R)	$S_{275-295}$ divided by $S_{350-400}$	Indicator of DOM source, reactivity, and molecular weight	Negatively correlated with DOM molecular weight; irradiation generally increases S_R
Fluorescence			
Specific fluorescence at various peaks (SpA, SpB, SpC, SpD, SpE, SpM, SpN, SpT) in $RU\ L\ mg^{-1}$	Fluorescence at a given excitation-emission pair divided by DOC concentration	Fluorescence per unit carbon used as DOM compositional indicators	Normalizes fluorescence peaks to DOC concentration; SpA, SpC, SpE, SpM, and SpD are associated with humic-like materials whereas SpB, SpN, and SpT are associated with fresh-like materials
Peak ratio (A:T)	Ratio of Peak A (ex260/em450) to Peak T (ex275/em340) intensity	Measure of humic-like (recalcitrant) versus fresh-like (labile) fluorescence	Higher values associated with greater humic-like materials

Table 2.2. Common absorbance fluorescence optical measurements used to characterize DOM composition and used in this study. Table adapted from Hansen et al. (2016, 2018) and references therein.

Fluorescence			
Peak ratio (C:A)	Ratio of Peak C (ex340/em440) to Peak A (ex260/em450) intensity	Measure of the relative amount of photosensitive humic-like DOM fluorescence	Higher values associated with a greater proportion of photosensitive humic-like materials
Peak ratio (C:M)	Ratio of Peak C (ex340/em440) to Peak M (ex300/390) intensity	Measure of the amount of diagenetically-altered (blue-shifted) fluorescence	Higher values associated with more blue-shifted fluorescence
Peak ratio (C:T)	Ratio of Peak C (ex340/em440) to Peak T (ex275/em340) intensity	Measure of humic-like (recalcitrant) versus fresh-like (labile) fluorescence	Higher values associated with greater humic-like materials
Fluorescence index (FI)	Ratio of 470 nm and 520 nm emission wavelengths at excitation 370 nm	Identifies relative proportions of terrestrial and microbial sources to the DOM pool	Higher values associated with more microbial DOM sources
Humification index (HIX)	Area under the emission spectra 435–480 nm divided by the peak area 300–345 nm + 435–480 nm at excitation 254 nm	Indicator of humic substance content or extent of DOM humification	Higher values associated with greater humification
Freshness index ($\beta:\alpha$)	Ratio of emission intensity at 380 nm divided by the maximum emission intensity between 420 nm and 435 nm at excitation 310 nm	Indicator of recently produced fresh-like DOM	Higher values indicate greater proportion of fresh DOM

2.2.4 Statistical analyses

Statistical analyses, including paired t-tests and correlations, were performed in R (R Core Team, 2022). The ggplot2 package (Wickham 2016) was used for data visualization. Visual inspection of histograms and quantile–quantile plots, and the Shapiro–Wilk test (rstatix package, shapiro_test function, Kassambara, 2021; Shapiro and Wilk, 1965) were used to evaluate normality, where a $p > 0.1$ indicated ~normal distribution (Royston, 1995). Parameters with significant Shapiro–Wilk’s W values ($p < 0.1$) were log-transformed to reduce skew. Levene’s test (car package, leveneTest function, Fox and Weisburg, 2019; Levene, 1960) was used to assess homogeneity of variance.

Paired-sample Student’s t-tests (rstatix package, t_test function, Kassambara, 2021; Student, 1908) were run to investigate seasonal (spring and summer) differences in mean values of water quality (turbidity, Z_{SD} , k_T , Chl a , TDN), DOC concentration, and compositionally based DOM absorbance and fluorescence optical parameters ($SUVA_{254}$, $S_{275-295}$, FI, HIX, $\beta:\alpha$). Spring and summer groups were split between samples collected April–June and July–September, respectively, to have approximately equal n in each group. The paired-sampled t-test assumes samples are dependent, normally distributed, and have no extreme outliers; this was confirmed prior to analysis. Cohen’s d was used to measure effect size, or the magnitude of the difference between each group, for significant ($p < 0.05$) t-test runs. Effect size is calculated as $(M_1 - M_2) / s$, where M_1 and M_2 are the means of the two groups and s is the standard deviation of all measurements. Effect size values range from small (0.2), medium (0.5), large (0.8), to very large (1.3) (Cohen, 1988). Significant t-test p -values were corrected using the false discovery rate (FDR) approach (Benjamini and Hochberg, 1995). The FDR quantifies the expected proportion of all positive (false and true) tests that reject the null hypothesis ($\mu_1 = \mu_2$) by ranking p -values in ascending order then multiplying each p -value by m/k where k is the ordered position of an individual p -value and m is the number of independent (pairwise) tests (Jafari and Ansari-Pour, 2019). In effect the FDR reduces the number of false positives while minimizing the occurrence of false negatives.

To investigate linear changes in DOM quantity and quality from the inflow to Buffalo Pound Lake through to its outflow, linear models (base package, lm function, R Core Team, 2022) were run using distance from the lake inflow and the mean of each parameter at each location (DOC concentration, TDN concentration, $SUVA_{254}$, $S_{275-295}$, FI, HIX, $\beta:\alpha$). Linear

models were considered significant at $p < 0.05$, and the number of observations at each site ranged from 10–22. Strong relationships were identified by R^2 values between ± 0.65 – 0.79 and very strong between ± 0.8 – 1.0 .

2.3 Results

2.3.1 Sourcewater variability

Local catchment (Q_{LC}), Lake Diefenbaker outflows (Q_{LD}), and Buffalo Pound Lake inflows (Q_{BP}) were variable across years, with Q_{LD} the dominant water source to Buffalo Pound Lake in all study years (Figure 2.3). Flows from the local catchment contributed comparatively little inflow to the lake, with the exceptions of singular episodes of increased catchment flow in 2016, 2018, and 2019, shown as the high points in the catchment flows in Figure 2.3. In all years Q_{LD} transiently reached or exceeded the 95th percentile of 1990–2019 flows while also falling to or below the 5th flow percentile for short periods.

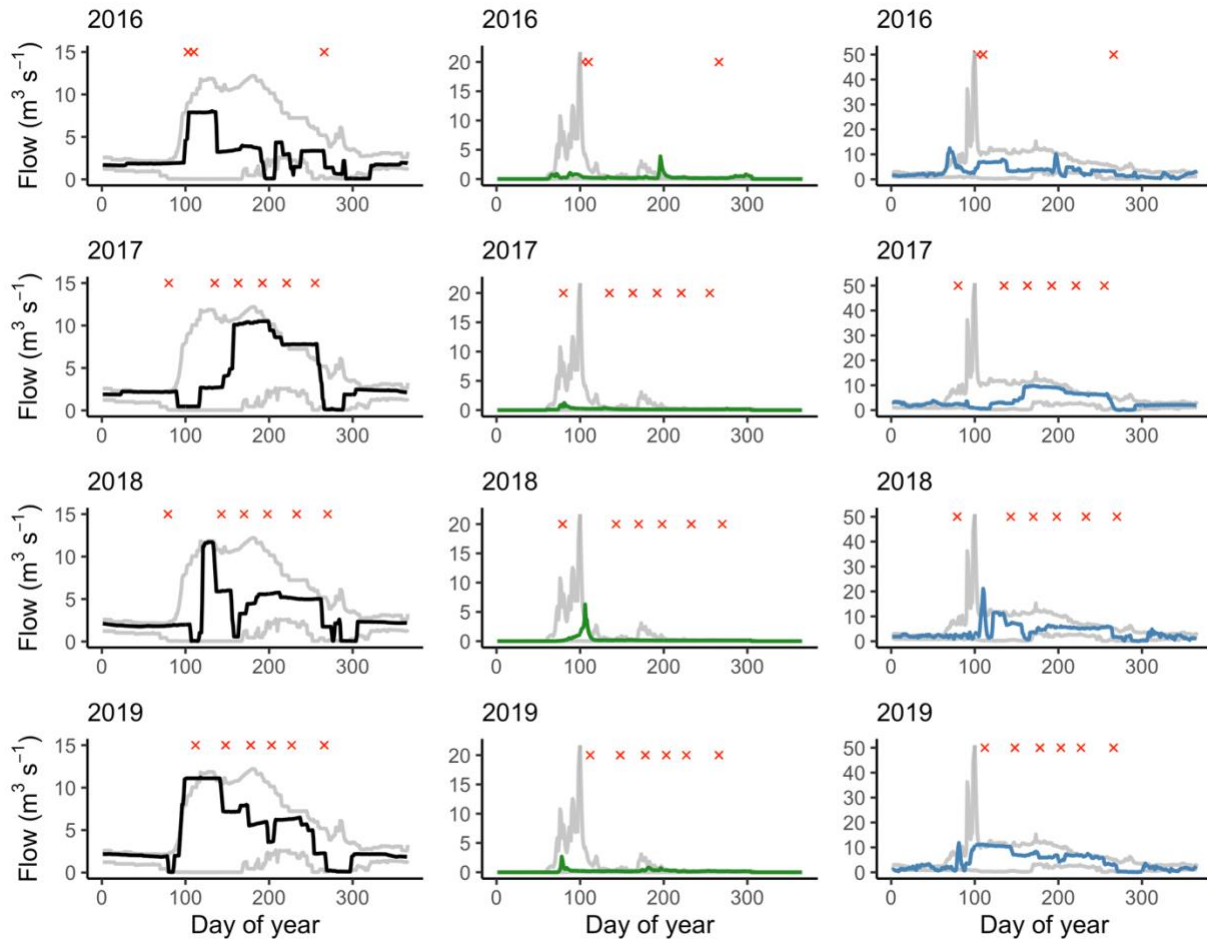


Figure 2.3. Flows from Lake Diefenbaker outflow (black), the local catchment (green), and Buffalo Pound Lake inflow (blue) from 2016–2019. Upper and lower grey lines are the 95th and 5th percentile of flows from 1990–2019 respectively. Red Xs are open water season sampling dates where DOM quantity and quality were measured. Note that the y-axis scales vary by column. Note also that estimated ungauged flows (Q_U) to Buffalo Pound Lake make up the difference shown between Q_{BP} and that shown from Q_{LD} and Q_{LC} , and that in any given year not all Q_{LD} and Q_{LC} contribute to Q_{BP} (Chapter 3).

2.3.2 Water quality and DOC concentration

2.3.2.1 Water quality

Turbidity averaged 7.9 ± 10.4 NTU (mean \pm standard deviation; $N = 146$) across sites and dates. In 2016 high turbidity (> 75 NTU) was recorded at the B1.7 and B3.8 but did not exceed 25 NTU at any other site in any other year (Figure 2.4a). Patterns among years were otherwise similar, with some lower turbidity and some minor variation throughout the lake. Specifically, turbidity was higher near the inflow (B1.7) and outflow (B29.1) in 2016, highest near the inflow (B1.7) and causeway (B3.8, B5.2) in 2017 and 2018, and highest at B19.8 (near mid-lake) in 2019. Summer turbidity values were lower than spring turbidity values (medium effect size) but this difference was not significant ($t(9.04) = -0.56$, $p = 0.182$, $d = 0.70$).

The light extinction coefficient (k_T) and Secchi disc depth (Z_{SD}) showed similar but inverse patterns, with water clarity improving beyond B1.7 and into the mid-lake sites and sites near the lake outflow (Figures 2.4b and 2.4c). Extinction coefficients and Z_{SD} were highly variable ($0.45\text{--}4.35\text{ m}^{-1}$ and $0.2\text{--}3.6\text{ m}$ respectively). Secchi disc depth reached the lake bottom (3.6 m) at B25.2 in 2019. Average values were $1.40 \pm 0.71\text{ m}^{-1}$ ($N = 131$) for k_T and $1.18 \pm 0.65\text{ m}$ for Z_{SD} ($N = 134$). Significant seasonal differences were not apparent for k_T ($t(8.88) = -0.31$, $p = 0.0936$, $d = 0.87$) or Z_{SD} ($t(8.28) = 0.21$, $p = 0.35$, $d = 0.49$).

Overall, Chl *a* concentrations showed considerable variation across the lake ($21.8 \pm 24.1\text{ }\mu\text{g L}^{-1}$, $N = 147$), peaking at B19.8 in 2019 ($141.5\text{ }\mu\text{g L}^{-1}$); median Chl *a* concentration was $12.4\text{ }\mu\text{g L}^{-1}$ (Figure 2.4d). Intraannual differences in Chl *a* were evident, particularly comparing 2019 to 2016 and 2017. Summer Chl *a* concentrations were significantly higher than spring concentrations with a large effect size ($t(11.07) = -0.63$, $p = 0.00786$, $d = 1.28$). A significant statistical result should be taken with caution as log-transformation did not improve left-skewness in Chl *a* concentrations. The large effect size suggests that there is potentially a real statistical difference in spring and summer Chl *a*; median Chl *a* concentrations were $11.6\text{ }\mu\text{g L}^{-1}$ in spring ($n = 75$) and $25.5\text{ }\mu\text{g L}^{-1}$ in summer ($n = 72$).

2.3.2.2 TDN and DOC concentrations

Total dissolved N concentrations increased from the lake inflow to the outlet and ranged from $0.22\text{--}0.64\text{ mg L}^{-1}$ (Figure 2.5a). On average TDN in the lake was $0.40 \pm 0.08\text{ mg L}^{-1}$ ($N = 86$). Peak average TDN concentrations were observed at B25.2 ($0.46 \pm 0.07\text{ mg L}^{-1}$, $n = 11$) and

B29.1 ($0.47 \pm 0.06 \text{ mg L}^{-1}$, $n = 11$). Seasonal differences between spring and summer TDN concentrations were not apparent ($t(7.86) = -0.30$, $p = 0.775$).

Dissolved organic carbon concentrations ranged from 3.7–8.1 mg L^{-1} and averaged $5.5 \pm 0.96 \text{ mg L}^{-1}$ ($N = 165$) across all sites and years. Across all years, DOC concentrations tended to increase from near the lake inflow to the outlet (Figure 2.5b), similar to observed patterns for TDN. For example, at B1.7, DOC concentration averaged $5.0 \pm 0.96 \text{ mg L}^{-1}$ ($n = 20$) and rose to $6.2 \pm 1.1 \text{ mg L}^{-1}$ ($n = 20$) at B29.1. Interestingly, B29.1 and B1.7 had the two highest observed DOC concentrations at 8.1 and 7.5 mg L^{-1} respectively. Adjacent to the water treatment plant intake (B25.2), DOC averaged $5.7 \pm 0.9 \text{ mg L}^{-1}$ ($n = 21$). Seasonally, among all sites, DOC concentrations averaged $5.5 \pm 0.2 \text{ mg L}^{-1}$ in spring and $5.3 \pm 0.7 \text{ mg L}^{-1}$ in summer ($t(8.22) = 0.63$, $p = 0.546$).

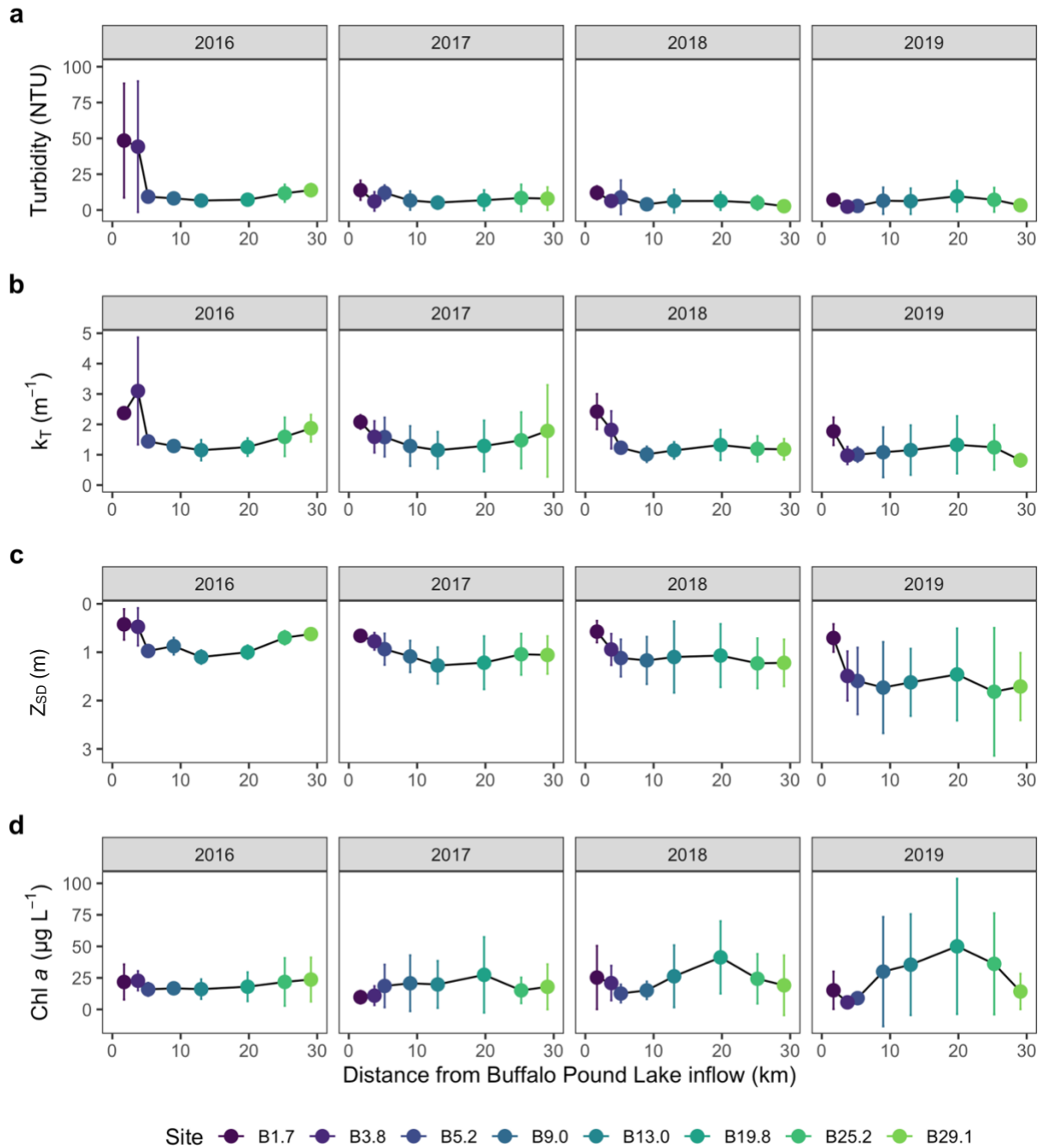


Figure 2.4. (a) Turbidity, (b) photosynthetically-available radiation (PAR) extinction coefficient (k_T), (c) Secchi depth (Z_{SD}), and (d) chlorophyll *a* concentration measured at 8 locations along Buffalo Pound Lake from 2016–2019. Points are mean values and error bars represent the standard deviation of mean values ($N = 3-6$).

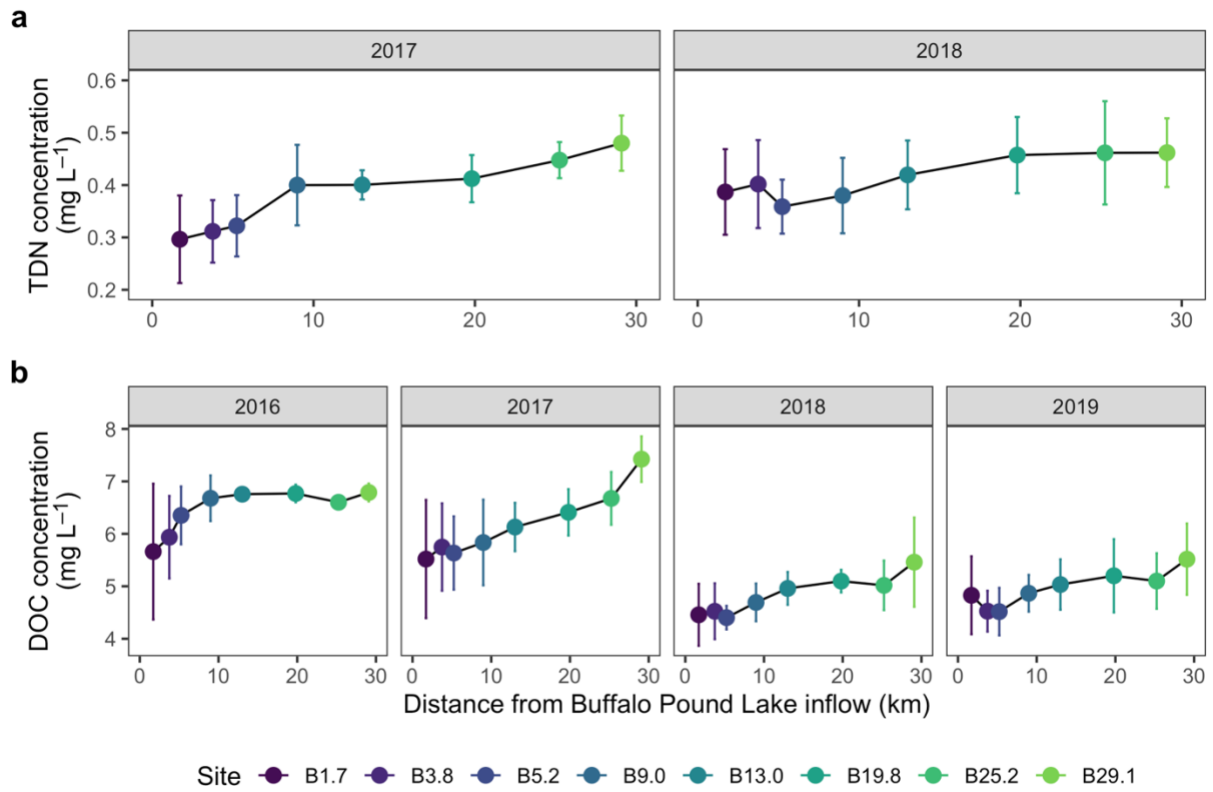


Figure 2.5. (a) Total dissolved nitrogen and (b) DOC concentrations measured at 8 locations along Buffalo Pound Lake from 2016–2019. Points are mean values and error bars represent the standard deviation of mean values ($N = 3-6$). TDN was not monitored in 2016 and 2019.

2.3.3 DOM compositional parameters

2.3.3.1 Absorbance

Overall SUVA₂₅₄ values averaged $2.1 \pm 0.3 \text{ L mg-C}^{-1} \text{ m}^{-1}$ ($N = 161$) and did not exceed $3.0 \text{ L mg-C}^{-1} \text{ m}^{-1}$. Like DOC concentration, SUVA₂₅₄ values were comparable in both spring and summer months ($t(13.61) = -0.033$, $p = 0.974$). In contrast to DOC concentration, patterns in SUVA₂₅₄ showed a marked decrease from inflow to outflow in all years (Figure 2.6a). At B25.2, SUVA₂₅₄ values ranged from 1.5–2.1 and averaged $1.9 \pm 0.2 \text{ L mg-C}^{-1} \text{ m}^{-1}$.

Spectral slope values tended to rise from lake inflow to outflow (Figure 2.6b); in 2016 and 2019 $S_{275-295}$ was similar from B1.7 to B13.0 with higher values observed from B19.8 to B29.1. Throughout the lake, $S_{275-295}$ values ranged from $0.016\text{--}0.026 \text{ nm}^{-1}$ but were predominately $> 0.020 \text{ nm}^{-1}$. On average $S_{275-295}$ was $0.023 \pm 0.002 \text{ nm}^{-1}$ ($N = 161$) and did not vary seasonally ($t(11.93) = -0.67$, $p = 0.517$).

2.3.3.2 Fluorescence

Fluorescence index values in Buffalo Pound Lake generally increased from inflow to outflow, except in 2016 where they plateaued at B13.0 (Figure 2.6c). Overall variation in FI values was low, with a range of 1.49–1.66 and average of 1.57 ± 0.03 ($N = 161$), and did not vary seasonally ($t(12.13) = -0.79$, $p = 0.442$).

Humification index values in the lake were generally high, ranging from 0.73–0.89 and averaging 0.83 ± 0.03 ($N = 161$) (Figure 2.6d). Patterns in HIX were more complex than other DOM compositional parameters. For example, in 2016 HIX was highest near the lake inflow, lowest near mid-lake, and rose again near the lake outflow. Interestingly HIX values were markedly lower in 2017, coinciding with low spring flows from Lake Diefenbaker and the local catchment (Figure 2.3). Seasonally there was little difference in average HIX values ($t(13.82) = -0.66$, $p = 0.523$).

Freshness index values ranged from 0.66–0.85 and averaged 0.77 ± 0.03 ($N = 161$) (Figure 2.6e), and a clear increase was observed from lake inflow to outflow across all years. Like other DOM compositional parameters there was no clear difference between spring and summer $\beta:\alpha$ ($t(13.94) = -0.96$, $p = 0.354$).

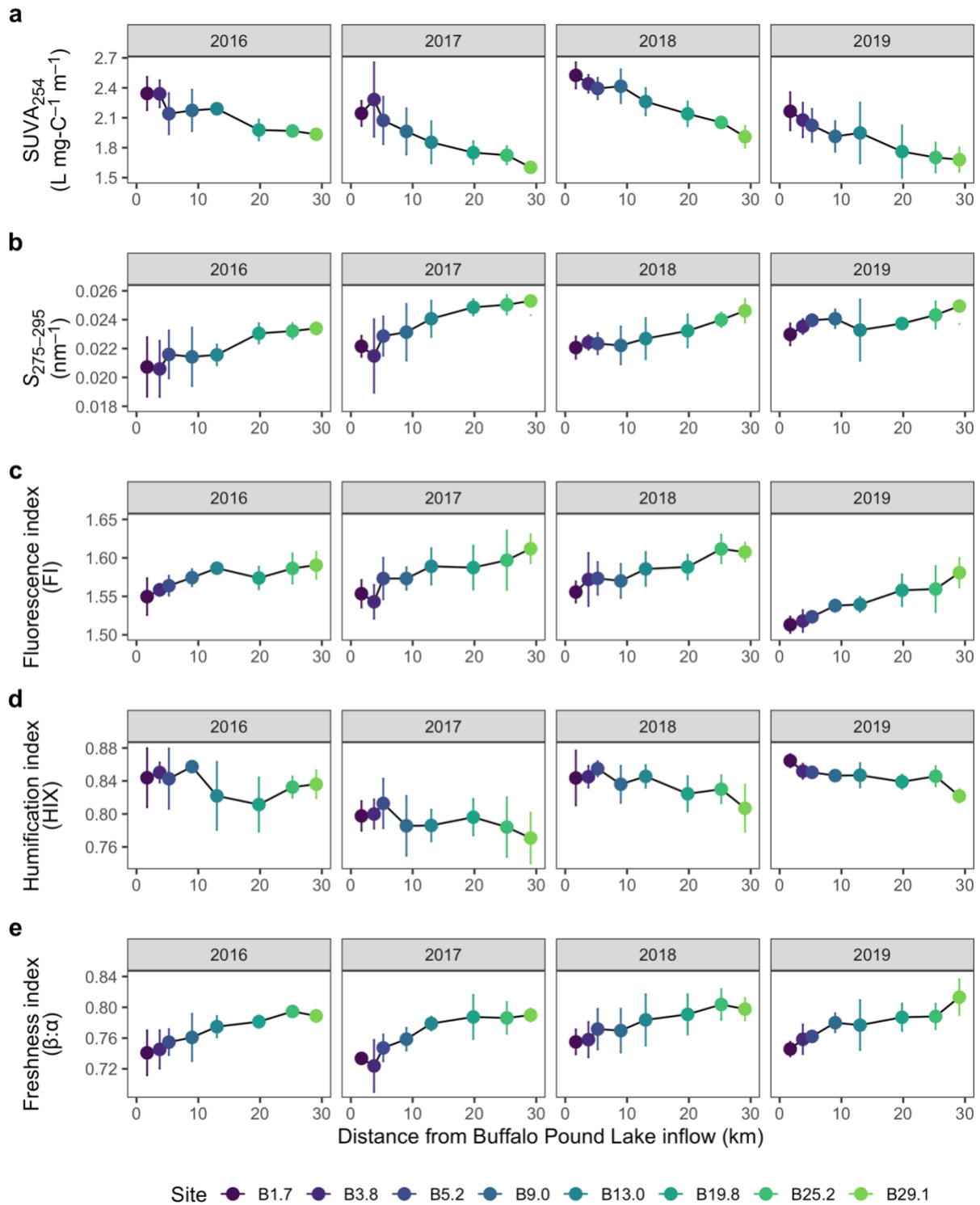


Figure 2.6. (a) SUVA₂₅₄, (b) S₂₇₅₋₂₉₅, (c) FI, (d) HIX, and (e) β:α measured at 8 locations along Buffalo Pound Lake from 2016–2019. Points are mean values and error bars represent the standard deviation of mean values ($N = 3-6$).

2.3.4 In-lake DOM patterns

We saw significant relationships between DOC, TDN, absorbance and fluorescence, and location of sampling over the course of the study. Concurrent increases in DOC and TDN concentrations, $S_{275-295}$, FI, and $\beta:\alpha$ were met with decreases in $SUVA_{254}$ and HIX (Figure 2.7).

Mean DOC concentration from 2016–2019 increased 1.2 mg L^{-1} from B1.7 to B29.1 ($R^2 = 0.94$, $p = 4.12 \times 10^{-5}$). Interannual patterns were also evident in DOC. Increases in DOC along the length of Buffalo Pound Lake were $< 1.0 \text{ mg L}^{-1}$ in 2016, 2018, and 2019, whereas in 2017 DOC increased 1.9 mg L^{-1} (Figure 2.7a, Figure A.8a). Mean DOC concentrations were distinctly higher in 2016 and 2017, ranging $5.5\text{--}7.4 \text{ mg L}^{-1}$. In 2018 and 2019 they were $4.4\text{--}5.5 \text{ mg L}^{-1}$.

In 2017–2018 mean TDN concentration increased 0.12 mg L^{-1} from B1.7 to B29.1 ($R^2 = 0.95$, $p = 3.04 \times 10^{-5}$) (Figure 2.7b). While an increase from B1.7 to B29.1 was observed interannually in 2017 and 2018 (Figure A.8b), the change was more pronounced in 2017 (increase from 0.30 to 0.48 mg L^{-1}) than 2018 (increase from 0.39 to 0.46 mg L^{-1}).

Along with increases in DOC concentration along the length of Buffalo Pound Lake, mean $SUVA_{254}$ values consistently decreased ($R^2 = 0.97$, $p = 6.90 \times 10^{-6}$) (Figure 2.7c). Interannual patterns in $SUVA_{254}$ were different than for DOC, however, with the lowest $SUVA_{254}$ values observed in 2017 and 2018 and the highest in 2016 and 2019 (Figure A.8c), suggesting $SUVA_{254}$ may initially be controlled by incoming source material then altered by in-lake degradation and processing.

Spectral slope values increased with increasing DOC and TDN concentrations but average overall change did not exceed 0.003 nm^{-1} from B1.7 to B29.1 ($R^2 = 0.95$, $p = 1.10 \times 10^{-6}$) (Figure 2.7d). Similar increases in $S_{275-295}$ from B1.7 to B29.1 were observed among years (Figure A.8d). We report only $S_{275-295}$ because poor absorption at near-visible wavelengths (350–400 nm) produced large variation in $S_{350-400}$ values at numerous sites across all years (Figures A.3, A.4a).

Fluorescence index values also increased along the length of Buffalo Pound Lake ($R^2 = 0.95$, $p = 2.01 \times 10^{-5}$); mean FI was 1.54 at B1.7 and 1.60 at B29.1 (Figure 2.7e). Interannual patterns were similar in 2016, 2017, and 2018, when FI at B1.7 was between 1.550 and 1.556, and between 1.591 and 1.612 at B29.1 (Figure A.8e). In 2019 FI was markedly lower at B1.7 (1.513) but reached 1.581 at B29.1 near the lake outlet.

Humification index values, like $SUVA_{254}$, tended to decrease on average from B1.7 to B29.1 ($R^2 = 0.87$, $p = 4.71 \times 10^{-4}$) (Figure 2.7f). Slopes and y-intercepts were very similar between 2016, 2018, and 2019, with HIX values at B1.7 between 0.844 and 0.865 and between 0.807 and 0.822 at B29.1 (Figure A.8f). In comparison, HIX in 2017 was notably lower across sites (0.798 at B1.7 and 0.771 at B29.1).

Increases in $\beta:\alpha$ from B1.7 to B29.1 ($R^2 = 0.94$, $p = 5.45 \times 10^{-5}$) suggest that, on average, microbially-produced DOM became more prominent along the length of the lake (Figure 2.7g). This pattern was similarly observed across all years but $\beta:\alpha$ values tended to be slightly higher near the inflow sites when DOC concentration was lower in this region of the lake (i.e., 2018–2019) (Figure A.8g). From B19.8 to B29.1 there was little interannual difference in $\beta:\alpha$ between 2016–2019 (Figure 2.7g).

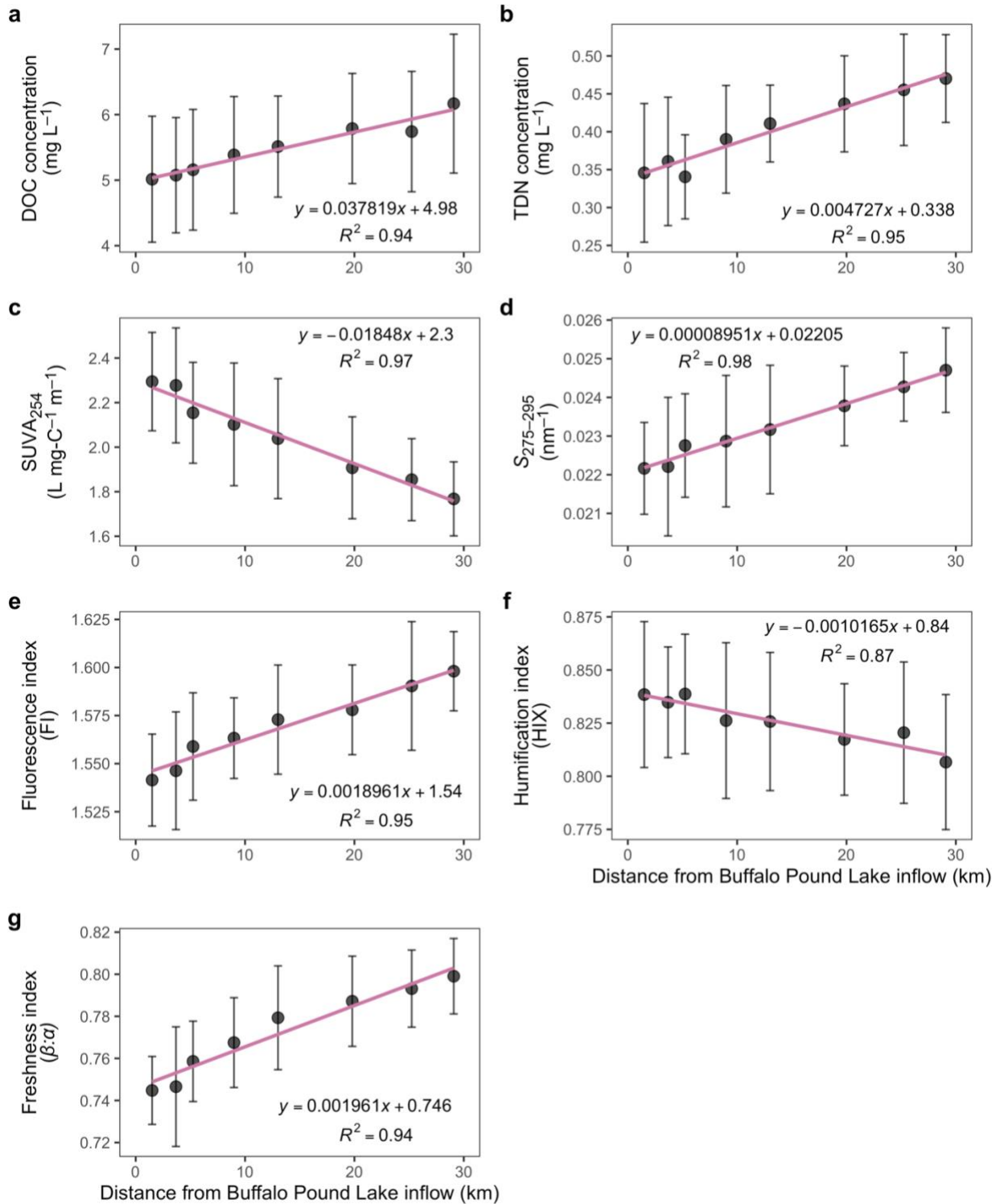


Figure 2.7. (a) Dissolved organic carbon concentration, (b) TDN concentration, (c) SUVA_{254} , (d) $S_{275-295}$, (e) FI, (f) HIX, and (g) $\beta:\alpha$ measured at 8 locations along Buffalo Pound Lake from 2016–2019. Points are mean values and error bars represent the standard deviation of mean values ($N = 10\text{--}22$). Lines (equations shown) are fitted linear model trend lines ($R^2 = 0.87\text{--}0.98$, $p < 0.0001$).

2.4 Discussion

While extensive work on cross-lake drivers of DOM chemodiversity has revealed the importance of precipitation, temperature, and water residence time on controlling DOM quality across ecosystems (Kellerman et al., 2014), there has been more limited work on within-ecosystem variability. Here we measured DOC and TDN concentrations and DOM quality across 8 locations in Buffalo Pound Lake, a shallow eutrophic reservoir with a drinking water treatment plant undergoing a \$325M upgrade to continue to provide safe drinking water to 270,000 people. Our results reveal strong gradients in DOM quantity and quality along the length of Buffalo Pound Lake reflective of in-lake DOM processing and production. We observed increases in DOC and TDN concentration as water transits the lake and a shift to more microbial and aliphatic DOM signatures and increasing autochthony nearer the outflow of Buffalo Pound Lake. During the years studied (2016–2019) inflows to Buffalo Pound Lake were dominated by releases of water from upstream mesotrophic Lake Diefenbaker with occasional, but limited, inputs from the local catchment. Under these hydrological conditions we expect minimal terrestrial DOM inputs directly to Buffalo Pound Lake, evidenced by moderate ($\sim 5\text{--}6\text{ mg L}^{-1}$) DOC concentrations; in years of deluge, monthly DOC concentrations in the lake have exceeded 12 mg L^{-1} (Chapter 3). Longer residence times associated with predominant inflows from Lake Diefenbaker during our study may have provided conditions favourable for enhanced autochthonous DOM production, which we associate with observed increases in DOC concentration, $S_{275-295}$, FI, and $\beta:\alpha$, and decreases in $SUVA_{254}$ and HIX along the length of the lake. Here we discuss the seasonal and longitudinal variation in water quality and DOM quantity and quality, framing our discussion in terms of the impact of variable sourcewater on in-lake DOM processes, with some broader implications on drinking water treatment in this critical drinking water source.

2.4.1 Seasonal variation in water quality and DOM quantity and quality

Lakes and reservoirs in cold regions receiving high amounts of terrestrial DOM may show distinct seasonal patterns in DOM quantity, quality, or both, driven by spring snowmelt (Jane et al., 2017; Miller and McKnight, 2010). We expected to see seasonal patterns in water quality and DOM quantity and quality because snowmelt is often the dominant period of flow and nutrient inputs in our study region (Ali and English, 2019; Painter et al., 2022a). We saw

little evidence of a seasonal effect as evidenced by little difference in TDN and DOC concentrations and DOM quality ($SUVA_{254}$, $S_{275-295}$, FI, HIX, and $\beta:\alpha$) despite significant differences in spring and summer turbidity, k_T , and Chl *a* concentrations. This could be a result of the highly managed nature of water inflows to the lake from Lake Diefenbaker, and decreasing water residence time associated with this flow source.

2.4.2 Spatial variability in DOM quantity and quality

Clear changes in DOM quantity and quality were observed between the deltaic inflow to Buffalo Pound Lake (e.g., sites B1.7, B3.8, B5.2) and locations near the lake outflow (e.g., sites B19.8, B25.2, B29.1). Increases in DOC and TDN concentration along the length of the lake were accompanied by a shift in DOM quality from more degraded, humic-lake DOM near the inflow to more fresh-like, aliphatic DOM near the outflow. The magnitude and rate of change of DOM quantity and quality varied among years (Figure A.8) but overall trends suggest a shift to increasing autochthony (Figure 2.7). There were also no significant differences in DOC concentration, $SUVA_{254}$, HIX, or $\beta:\alpha$ among sites near the inflow that were perpendicular to the flow axis (Supplementary Information section A.1.1), reinforcing that spatial variation in DOM quantity and quality is along the flow axis of the lake.

The BPWTP routinely measures $SUVA_{254}$ as part of its routine water quality monitoring. On average $SUVA_{254}$ decreased $\sim 0.5 \text{ L mg-C}^{-1} \text{ m}^{-1}$ from B1.7 to B25.2, where raw water is collected and pumped to the BPWTP. The $SUVA_{254}$ levels we observed ($< 3.0 \text{ L mg-C}^{-1} \text{ m}^{-1}$) during drier years may be associated with less reactive and refractory DOM, easing DOC removal during water treatment and reducing the formation of disinfectant byproduct precursors (Weishaar et al., 2003).

Lower $S_{275-295}$ values generally indicate higher molecular weight and more aromatic DOM (Chin et al., 1994; Hansen et al., 2016; Helms et al., 2008). The range of $S_{275-295}$ we report ($0.016\text{--}0.026 \text{ nm}^{-1}$) is comparable to values reported for ocean ($0.020\text{--}0.030 \text{ nm}^{-1}$) and coastal waters ($0.010\text{--}0.020 \text{ nm}^{-1}$) (Del Vecchio and Blough, 2002). Hansen et al. (2016) observed increases in $S_{275-295}$ with prolonged light exposure in peat soil, wetland plants, and algae leachates, attributing these changes to either loss of higher molecular weight DOM due to disaggregation or an increase in lower molecular weight (MW) products of condensation reactions absorbing light at these wavelengths (Obernosterer et al., 1999; Stepanauskas et al.,

2005). A survey of 44 prairie freshwater and saline lakes and wetlands demonstrated that, in the freshwater systems, light in the UV-B range (280–320 nm) penetrated much deeper than the UV-A range (320–400 nm) (Arts et al., 2000). In our study S_R (the ratio of $S_{275-295}$ to $S_{350-400}$) was > 1 across all years, and tended to increase along the length of Buffalo Pound Lake (Figure A.4b). Likewise, Helms et al. (2008) observed a photochemically-induced shift from high MW terrestrially-derived DOM ($S_R < 1$) to low MW DOM ($S_R > 1$) and an increase in $S_{275-295}$ as water transited an estuary to the open ocean. This suggests that the Buffalo Pound Lake DOM pool may have shifted to lower MW compounds from inflow to outflow but overall lacked a large portion of high MW DOM. Water clarity in Buffalo Pound Lake generally improved downstream of the inflow and causeway (Figure 2.4), providing conditions favourable for light exposure and photodegradation.

In natural waters FI values typically fall between 1.2 and 1.8 (Carpenter et al., 2013; Cory et al., 2010a; Fleck et al., 2014, 2014; Hansen et al., 2016; Helms et al., 2013; Jaffé et al., 2008; Wilson and Xenopoulos, 2009). The FI was originally derived to characterize the fulvic acid fraction of DOM, and associates lower FI values with DOM derived from degraded plant and soil organic matter from terrestrial sources, and higher values with microbial sources, including DOM derived from extracellular release and leachate from algae and bacteria (McKnight et al., 2001). A shift in FI of at least 0.1 can indicate a difference in fulvic acid source (McKnight et al., 2001). In this study FI ranged 1.49–1.66 overall, shifting toward more fresh-like, perhaps microbially-sourced, DOM at sites close to the lake outflow. These increases in FI coupled with declining $SUVA_{254}$ along the length of Buffalo Pound Lake suggest a decreasing level of DOM aromaticity as water transits the system (Cory et al., 2010b; McKnight et al., 2001).

Freshwater HIX values commonly range between 0.6 and 0.9 (Chen et al., 2011; Fleck et al., 2014; Ohno, 2002) with higher values indicating a greater degree of humification. The high (0.73–0.89) HIX values observed here suggest Buffalo Pound Lake DOM is derived from terrestrial sources despite Lake Diefenbaker being its primary water source. Patterns in HIX were less clear from the lake inflow to outflow. For example, similar average HIX was observed at mid-lake sites B9.0 and B13.0 and near the BPWTP intake site (B25.2). However, HIX clearly decreased when viewed along the whole length of the lake, suggesting photodegradation or biological processing reduced the degree of humification in the DOM pool, or the addition of

new DOM via internal production added more fresh-like DOM decreased the relative proportion of humic-like DOM. Interestingly, Hansen et al. (2016) observed increasing HIX in plant- and algae-derived DOM with increasing length of dark incubation (up to 111 days), noting that microbial consumption in the absence of photoexposure reduced the labile portion of the DOM pool and facilitated DOM humification.

The freshness index ($\beta:\alpha$) reflects the ratio of fresh-like (β) DOM to humic-like (α) DOM where higher values are associated with a greater contribution of recently produced DOM (Parlanti et al., 2000; Wilson and Xenopoulos, 2009). Freshness index values between 0.5–0.9 were reported for peat soil, wetland plants, and algae leachates (Hansen et al., 2016) and 0.5–0.68 for temperate watershed draining agricultural areas in Ontario, Canada (Wilson and Xenopoulos, 2009). Here we report $\beta:\alpha$ values ranging 0.66–0.85 with increases in $\beta:\alpha$ from the lake inflow to outflow, suggesting an increasing proportion of recently produced, microbial-like DOM consistent with increases in TDN, $S_{275-295}$, and FI, and decreases in SUVA₂₅₄ and HIX.

The morphometry of Buffalo Pound Lake (~29 km long, 1 km wide, and ~3 m mean depth) may lend itself to processes associated with slow-moving rivers as opposed to rounder lakes. Changes in DOM quantity and quality along the length of Buffalo Pound lake are consistent with the pipe vs. reactor hypothesis for in-river DOM processing and production (Casas-Ruiz et al., 2017) where increasing residence time is positively correlated with the magnitude of DOM change and processing. Under this hypothesis higher residence times are associated with available time for biophysical DOM reactions to occur, and a shift toward DOM of more autochthonous character occurs where autochthonous DOM production may outweigh DOM processing (Casas-Ruiz et al., 2017). Our results contrast those reported for Lake Võrtsjärv—a large, shallow temperate lake in Estonia—where DOC concentrations and SUVA₂₅₄ were higher at the lake inflow than at the outflow (Piiroo et al., 2012). However, Kalinin et al. (2016) found higher DOC and TDN concentrations at the outflow of Bull Trout Lake—a moraine lake in the Sawtooth Mountains of Indiana, USA—compared to its inflow, attributing these differences to autochthonous production in the lake. These contrasting results suggest that DOM in individual lakes may be subject to different processes based on sourcewater DOM quantity and quality, nutrient and solute dynamics, and local climate and hydrology. In Buffalo Pound Lake, records for this four year period during which conditions were relatively

dry indicate the potential for more DOC of an increasingly autochthonous character near the lake outlet.

2.4.3 Implications for drinking water treatment

Buffalo Pound Lake has moderate DOM for a drinking water source, which has contributed to issues associated with disinfectant byproduct (DBP) formation. Fortunately, conditions in recent years have lessened DOM concentrations and prevented exceedance of drinking water regulations; however, treatment remains challenging given the need to balance risks associated with harmful algal blooms (Painter et al., 2022a, 2022b) and DOM impacts on treatability and DBP formation (Williams et al., 2019). Among the constituents measured here, particularly those that may reflect DOM source, composition, and level of processing (e.g., HIX, FI, $\beta:\alpha$), less prechlorination would likely be needed for disinfection but the type of DBP formation may still be problematic. For example, Williams et al. (2019) linked several different federally regulated trihalomethane and haloacetic acids to differences in DOM source and composition in Buffalo Pound Lake. Chlorination decisions would ultimately benefit from ongoing monitoring of DOM quality. The relative stability in DOM quantity and quality we observe here, when Lake Diefenbaker is the dominant water source to the lake and residence time is longer, adds to our understanding of DOM dynamics in a system with variable source waters and will inform effective drinking water treatment.

2.5 Conclusions

The magnitude and rate of change in DOC concentration, and the shifts toward increasing autochthony observed along the length of Buffalo Pound Lake underscore the role of autochthonous DOM production and/or build up in driving DOM cycling and transformation within the lake. In each year of this study we observed consistent increases in DOC concentration coupled with shifts in fluorescence toward more autochthonous DOM signatures along the lake, demonstrating that DOM quality is highly dynamic during the open-water season. Our results improve understanding of DOM cycling and transformation in Buffalo Pound Lake when Lake Diefenbaker is the dominant water source, and show that DOM quality measurements in addition to DOC concentration can provide insights into the source and composition of DOM that are unattainable with DOC concentration alone. While DOC concentrations were moderate

(5–6 m L⁻¹) during our study years and conditions were relatively dry, abnormally wet years—when runoff from the local catchment is an important water source—can raise DOC concentrations in the lake substantially (Chapter 3), and may alter DOM quality within the lake. Further study of this nature across a wider range of hydrological conditions is needed to understand the effects of variable water source on DOM quality in Buffalo Pound Lake. Additional DOM quality measurements in times of deluge would be beneficial to the Buffalo Pound Water Treatment Plant, as it is during these wet years that DOC removal becomes costly and limiting disinfection byproduct formation during water treatment are particularly challenging.

2.6 Acknowledgements

Research funding for this work was provided by NSERC Discovery Grants to Helen M. Baulch and Colin J. Whitfield, and an NSERC Graduate Scholarship – Master’s to Anthony A. P. Baron. We owe thanks to the Saskatchewan Water Security Agency for contributing data and David Vandergucht doing much of the fieldwork. Thanks are also owed to Blair Kardash at the Buffalo Pound Water Treatment Plant, whose discussions throughout and participation in co-design of this project were invaluable to this work. We would also like to thank members of the Bigfoot and SaskWatChe labs for support and feedback throughout each stage of this project.

2.7 Author contributions

A.A.P Baron: Conceptualization, Methodology, Software, Formal Analysis, Data Curation, Writing – Original Draft, Writing – Review & Editing, Visualization; **H.M. Baulch:** Conceptualization, Methodology, Investigation, Data Curation, Writing – Review & Editing, Supervision, Project Administration, Funding Acquisition; **C.J. Whitfield:** Conceptualization, Methodology, Investigation, Data Curation, Writing – Review & Editing, Supervision, Project Administration, Funding Acquisition; **C.J. Williams:** Data Curation, Writing – Review & Editing; **J.M. Davies:** Data Curation, Writing – Review & Editing.

Segue between Chapter 2 and 3

In Chapter 2 an in-depth whole-lake study of dissolved organic matter (DOM) dynamics is presented spanning four open-water seasons. Our principal findings highlight the importance of water source on moderating dissolved organic carbon (DOC) concentration and DOM quality in Buffalo Pound Lake, but are limited to four years (2016–2019) where Lake Diefenbaker is the dominant water source, and catchment runoff is infrequent and episodic with no major water contributions. The Canadian prairie climate is highly variable, and can fluctuate between extreme wet and extreme dry conditions. For example, an extensive drought between 1999–2005 was followed less than a decade later by widespread flooding caused by exceptionally wet conditions. In Chapter 3 we aim to explore long-term (1990–2019) changes in DOC concentration in Buffalo Pound Lake to further understand the role of water source in driving DOC concentration, along with in-lake drivers that include nutrient and solute concentrations. We expect that at the scale of four years (Chapter 2), signals, or forcings, that affect DOM quantity and quality in the lake may be masked. Thus, in Chapter 3 our overarching objective is to further explore the importance of climate (wet vs. dry conditions), variable flow source (Lake Diefenbaker vs. the local catchment), and nutrient and solute dynamics that may be associated with eutrophication or changes in land-use that may impact DOM quantity and quality.

Chapter 3: Extreme variation in DOC and the importance of climate and flow source for Buffalo Pound Lake, Saskatchewan

Anthony A. P. Baron¹, Helen M. Baulch^{1,2}, Ali Nazemi³, Colin j. Whitfield^{1,2}

¹School of Environment and Sustainability, University of Saskatchewan, Saskatoon, Saskatchewan, Canada.

²Global Institute for Water Security, University of Saskatchewan, Saskatoon, Saskatchewan, Canada

³Department of Building, Civil and Environmental Engineering, Concordia University, Montréal, Quebec, Canada

3.0 Abstract

Dissolved organic carbon (DOC) is an important water quality characteristic of freshwater ecosystems. Elevated DOC concentrations are a major concern for drinking water treatment plants that draw from lakes and reservoirs owing to effects on disinfection byproduct (DBP) formation, risks of bacterial regrowth in water distribution systems, and increasing treatment costs. Long-term trends in DOC have been observed across many regions of the Northern Hemisphere, yet there has been little agreement over the drivers of these trends. Here, we reveal the roles of changing source water and in-lake water chemistry as drivers of DOC fluctuation in Buffalo Pound Lake, Canada, a shallow eutrophic drinking water reservoir in the Great Plains of North America. Using 30 years (1990 to 2019) of DOC, nutrients, sulfate (SO_4^{2-}), and streamflow data, we studied the long-term change in DOC under periods of influence from both landscape runoff and managed flow from a large upstream mesotrophic reservoir, Lake Diefenbaker. The period encompassed both extreme wet and extreme dry conditions. Using wavelet coherence analyses we identified Lake Diefenbaker flow as significantly coherent with DOC concentration across the 30-year record. Additionally, SO_4^{2-} , total phosphorus, ammonium, and chlorophyll *a* concentrations were all coherent with DOC. These parameters were included as predictors in a generalized additive model (GAM), which aimed to describe fluctuations in DOC concentration. The GAM accounted for 56% of the deviance in DOC from 1990 to 2019, suggesting that water source and in-lake nutrient and solute chemistry are effective predictors of DOC concentration in Buffalo Pound Lake. Though we expected flows from the local catchment (natural prairie runoff conditions) to be of greater

importance statistically, we suspect that the ephemeral and episodic nature of this water source partially masked its effects on DOC. We suggest that climatic change and changes in water and catchment management, including flows and agricultural land-use, may drive source water quality in this already water-scarce region. Our results will inform the design of an ongoing \$325M upgraded water treatment plant aiming to address the complex source water quality challenges of this shallow lake, which requires consideration of past changes in water quality, and likely future change.

3.1 Introduction

Numerous studies over the last four decades have assessed long-term trends in dissolved organic carbon (DOC) in freshwater lakes and reservoirs in the Northern Hemisphere, primarily in forested regions. Several studies report increasing DOC concentrations across regions including eastern Canada (Couture et al., 2011; Hudson et al., 2003), the northeastern United States (Rodríguez-Cardona et al., 2022), northern Europe (Futter et al., 2014; Pärn and Mander, 2012), central Europe (Hruška et al., 2009), and the United Kingdom (Evans et al., 2005). Others report no significant trends in DOC concentration (Dillon and Molot, 2005; Jane et al., 2017) or decreasing trends over time (Rodríguez-Murillo et al., 2015). These different findings from different study systems have sparked much debate over the factors that govern DOC concentrations across time and in different regions, and have led to a search for common drivers of these changes (e.g., Pagano et al., 2014; Temnerud et al., 2014; Winterdahl et al., 2014). Several common hypotheses have emerged that aim to unravel the drivers of observed patterns in DOC concentration in freshwater systems, with a substantial focus on declining anthropogenic sulfur dioxide emissions and consequent declines in deposition (Monteith et al., 2007). In regions not heavily impacted by acidification, or where sulfate (SO_4^{2-}) deposition has shown minimal effect on DOC, trends in DOC have been linked to climatic and hydrological factors such as changes in temperature, precipitation, or runoff (Hongve et al., 2004; Weyhenmeyer and Karlsson, 2009), cycles in sea salt (i.e., chloride) deposition (Evans et al., 2006), atmospheric nitrogen (N) deposition (Evans et al., 2008), land management and land-use (Yallop and Clutterbuck, 2009), and increased atmospheric carbon dioxide concentrations (Freeman et al., 2004).

The sum of all DOC exports to a lake is highly correlated with precipitation and annual runoff, hence is regulated by local hydrology and climate, as well as landscape features which influence DOC production and transport (Pace and Cole, 2002; Porcal et al., 2009). At the landscape scale, allochthonous DOC leached from terrestrial soils is transported to streams and lakes, and the amount of DOC leached from soils is regulated by soil moisture and flow paths from soil to stream or lake (Clark et al., 2010; Sobek et al., 2007). Landscape features that influence DOC concentration in lakes include drainage ratio (catchment:lake area), hydrological connectivity of water sources such as wetlands and streams (Laudon et al., 2011; Schiff et al., 1997), land-use (Williams et al., 2010; Wilson and Xenopoulos, 2009), wetland area (Dillon and Molot, 1997), proportion of the catchment that is open water (Kortelainen, 1993), and watershed slope and topography (Sobek et al., 2007; Xenopoulos et al., 2003).

The Canadian prairie region, a vast area of 1.8×10^6 km², is characterized by poorly developed stream networks with abundant pothole ponds (wetlands) that formed during the recession of the last ice age. It is also characterized by relatively flat topography, and extreme climatic and hydrological variability that produces periods of deluge and severe drought (Pham et al., 2009; Pomeroy et al., 2007; Vogt et al., 2018). Widespread flooding across the prairies in 2011 (Brimelow et al., 2014) and a multi-year drought from 1999–2005 (Hanesiak et al., 2011) are two recent examples of these phenomena. Prairie soils contain high concentrations of DOC, SO₄²⁻, phosphorus (P), and nitrogen (N), and concentrations of these nutrients and solutes are reflected in pothole ponds (Arts et al., 2000; Labaugh et al., 1987; Waiser, 2006). Dissolved organic matter (DOM) in these systems is often extremely high owing to evapoconcentration, and runoff from prairie soils, ponds, and agricultural croplands is often rich in DOC, nutrients, and solutes (Brunet and Westbrook, 2012; Liu et al., 2021; Nachshon et al., 2014). These conditions make prairie lakes and reservoirs especially prone to eutrophication and frequent cyanobacterial blooms. Widespread agriculture and wetland drainage in the prairies, along with the highly managed nature of surface waters through dams and impoundments, further work to impact water quality in receiving lakes (Maheaux et al., 2016; Painter et al., 2022a). Extremes in climate, including drought, have had comparable effects in European watersheds (Lepistö et al., 2014; Pärn and Mander, 2012; Worrall et al., 2006); drought periods are typically characterized by reduced allochthonous DOC loads and increased autochthonous DOC contributions, with large influxes of allochthonous DOC upon a return to wet conditions. Periods of elevated runoff

are known to export more DOC from the catchment, and may increase DOC concentrations in receiving rivers and lakes if DOC inputs outweigh dilution effects (Clark et al., 2010).

Although endorheic saline prairie lakes are well known for their often extremely high DOC concentration owing to prolonged evapoconcentration (Arts et al. 2000; Osburn et al. 2011; Waiser and Robarts 2000), DOC concentrations in freshwater lakes of the region have received less attention, and few, if any, long time series of DOC concentration exist. Buffalo Pound Lake is a key water source in Saskatchewan, Canada providing drinking water for a quarter of the province. Study of the long-term change in DOC concentration is of particular interest to the Buffalo Pound Water Treatment Plant (BPWTP) to maintain safe drinking water and limit the production of disinfection byproducts like trihalomethanes and haloacetic acids. DOC is also a critical limnological factor within lakes and reservoirs due to its role in regulating the physical, chemical, and biological structure and function of these systems. The chemical and physical properties of DOC dictate the amount and spectral properties of light available for aquatic organisms and can affect lake thermal regime and mixing; influence aquatic ecosystem metabolism and nutrient cycling; and impact the mobility, reactivity, and bioavailability of metals and organic contaminants (Prairie, 2008; Wetzel, 2001a).

This study investigates long-term variation in DOC concentration in Buffalo Pound Lake over a 30-year period (1990–2019) encompassing both wet conditions and severe drought, with varied water flows and management. Our objectives were to understand relationships between DOC, flows from upstream Lake Diefenbaker and the local catchment, and a suite of in-lake water chemistry parameters. Wavelet coherence and phase analyses were used to identify temporally-dependent patterns between time series that are typically masked by traditional correlation methods. These relationships were further investigated with generalized additive modeling (GAM) to understand the predictor-response relationship between DOC concentration, flows, and water chemistry over the 30-year period. We hypothesized that at longer timescales flows into Buffalo Pound Lake would be important determinants of patterns in DOC concentration, while changes in lake water chemistry would impact DOC at shorter timescales.

3.2 Methods

3.2.1 Study site

Buffalo Pound Lake is a shallow eutrophic multipurpose reservoir located near the headwaters of the Qu'Appelle River drainage system in southern Saskatchewan, Canada

(50.65127° N, 105.508225° W) (Figure 3.1, Table 3.1). Climate in this region is subhumid continental with very cold, long winters and short, warm summers. Mean annual precipitation is 320 mm (McGowan et al., 2005) and average annual temperature is ~3°C (Haig et al., 2021). Buffalo Pound Lake is the drinking water source for ~25% of the population in Saskatchewan, servicing the cities of Regina (population 249,000) and Moose Jaw (population 34,000). The lake is also the site of a Saskatchewan provincial park and a popular recreation spot for activities that include fishing, swimming, and camping. It is a natural lake that was impounded to raise water levels beginning in 1939 by damming the outflow of the lake to the Moose Jaw River. The lake is long and narrow (~29 km by 1 km) with an average depth of 3 m (max depth 5.6 m) and storage capacity of $9 \times 10^7 \text{ m}^3$ (BPWTP, 2020). Its shallow depth and exposure to regular wind-induced mixing result in a polymictic system that only periodically establishes thermal stratification (Finlay et al., 2019). Buffalo Pound Lake drains a 3310 km² agricultural catchment with nutrient-rich soils that favour high nutrient influx and eutrophic conditions (Finlay et al., 2019; Hammer, 1971). This drainage area represents the gross drainage area of the Buffalo Pound Lake—the area that might be expected to entirely contribute runoff under extremely wet conditions (Godwin and Martin, 1975). In contrast, Buffalo Pound Lake’s effective drainage area, defined as that portion of the watershed that contributes flow in 1:2 runoff years (Godwin and Martin, 1975), is just 38% of the gross drainage area. The dominant water source to the lake is from controlled releases out of the Qu’Appelle River Dam on Lake Diefenbaker reservoir. Flows from Lake Diefenbaker originate outside of the natural catchment boundary (BPWTP, 2020). Between 2015–2020, mean annual water release from Lake Diefenbaker ranged from 1.8–4.8 m³ s⁻¹ (BPWTP, 2021).

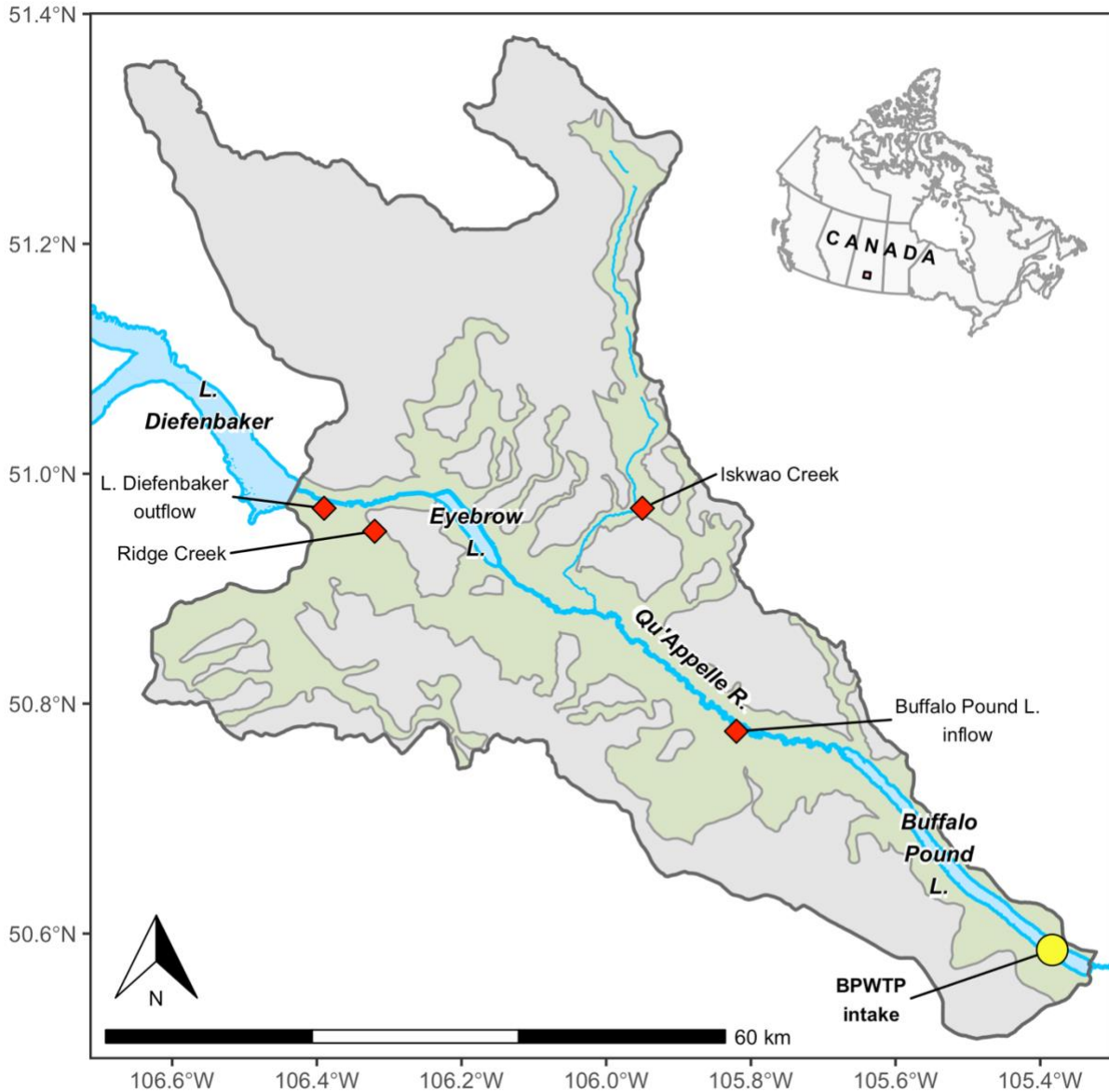


Figure 3.1. Map of Buffalo Pound Lake, Saskatchewan, Canada, highlighting its gross (grey) and effective (green) drainage areas, including upstream Lake Diefenbaker and the Qu'Appelle River. The middle of Buffalo Pound Lake is located at 50.65127° N, 105.508225° W. Red diamonds denote Water Survey of Canada (WSC) streamflow gauging stations in the Buffalo Pound Lake watershed with complete or reconstructed records over the study period (see Section 3.2.3 and Table B.1). The inset map of Canada was plotted using the R package mapcan (McCormack and Erlich, 2019). Gross and effective drainage area shapefiles were obtained from the Prairie Farm Rehabilitation Administration (PFRA). Lake and river geospatial data were retrieved through the Government of Canada's Open Government License (Statistics Canada, 2006, 2011).

3.2.2 Data

3.2.2.1 Water chemistry

The BPWTP laboratory is accredited to the ISO/IEC 17025 standard and adapts their analysis methods using Standard Methods for the Examination of Water and Wastewater (APHA, 2012). Water samples collected between 1990 and 2019 were analyzed on weekly, semi-monthly, or monthly bases (Table 3.1). Described here are the current methods the BPWTP uses to analyze water chemistry. The accredited BPWTP laboratory did change instruments over the long history of this data set; however, new instruments were cross validated and subjected to testing requirements associated with accreditation (B. Kardash pers. comm.). Prior to 2015 DOC samples were acidified prior to analysis to remove inorganic carbon, then analyzed via nondispersive infrared detector (injection with sodium persulfate and treatment with UV light to convert to carbon dioxide) on a Tekmar/Dohrmann Phoenix 8000 Carbon Analyzer. Since 2015 DOC concentrations have been analyzed on a General Electric (GE) M5310M Laboratory total organic carbon (TOC) Analyzer with GE-patented Sievers Selective Membrane Conductometric design that uses a gas-permeable membrane that separates CO₂ from the DOC sample. The membrane separates the (dissolved) sample side (total carbon, TC) of the Analyzer from the inorganic carbon (IC) side. The IC side is a closed loop consisting of two conductivity cells (one for the TC stream and one for the IC stream), a deionized water pump and water reservoir, and an ion exchange resin bed. The CO₂ from the TC and IC sample streams are measured by the respective conductivity cells, and used to calculate concentration of TC (i.e., DOC) and IC (i.e., dissolved inorganic carbon, DIC). Sulfate (SO₄²⁻) and nitrate (NO₃⁻) concentrations (as S and N respectively) are determined via ion chromatography using a Dionex ICS-1100 Ion Chromatograph. Ammonium (NH₄⁺ as N) concentrations are determined colorimetrically by Nessler's reagent addition after samples are buffered in boric acid solution and distilled. Chlorophyll *a* pigments are extracted with acetone and concentrations are measured via spectrophotometry, but are not corrected for the presence of pheophytin. Samples for total phosphorus (as P) analysis are digested with strong acid and persulfate, then analyzed via the molybdenum blue method at 690 nm on a spectrophotometer. Soluble reactive phosphorus (as P) concentrations are analyzed using the ammonium molybdate method then measured at 690 nm on a spectrophotometer.

The variable frequency of water chemistry analyses permitted using month-averaged measurements ($N = 360$) across the 30-year time series with few missing data points (0.28–3.6%) across the seven parameters presented in Table 3.1. Statistical analyses (described below) required a complete record, necessitating (very limited) imputation. Because many water chemistry parameters were highly variable over decadal scales, replacing missing values with (seasonal) mean or median consistently produced values outside the reasonable range for a given month and year based on visual inspection. To overcome this the k -nearest neighbour regression approach (Altman, 1992; Fix and Hodges, 1951) was used, replacing missing values with the mean of $k = 1$ nearest neighbours.

3.2.2.2 *Streamflow measurements*

Streamflow time series collected by the Saskatchewan Water Security Agency (WSA) from 1972–2019 at four hydrometric gauging stations upstream of Buffalo Pound Lake (Figure 3.1, Table B.1) were used. Lake Diefenbaker outflow (Q_{LD}) and Buffalo Pound Lake inflow (Q_{BP}) comprise streamflow measurements along the Qu’Appelle River, and Ridge Creek and Iskwao Creek are tributaries sourced from the local catchment (Q_{LD}) that flow into the Qu’Appelle River between Lake Diefenbaker and Buffalo Pound Lake (see section 3.2.3).

Table 3.1. Analytical methods (APHA, 2012) used at the BPWTP ISO/IEC 17025 accredited laboratory, and sampling frequency and duration. Analytical instruments reported here correspond to current methods used by the BPWTP. All instrument changes between 1990 and 2019 were cross validated and subjected to testing requirements associated with accreditation (B. Kardash pers. comm.). MM refers to the plant’s Methods Manual procedures, with these methods based on APHA (2012) methods.

Analyte	Unit	Laboratory method or APHA method	Method summary (current instrumentation noted)	Sampling frequency
DOC	mg C L ⁻¹	MM #20, v. 2.1; APHA Method 5310A and C	1990–2014: organic carbon oxidized to CO ₂ is measured using a Tekmar/Dohrmann Phoenix 8000 Carbon Analyzer; 2015–2019: total (dissolved) organic carbon and DIC are separated into conductivity cells by gas-permeable membrane to separate CO ₂ , then measured conductivity in each cell is used to calculate DOC and DIC	Weekly (1990–2019)
SO ₄ ²⁻	mg S L ⁻¹	MM #3, v.2.7; modified from APHA Method 4110B	Ion chromatography using a Dionex ICS-1100 Ion Chromatograph	Weekly (1990–2002); semi-monthly to monthly (2003–2019)
TP ^(a)	µg P L ⁻¹	MM #202, v. 3.1; APHA Methods 4500-P B(5) and D	Digestion with strong acid and persulfate [APHA Method 4500-P B(5)] followed by colorimetric analysis using molybdenum blue method at 690 nm [APHA Method 4500-P D]	Weekly (1990–2002); semi-monthly to monthly (2003–2019)
SRP ^(a)	µg P L ⁻¹	MM #203, v. 3.1; APHA Method 4500-P C	Soluble phosphorus ions complexed with ammonium molybdate to form ammonium-phosphomolybdate and reduced to molybdenum blue with stannous chloride, then absorbance measured at 690 nm	Weekly (1990–2002); monthly (2003–2019)
Chl α ^(a)	µg L ⁻¹	MM #206, v. 2.1; APHA Method 10,200-H 1&2	Extraction of filtrate using aqueous acetone, and analysis via spectrophotometer as per APHA Method 10,200-H with the modification that results are not corrected for pheophytin α or pheophorbide α.	Weekly (1990–2002); monthly (2003–2012); weekly to semi-monthly (2012–2019)
NO ₃ ⁻ -N ^(a)	mg N L ⁻¹	MM #3, v. 2.3; APHA Method 4110-A, B, C	Ion chromatography using a Dionex ICS-1100 Ion Chromatograph	Weekly (1990–2002); semi-monthly to monthly (2003–2019)
NH ₄ ⁺ -N ^(a)	mg N L ⁻¹	MM #201, v. 2.2 APHA Method 4500-P C	Water sample is buffered at pH 9.5 with a borate buffer and distilled into a boric acid solution. Ammonia in the distillate is then determined colorimetrically by addition of Nessler’s reagent	Weekly (1990–2002); semi-monthly to monthly (2003–2019)

(a) Method summary from Cavaliere and Baulch (2020)

3.2.3 Hydrological calculations

Inflows and outflows at Buffalo Pound Lake are managed to maintain lake levels within an established operating range that has some seasonal variability. During the summer months, the operating range is 30 cm; however, due to the importance of the water supply and recreational interests, the lake is typically managed within 10 cm nearer the upper end of the operating range. Levels are typically reduced by about 15–20 cm over the winter months. Water levels in the lake are controlled predominately by water releases from Lake Diefenbaker; however, the lake regularly experiences a transient period of higher inflows from the local catchment during spring snowmelt. Water quality characteristics in flows from the local catchment, including DOC concentration and DOM quality, are distinct from Lake Diefenbaker. To understand water source dynamics in the Buffalo Pound Lake watershed we compared flows from Lake Diefenbaker (Q_{LD}), the local catchment (Q_{LC} , see below), and the inflow to Buffalo Pound Lake (Q_{BP} ; Figure 3.1). Complete streamflow records for Lake Diefenbaker and Ridge Creek were available from 1972–2019. Iskwao Creek was gauged from 1972–2006 during the warm season (April to November) and Buffalo Pound Lake was gauged from 1968–1994 and 2015–2019.

Iskwao Creek cold season flows (i.e., December to March) and flows from 2007–2019 (ungauged period) were estimated using non-linear regression based on a training data set of Ridge Creek flows from 1972–1992 (Nazemi, unpublished data):

$$Q_{IC} = \begin{cases} 0.3112Q_{RC}^{0.4537} & \text{if cold season} \\ 0.4957Q_{RC} + 0.1185 & \text{if warm season and } Q_{RC} > 0 \\ 0 & \text{if warm season and } Q_{RC} = 0 \end{cases} \quad (1)$$

where Q_{RC} is Ridge Creek flow ($\text{m}^3 \text{s}^{-1}$), Q_{IC} is Iskwao Creek flow ($\text{m}^3 \text{s}^{-1}$), and warm season is April to November. Flow from the local catchment (Q_{LC}) was then estimated by scaling up to the effective area of Buffalo Pound Lake to estimate inflow from similar ungauged streams that contribute water to the lake during high precipitation events and snowmelt according to:

$$Q_{LC} = \frac{(Q_{RC} + Q_{IC})}{(A_{RC} + A_{IC})} \times A_{BP} \quad (2)$$

where Q_{LC} is local catchment flow ($\text{m}^3 \text{s}^{-1}$) and effective areas (A , m^2 in equation) for Buffalo Pound Lake, Ridge Creek, and Iskwao Creek are 1282, 233, and 113 km^2 respectively.

Much of the Qu'Appelle River between Lake Diefenbaker and Buffalo Pound Lake is ungauged, including Eyebrow Lake where flow from Lake Diefenbaker is periodically retained (e.g., following a drop in lake water levels). Flow for the ungauged portion of the catchment (Q_U , in $\text{m}^3 \text{s}^{-1}$), was also estimated using non-linear regression based on Q_{RC} (Nazemi, unpublished data):

$$Q_U = \begin{cases} 0.01292Q_{RC}^3 - 0.303Q_{RC}^2 + 1.249Q_{RC} - 0.0956 & \text{if cold season} \\ -0.05958Q_{RC}^2 + 2.77Q_{RC} - 0.1463 & \text{if warm season} \end{cases} \quad (3)$$

Estimated Q_U includes both positive and negative values. Negative values are related to episodes where the ungauged instream part, including Eyebrow Lake, retains part of the water coming from upstream sources (i.e., Q_{LD} as well as Q_{LC}). The equations for estimating missing Q_{IC} and Q_U were selected based on Bayesian Information Criterion among a pool of 420 forms of linear and non-linear regression forms. Buffalo Pound Lake inflow (Q_{BP} , in $\text{m}^3 \text{s}^{-1}$) was gauged from 1990 to mid-1995. The Q_{BP} ungauged period from mid-1995–2015 was estimated as:

$$Q_{BP} = Q_{LD} + Q_{RC} + Q_{IC} + Q_U \quad (4)$$

During the training period (1972–1992) the coefficient of determination (R^2) for estimating Q_{BP} was 0.87.

3.2.4 Statistical analyses

There were two major goals of our statistical analysis. First, we aimed to understand frequency-dependent relationships between DOC concentration and a suite of environmental predictors that include upstream flows (Q_{LD} , Q_{BP} , Q_{LC}) and in-lake water chemistry (SO_4^{2-} , TP, SRP, Chl a , NO_3^- , NH_4^+) using wavelet coherence analysis (Grinsted et al., 2004; Sheppard et al., 2016, 2017; Walter et al., 2021). Wavelet-based methods can be used to measure synchrony and coherence between environmental and biological variables, and investigate relationships that are not readily detected by conventional correlation methods (Reuman et al., 2021). Specifically,

wavelet coherence analysis can reveal the direction (analogous to positive or negative correlation) and phase (positive or negative time-lag) between two variables at different timescales. Predictors identified as significantly coherent with DOC ($\alpha = 0.05$) by wavelet coherence analysis were subsequently used to investigate our second objective, where we used generalized additive modeling (GAM) to understand predictor–response relationships between DOC concentration, flows, and in-lake water chemistry.

All statistical analyses were carried out in R version 4.1.3 (R Core Team, 2022). Wavelet analyses were done using the Wavelet Approaches to Synchrony (*wsyn*) R package (version 1.0.4; Reuman et al., 2021). Plotting for wavelet analyses was done with the R packages *base* (R Core Team, 2022) and *spatstat.core* (version 2.4.2; Baddeley et al., 2015). Generalized additive models were fit using the R package *mgcv* (version 1.8.40; Wood, 2017), and graphics were plotted with *ggplot2* (version 3.3.6, Wickham, 2016), *gratia* (version 0.7.3; Simpson, 2021), and *patchwork* (version 1.1.1; Pedersen, 2020). Further details on wavelet analyses and GAMs are provided below.

3.2.4.1 Wavelet coherence and phase

Wavelet-based methods can be used to measure synchrony and coherence between environmental and biological variables, and investigate relationships that are not readily detected by conventional correlation methods (Reuman et al., 2021). We applied the continuous Morlet wavelet transform $W_{\sigma}(t)$ (Addison, 2002) to each time series following approaches outlined by Sheppard et al. (2016, 2017, 2019). The wavelet transform $W_{\sigma}(t)$ uses small localized wavelike functions to transform time series signals into representations which present the signal information in a more useful form (Addison, 2002). For this study, scaling was applied such that one wavelet oscillation was equal to two months ($\sigma = 2$) because a two-month period is the highest-frequency fluctuation that can be identified in monthly time series. Wavelets were generated across a range of timescales, from two to 120 months (10 years). Wavelet transforms require scalloping to remove poorly estimated values at the tails of time series (Addison, 2002), depicted as the ‘rocket ship nose cone’ in Figure B.1. For a 30-year time series of monthly observations, scalloping limits wavelet periods to a maximum of ~120 months, or approximately one-third of the length of the full time series.

Coherence between two variables is a measure of the strength of association between those variables in a timescale-specific way that is not confounded by lagged or phase-shifted

associations (Reuman et al., 2021). In other words, wavelet coherence quantifies the degree to which two time series have correlated magnitudes of oscillation and consistent phase differences through time, as a function of timescale (Walter et al. 2021), with magnitude ranging from 0 (no relationship) to 1 (perfect coherence). The ‘wavelet mean field’ normalization method (Sheppard et al. 2016) was used to measure wavelet coherence because its coherence magnitude increases both with increasing synchrony between time series and when oscillations in time series at time t and timescale σ have similar phase (direction and time-lag). This method also permits testing for significant coherence across multiple timescales. Two timescale bands were tested for significance. Short timescales (≤ 18 months) were selected based on Buffalo Pound Lake intra-annual/seasonal dynamics and potential lagged relationships between DOC and environmental predictors. Long timescales (> 18 months—i.e., up to 120 months) were selected based on multi-year to decadal patterns observed in DOC concentration and timescales where DOC had high $|W_\sigma(t)|$ (e.g., warm regions in Figure B.1).

Phase (direction and time-lag) was also investigated for environmental predictors that were significantly coherent with DOC concentration. Coherent variables may be in-phase (positively correlated) or anti-phase (negatively correlated), and are typically (positively or negatively) time-lagged as it is unlikely that two environmental variables will be perfectly in-phase or anti-phase (Figure B.2). To understand phase difference relationships between significantly coherent DOC–predictor pairs we computed the average phase ϕ across the corresponding timescale band (Walter et al., 2021). Because phase ϕ is an angular measurement, sine- or cosine-transforming this value provides information about how close the relationship is to being in-phase [$\cos(\phi)$], and whether the time-lagged relationship between time series tends to be positive or negative [$\sin(\phi)$] (Walter et al. 2021). Cosine transformation assigns in-phase relationships ($\phi = 0$) to 1, anti-phase relationships ($\phi = \pm \pi$) to -1 , and quarter-phase (i.e., time-lagged) relationships ($\phi = \pm \pi/2$) to 0. Sine transformation assigns both in-phase ($\phi = 0$) and anti-phase ($\phi = \pm \pi$) relationships to a value of 0 because they exhibit no time lag. When a change in DOC leads ahead of a predictor variable ($\phi = -\pi/2$) the relationship is lagged negative, whereas when a change in DOC lags behind a change in a predictor ($\phi = \pi/2$) the relationship is lagged positive.

To test for significant coherence all time series were transformed using standard optimal Box-Cox normalization prior to wavelet transformation (Sakia, 1992). Box-Cox transformation improves normality and ensures variability in individual time series is not dominated by extreme values (Sheppard et al., 2019). Significance testing for wavelet methods relies on Fourier surrogate techniques where time series are normally distributed (Schreiber and Schmitz, 2000), so fair comparisons and statements of significance can only be made if underlying data are normally distributed (Sheppard et al., 2019). Box-Cox transformation removes the linear trend for each time series and re-scales the variance to 1 producing transformed times series with mean of 0 and approximately normal distributions. Fourier transform based methods for generating surrogate coherence data sets can be used to test for statistically significant coherence relationships between wavelet-transformed variables (Sheppard et al., 2017). These Fourier transformed data retain the original characteristics (e.g., temporal autocorrelation) of the time series and test whether coherence values are likely to occur under the null hypothesis that no actual coherence and phase relationships exist between variables. For each DOC–predictor time series pair 10,000 surrogate randomizations were run to facilitate more accurate significance testing results and reduce variability on repeat runs (Reuman et al., 2021; Sheppard et al., 2017).

3.2.4.2 Generalized additive models

Predictors identified as significant by coherence analysis were used to model the DOC time series using a GAM. The GAM approach was chosen because it can account for nonlinearity in trends whereas other methods are limited to identifying increasing or decreasing linear (monotonic) trends (e.g., (seasonal) Mann-Kendall test) or require *a priori* selection of the functional form of trends in time series or selection from less flexible polynomial models (e.g., parametric linear or generalized linear models) (Finlay et al., 2019; Simpson, 2018). Conversely, GAMs estimate the functional form from the data allowing nonlinear relationships to be fit using splines. Splines can also reduce bias issues and over-fitting at the tails of data sets, which is a common problem with polynomial models (Finlay et al., 2019). In practice a GAM is a generalized linear model with a linear predictor and a series of smooth functions of covariates, taking the general form:

$$y_i = \beta_0 + f_1(x_{i1}) + f_2(x_{i2}) + \dots + f_n(x_{in}) + \epsilon_i \quad (5)$$

where y_i is the response variable; β_0 is the model intercept; x_{i1} , x_{i2} , and x_{in} are covariates; f_1 , f_2 , and f_n are non-parametric smoothing functions; and ϵ_i are independent $N(0, \sigma^2)$ random errors (Wood, 2017). All predictors (i.e., $f(x_i)$) were estimated using thin plate regression splines and penalized using restricted maximum likelihood-based smoothness selection procedures (Wood, 2011). Initial basis dimension (k) of each smooth function was checked following the procedure described in Pya and Wood (2016)—if the initial k was deemed too low (i.e., if k -index < 1 and estimated degrees of freedom was close to k'), a larger basis size was used and the model refitted. The Tweedie distribution (Tweedie, 1984) was used as the model conditional distribution because histograms of most of the environmental predictors showed deviation from normality and resembled some form of the gamma distribution, which is also included in the Tweedie family of distributions and identified when the Tweedie power parameter, p , is 2. In our model p was 1.99, indicating the gamma distribution was a good fit; however, selecting the Tweedie distribution *a priori* avoided the potential of erroneously choosing gamma as the conditional distribution. Model fit was assessed through qualitative inspection of quantile–quantile residuals, residuals vs. linear predictor, histogram of residuals, and observed vs. fitted values plots. Uncertainty in the estimated DOC trend was simulated using 10,000 trends from the posterior distribution of the fitted values. The simulated trends are consistent with the estimated trend but include the uncertainty in the estimates of the spline coefficients (Finlay et al., 2019). The posterior simulation involves drawing 10,000 samples from the multivariate normal distribution then deriving the difference between peak and minimum DOC for each sample (trend). The upper and lower 2.5% probability quantiles of the distribution of the 10,000 differences in trend for each year form a 95% credible confidence interval on the difference estimated from the fitted trend (Finlay et al., 2019).

3.3 Results

3.3.1 Time series of DOC and environmental predictors

Flow sources varied over the 30-year period with no distinct long-term or multi-year patterns (Figure 3.3a–c). Buffalo Pound Lake inflows (Q_{BP}) and flows from Lake Diefenbaker (Q_{LD}) each showed seasonal patterns, peaking around late spring to early summer and reduced during winter months when water demands are lower and the lake is covered with ice. Local

catchment flows (Q_{LC}) typically peaked in late spring to early summer and did not contribute water to Buffalo Pound Lake in winter months or dry years. Streamflow at Q_{LD} averaged 3.2 ± 2.6 (range: 0–12.4) $\text{m}^3 \text{s}^{-1}$, while averages were 3.6 ± 2.8 (range: 0.1–18.9) $\text{m}^3 \text{s}^{-1}$ at Q_{BP} . Catchment flows (Q_{LC}) were much lower, averaging 0.3 ± 0.8 (range: 0–8.3) $\text{m}^3 \text{s}^{-1}$. In years where Q_{LC} was low or absent, particularly in the late 1990s and early 2000s, Q_{BP} generally followed patterns of water release from Lake Diefenbaker. In most years, fluctuations in Q_{BP} were comparable to those of Q_{LD} , owing in large part to water releases from a dam above Q_{LD} being the major water source to Buffalo Pound Lake. Several years in the local catchment record showed evidence of wetter-than-normal conditions (e.g., 1997, 2011, 2014) with short-term episodes of considerable discharge. These episodes correspond to peaks in Q_{BP} and were generally associated with low Q_{LD} flows.

Dissolved organic carbon concentrations fluctuated considerably over the 30-year observation period, ranging 3.3–12.4 mg L^{-1} (Figure 3.2). Mean (\pm standard deviation) DOC concentration was $6.8 \pm 1.8 \text{ mg L}^{-1}$. Several notable fluctuations occurred over multi-year periods. For example, after sustained high concentrations from 1997–2000 (mean 9.5 mg L^{-1}), DOC fell to 4.4 mg L^{-1} by 2004 and remained near- or below-average until the mid-2010s. Between 1990 and 2000, there was a gradual increase in DOC concentration where, despite shorter-term increases and decreases, DOC concentrations increased from 3.9 mg L^{-1} in 1990 to 9.3 mg L^{-1} in 2000. Other notable changes occurred at shorter timescales: in 1991 DOC concentrations were $\leq 5.0 \text{ mg L}^{-1}$ from January to July, spiked to 10.5 mg L^{-1} in August, and fell to 5.5 mg L^{-1} by December. The mid-2010s also saw a sharp increase in DOC concentration followed by below-average levels within a 4-year span.

Water chemistry was also highly variable over the 30-year period (Figure 3.3g–i), with evidence of dramatic changes in the chemistry of Buffalo Pound Lake over time. For example, SO_4^{2-} concentrations ranged 56.8–340 mg L^{-1} , and were relatively stable from 1990–2009 before rapidly rising up to 250 mg L^{-1} between 2011 and 2017 (Figure 3.3d). By the end of 2019, SO_4^{2-} returned to levels observed during 1990–2010. Nitrate also showed two distinct patterns. After averaging $0.20 \pm 0.28 \text{ mg L}^{-1}$ from 1990–1999 and peaking at 1.5 mg L^{-1} in 1997, NO_3^- concentrations were nearly an order of magnitude lower from 2000–2019, averaging $0.05 \pm 0.08 \text{ mg L}^{-1}$ (Figure 3.3h). Total phosphorus, SRP, Chl *a*, and NH_4^+ concentrations rose rapidly in 1991 (Figure 3.3e–g, i), concomitant with the rise in DOC in that year. After 1991, chemical

concentrations were average or below average, followed by increases in concentrations into the early 2000s. The mid 2010s also showed elevated levels of SO_4^{2-} , TP, Chl *a*, and NH_4^+ concurrent with elevated DOC concentrations during this time.

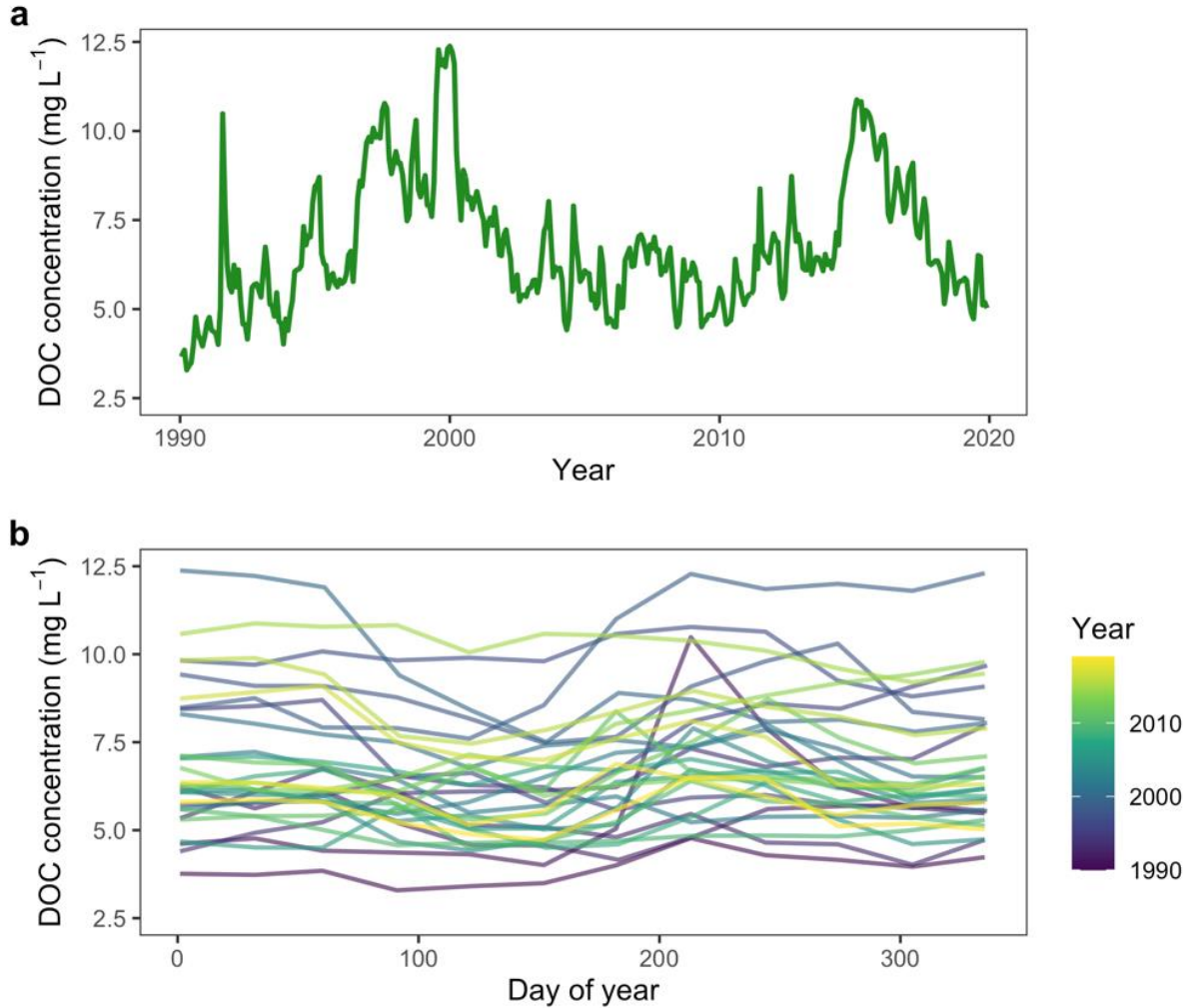


Figure 3.2. Monthly Buffalo Pound Lake DOC concentrations from 1990–2019 by (a) year, showing the pattern in DOC concentration over the full time series, and (b) day of year, showing the intraannual variation in DOC concentration.

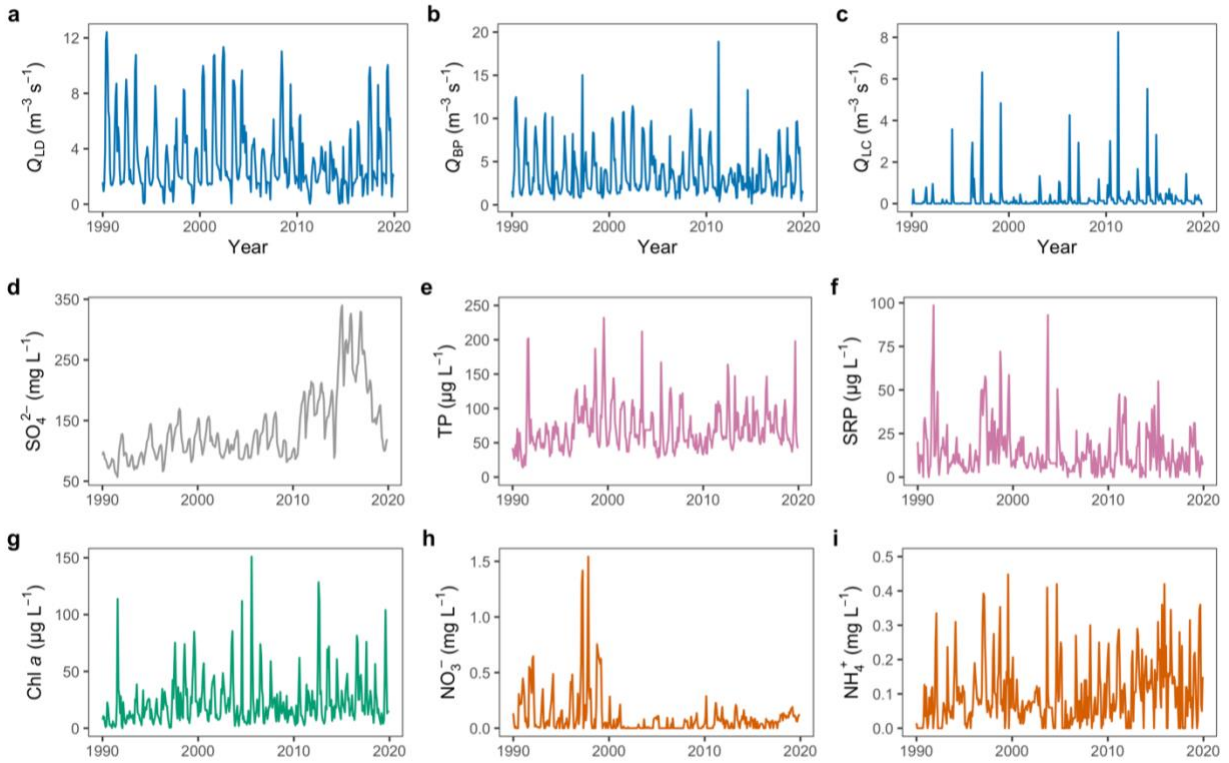


Figure 3.3. (a–i) Monthly time series of flows from Q_{LD} , Q_{BP} , Q_{LC} , and SO_4^{2-} , TP, SRP, Chl *a*, NO_3^- , and NH_4^+ , concentrations from 1990–2019.

3.3.2 Wavelet coherence and phase

Coherences between DOC and nine environmental predictors at short (≤ 18 -month) and long (> 18 -month) timescales were highly variable, ranging from 0.05–0.74 (median of 0.31) (Figure 3.4, Table B.3). At short timescales coherence magnitudes ranged 0.08–0.50 (median of 0.15) and at long timescales 0.05–0.74 (median of 0.54). Four DOC–predictor pairs were significant at short timescales ($\alpha = 0.05$ significance level): SO_4^{2-} , TP, Chl *a*, and NH_4^+ . At long timescales SO_4^{2-} , TP and Q_{LD} were significantly coherent with DOC ($\alpha = 0.05$ significance level). We observed higher coherence magnitudes at long timescales compared to short timescales (Table B.3), potential evidence of a bias in wavelet coherence where greater coherence magnitudes tend to be returned at long timescales (Walter et al., 2021).

Phase relationships spanned the range of possible values (0 to $\pm \pi$) (Figure B.4). For DOC–predictor pairs with significant coherence, most relationships were approximately in-phase ($-\pi/4 < \phi < \pi/4$) at both short and long timescales (Figure 3.5, Table 3.2). At short timescales DOC was strongly in-phase with TP, Chl *a*, and NH_4^+ ($0 < \phi < \pi/4$), and tended to lag behind fluctuations in SO_4^{2-} ($-\pi/2 < \phi < -\pi/4$). Interestingly, the phase relationship between DOC and SO_4^{2-} shifted to strongly in-phase ($-\pi/4 < \phi < 0$) at long timescales, and TP remained strongly in-phase with DOC ($0 < \phi < \pi/4$). Unlike SO_4^{2-} and TP, fluctuations in DOC tended to lag behind fluctuations in Q_{LD} ($-\pi/2 < \phi < -\pi/4$).

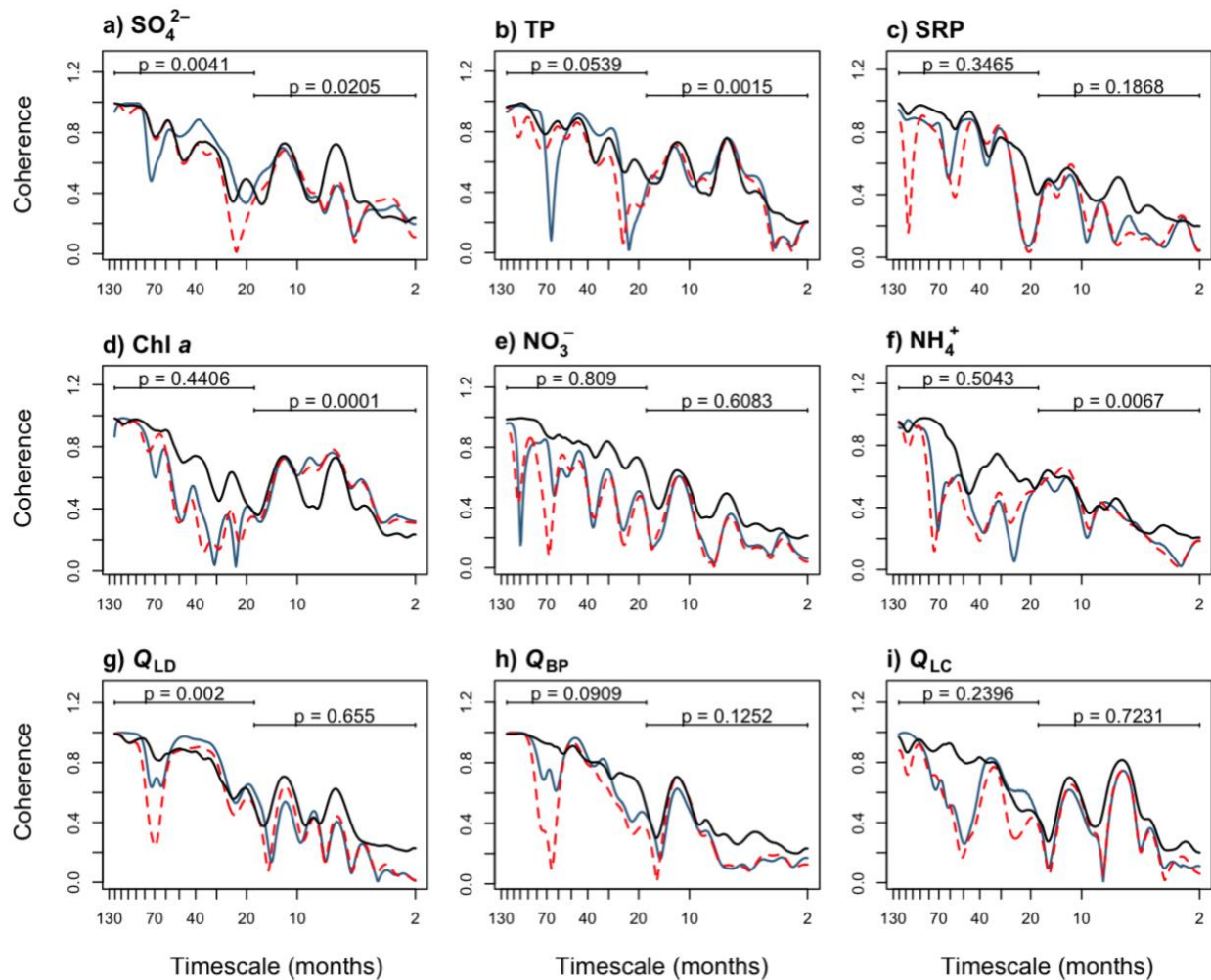


Figure 3.4. (a–i) Wavelet coherence using the wavelet mean field (Sheppard et al., 2016) for nine DOC–environmental predictor pairs. Coherence magnitude (y-axis, range 0–1) represents the sum of the mean squared magnitude of the wavelet mean field over all timescales. The x-axis (log scale, reversed) depicts the range of timescales (2 to 120 months) for which coherence can be reliably investigated for each time series (1/3 of the total length of the original time series). The blue solid line is coherence. The solid black line is the 95th quantile of coherences of surrogate data sets ($n = 10,000$ surrogates). Coherence is significant ($\alpha = 0.05$) for timescales in which the red dashed line is above the black line. Bars above the coherence line are timescales over which coherence was tested for significance. Timescales are defined as short (≤ 18 months) and long (> 18 months).

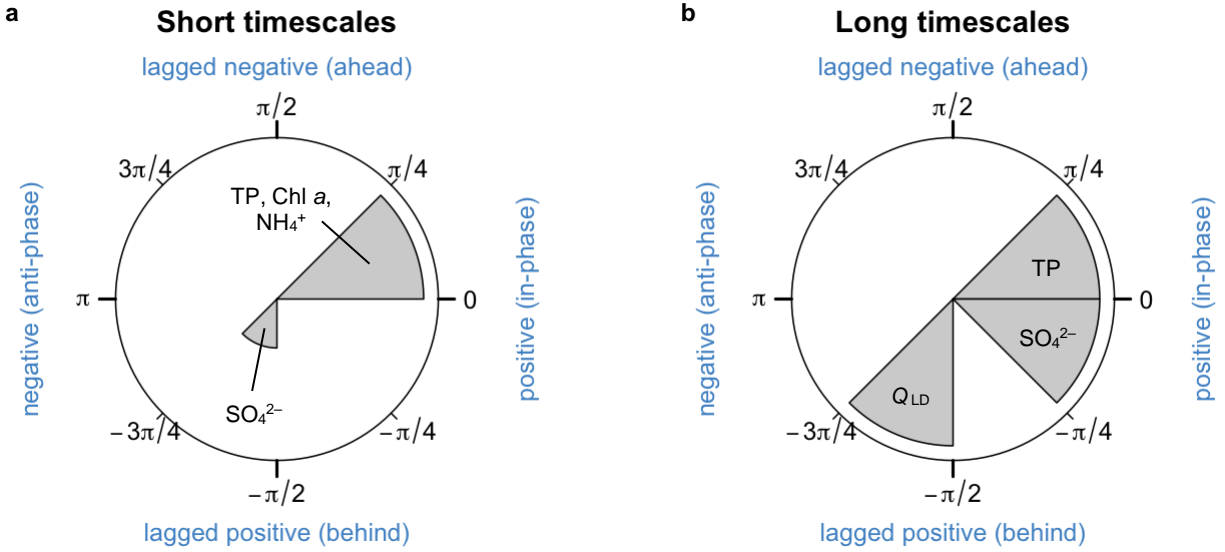


Figure 3.5. Distributions of phase differences at **(a)** short (≤ 18 -month) and **(b)** long (> 18 -month) timescales for environmental predictors that were significantly coherent with DOC concentration. Radius length is proportional to the frequency of each type of relationship observed (lagged, in-phase, anti-phase), where longer radii indicate higher frequency (as in **(a)**). Lagged negative refers to fluctuations in DOC leading ahead of fluctuations in a predictor; lagged positive refers to fluctuations in DOC lagging behind fluctuations in a predictor (e.g., SO_4^{2-} in **(a)** and Q_{LD} in **(b)**). In-phase relationships are analogous to positive correlation, whereas anti-phase relationships are analogous to negative correlation. See Table 3.2 for details.

Table 3.2. Coherence and phase relationships between DOC and environmental predictors that had significant coherence ($\alpha = 0.05$) at short (≤ 18 -month) and long (> 18 -month) timescales. Mean coherence p -values are calculated over the reported timescale band for each significant relationship. $\cos(\phi)$ and $\sin(\phi)$ are transformations of the average phase ϕ over the reported timescale band where $\cos(\phi)$ describes how close the relationship between DOC and each parameter is to being in-phase and $\sin(\phi)$ focuses on whether the time-lagged relationship between DOC and each predictor tends to be positive or negative. Because phases are angular measurements, ϕ ranges between $-\pi$ and π , and $\cos(\phi)$ and $\sin(\phi)$ range between -1 and 1 . Relationships are identified as in-phase when $\cos(\phi) \approx 1$, anti-phase when $\cos(\phi) \approx -1$, and quarter-phase when $\cos(\phi) \approx 0$. When $\sin(\phi) \approx -1$ the relationship is time-lagged positive (i.e., a change in DOC precedes a change in the predictor), whereas when $\sin(\phi) \approx 1$ the relationship is time-lagged negative (DOC lags behind the predictor). When relationships are perfectly in-phase or anti-phase (i.e., not time-lagged), $\sin(\phi) = 0$.

Environmental predictor	Timescales	Mean coherence	p-value	ϕ	$\cos(\phi)$	$\sin(\phi)$	Phase relationship
SO ₄ ²⁻	Short	0.21	0.019	-2.01	-0.43	-0.90	DOC lags behind SO ₄ ²⁻
TP	Short	0.36	0.0016	0.33	0.95	0.33	TP very strongly in-phase with DOC
Chl <i>a</i>	Short	0.50	0.00010	0.55	0.85	0.52	Chl <i>a</i> strongly in-phase with DOC
NH ₄ ⁺	Short	0.26	0.0065	0.16	0.99	0.16	NH ₄ ⁺ very strongly in-phase with DOC
SO ₄ ²⁻	Long	0.67	0.0048	-0.22	0.98	-0.22	SO ₄ ²⁻ very strongly in-phase with DOC
TP	Long	0.57	0.045	0.45	0.90	0.43	TP very strongly in-phase with DOC
Q _{LD}	Long	0.74	0.0015	-1.84	-0.26	-0.97	DOC lags behind Q _{LD}

3.3.3 Generalized additive modeling

Five environmental predictors were found to be significantly coherent with DOC concentration as identified by wavelet coherence analyses at either short (≤ 18 -month) or long (> 18 -month) timescales, or both (section 3.2): SO_4^{2-} , TP, Chl *a*, NH_4^+ , and Q_{LD} . A simple GAM (effective degrees of freedom = 16.9) with a thin plate regression spline for each covariate explained 56% of the deviance in DOC concentration over the 30-year period, with an adjusted R^2 of 0.50 (). Sulfate, TP, NH_4^+ , and Q_{LD} all explained significant variation in DOC concentration ($p < 0.001$ for NH_4^+ and Q_{LD} , and $p < 0.0001$ for SO_4^{2-} and TP). The Chl *a* smooth term was the only non-significant predictor ($p = 0.15$; Figure 3.6a). Total phosphorus and Q_{LD} showed linear positive and negative relationships with DOC concentration respectively (Figure 3.6b,e). At NH_4^+ concentrations $< \sim 0.1 \text{ mg L}^{-1}$ (61% of the observed NH_4^+ data), NH_4^+ had an approximately linear positive effect on DOC concentration but did not have much predictive power at concentrations $> 0.1 \text{ mg L}^{-1}$ as shown by the increasingly large confidence interval (CI; shaded region) at higher NH_4^+ levels (Figure 3.6c). The relationship between DOC and SO_4^{2-} (Figure 3.6d) was generally positive but was more variable than the other environmental drivers. For example, at SO_4^{2-} concentration from $\sim 150\text{--}200 \text{ mg L}^{-1}$ increases in SO_4^{2-} were concurrent with decreases in DOC; however, at SO_4^{2-} concentrations $< 150 \text{ mg L}^{-1}$ (71% of the observed SO_4^{2-} data) DOC tended to increase with increases in SO_4^{2-} . At higher concentrations of SO_4^{2-} , TP, and NH_4^+ and elevated Q_{LD} flow the GAM lost predictive power (large CI for right tails of each smooth) but performed well in lower to moderate ranges (Figure 3.6). In the observed vs fitted values plot (Figure B.5d) the GAM provided a near 1:1 fit between observed and fitted DOC at concentrations $< \sim 7\text{--}8 \text{ mg L}^{-1}$ but considerable variation was apparent in the model fit at concentrations $> 8 \text{ mg L}^{-1}$. Fitting the GAM to the DOC time series (Figure 3.7) revealed that using these predictors to estimate DOC concentration was useful at identifying multi-year trends (e.g., in the 1990s and mid-2010s) but suffered from over-fitting intra-annual fluctuations.

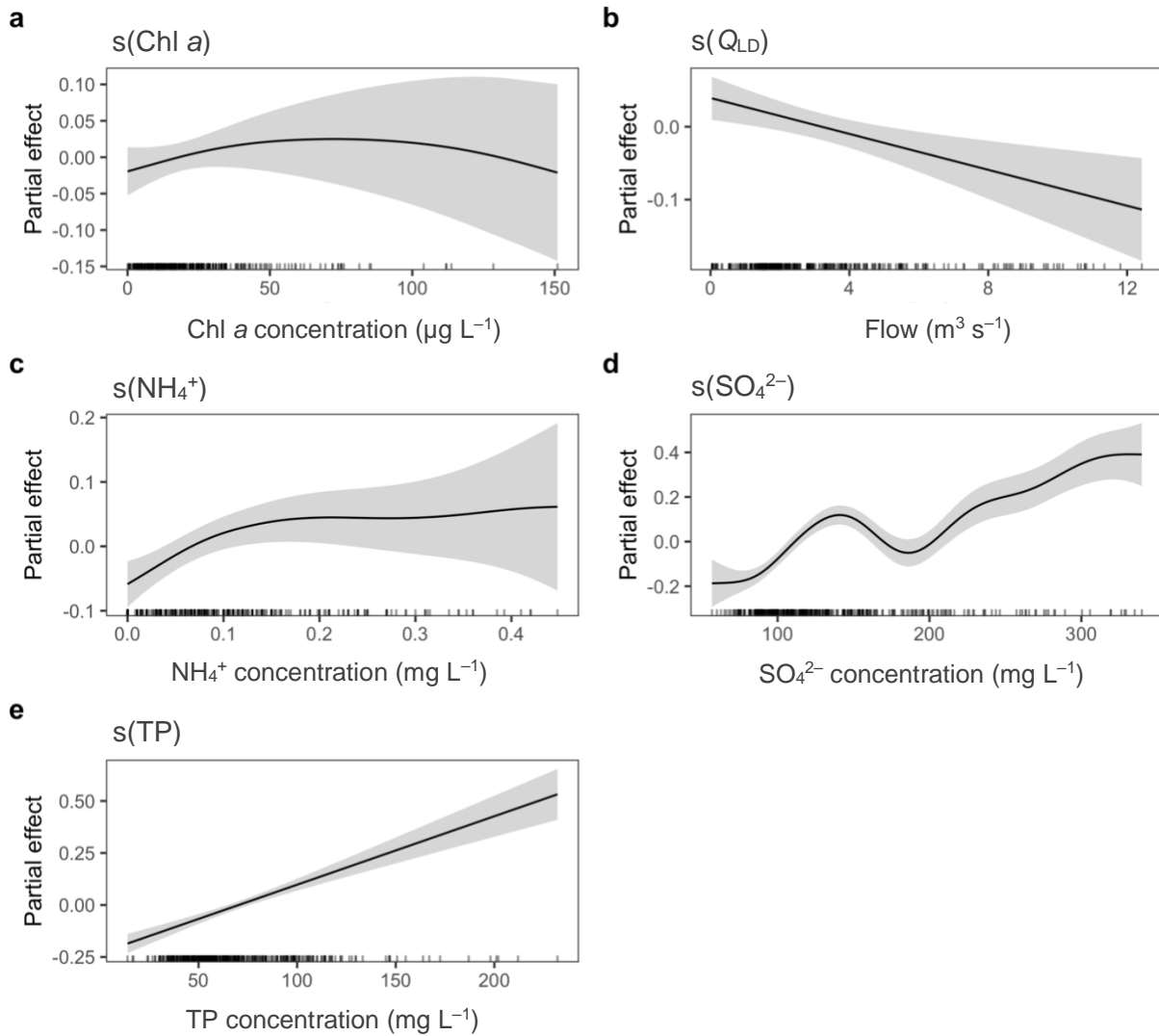


Figure 3.6. Partial effects of (a) Chl *a*, (b) Q_{LD} , (c) NH_4^+ , (d) SO_4^{2-} , and (e) TP for the GAM fitted to the DOC time series with significantly coherent environmental predictor covariates. The *x*-axes show observed values for each environmental predictor. The *y*-axes show the partial effects of thin plate regression spline smooths (black lines) for each environmental predictor. Grey shaded regions are the 95% confidence interval. The rug (inset on *x*-axis) displays the distribution of observed values. Chlorophyll *a* was the only non-significant covariate ($p = 0.15$); all other environmental predictors were significant at $p < 0.001$.

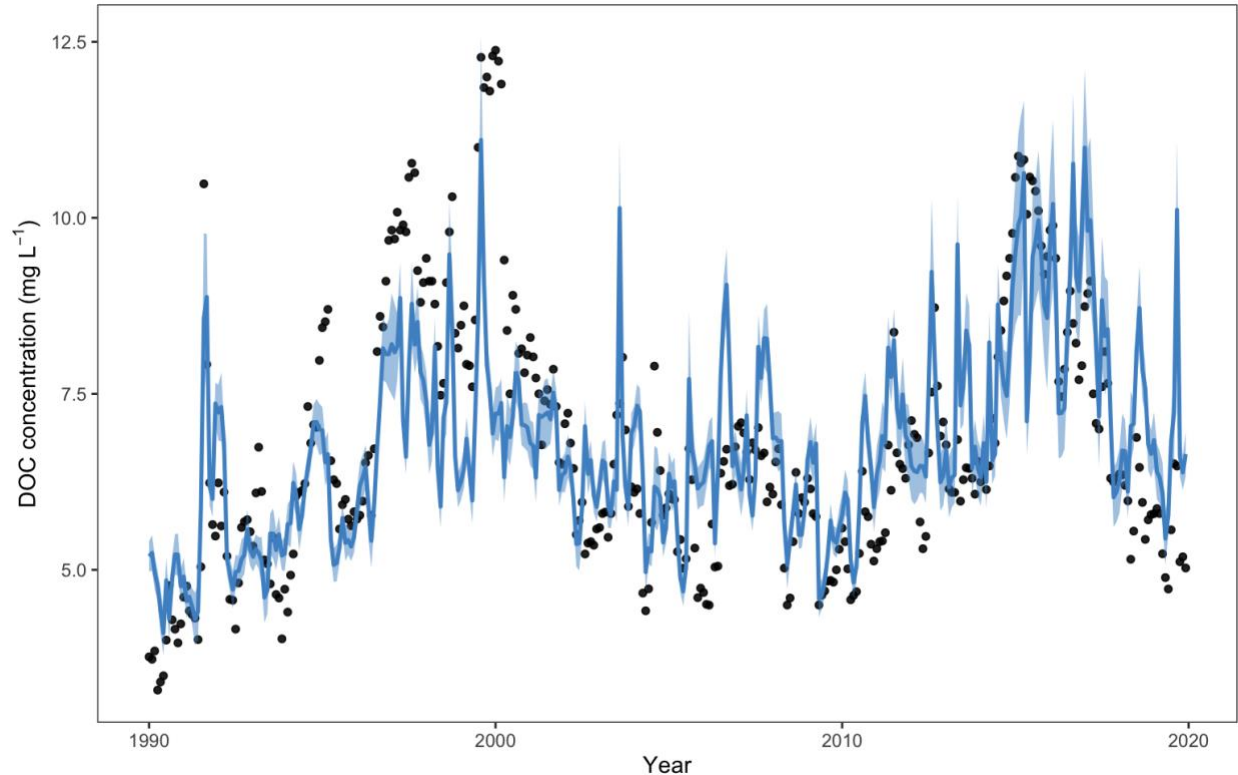


Figure 3.7. Raw DOC concentration time series (black points) overlain with the GAM fit with SO_4^{2-} , TP, Chl *a*, NH_4^+ , and Q_{LD} (blue line). The shaded blue area is the 95% confidence interval of the GAM model fit using 10,000 samples drawn from the posterior multivariate normal distribution. This model explained 56% of the deviance in DOC concentration with an R^2_{adj} of 0.50.

3.4 Discussion

3.4.1 Variability in DOC concentration and flow conditions

Globally, numerous drivers of changing DOC concentrations have been identified, from declining atmospheric SO_4^{2-} (Monteith et al., 2007) and N deposition (Evans et al., 2008), to land management and land-use (Yallop and Clutterbuck, 2009), and to patterns in temperature, precipitation, or runoff (Hongve et al., 2004; Weyhenmeyer and Karlsson, 2009). Within Buffalo Pound Lake, a shallow reservoir in a DOC-rich landscape (Labaugh et al., 1987; Waiser, 2006) with high climatic variability (Pham et al., 2009; Pomeroy et al., 2007; Vogt et al., 2018), climate and flow source appear to have an overriding influence on DOC concentrations. Here, in this highly flow-managed lake, flow sources are related to weather and climatic patterns. In dry years more water is released from upstream Lake Diefenbaker to maintain water levels at Buffalo Pound Lake and other lakes downstream. In wet years runoff from the local catchment increases, delivering nutrients, solutes, and DOC from prairie croplands and wetlands to Buffalo Pound

Lake through tributaries like Ridge Creek and Iskwao Creek. Dry years constitute a more “managed” flow regime (where Lake Diefenbaker dominates flows) whereas wet years (where landscape runoff dominates) bring the system back to a more “natural” state. Under the “natural” regime allochthonous DOC influxes may be large, as prairie wetlands can be important flow sources during wet periods when hydrologic connectivity is high (Ali and English, 2019; Nachshon et al., 2014) and these prairie wetlands can have extremely high DOC concentrations due to evapoconcentration (in excess in 100 mg L^{-1} in some ponds) (Arts et al., 2000; Waiser, 2006). Wetlands are not the only substantive DOC source in the landscape. High concentrations of DOC have also been observed in snowmelt runoff from agricultural fields in the prairies. For example, flow-weighted mean DOC concentrations in snowmelt runoff under conventional and rotational tillage practices in the prairies are also relatively high: 15.8 mg L^{-1} under conventional tillage and 20.0 mg L^{-1} with rotational tillage (Liu et al. 2014). In addition to soils, crop residues can be an important DOC source in the prairies, but DOC release from residues may be highly dependent on crop type (Elliott, 2013; Elliott et al., 2008).

Lake DOC concentrations in cold regions tend to vary both seasonally and interannually. Seasonal cycles alter the rates of biological DOC production and hydrological export (Clark et al., 2010), and DOC influxes often peak during spring snowmelt while biological DOC production peaks in summer (Buffam et al., 2007; Clark et al., 2010; Laudon et al., 2004). High intensity precipitation events can also supply DOC to lakes, and interannual variation in rain and snowfall can account for much among-year DOC variability by heightening differences in catchment runoff between wet and dry years (Clark et al., 2010) or altering the regional water balance (Jane et al., 2017). In cold regions where lakes are ice covered for a portion of the year, DOC exclusion from ice can be important factor driving winter metabolism and DOC concentrations (Guo et al., 2012; Kurek et al., 2022), whereas photo- and biodegradation processes (Hansen et al., 2016) and autochthonous DOC production (Chapter 2) may dominate during the open-water season. In many lakes seasonal variation in DOC concentration can be one to two orders of magnitude greater than the long-term rate of change over decadal time scales (Clark et al., 2010). Within Buffalo Pound Lake we observed both high inter- and intraannual variability, with large variations in DOC concentration occurring over multi-year periods (e.g., up to a 10 mg L^{-1} increase in monthly concentrations over a decade) and fluctuation as high as 7 mg L^{-1} within a single year. This lake has a short residence time compared to many (8 months to

2.5 years; BPWTP, 2016; Vogt et al., 2018), which may make it more responsive to rapid change as a result of changes in inflows. Both allochthonous and autochthonous DOC sources are important in Buffalo Pound Lake (e.g. Chapter 2) but variable residence time and other external conditions (e.g., climate) make it difficult to disentangle multiple interactive factors driving DOC concentration. The observed variability in these conditions and DOC concentration, including large within- and among-year fluctuations in DOC, lead to a complex DOC–predictor picture which we aimed to explain using wavelet analysis and GAMs.

3.4.2 DOC–predictor relationships

Wavelet analyses demonstrated that flows from Lake Diefenbaker were coherent with DOC concentrations in Buffalo Pound Lake at long timescales, with Lake Diefenbaker outflows tending to precede fluctuations in DOC concentration. Specifically, Lake Diefenbaker flows appear to have a flushing, or diluting impact. Lake Diefenbaker is fed by the South Saskatchewan River, a sand-bottom river with low DOC concentrations whose origins are in the Rocky Mountains. We expected to see a contrasting role of the local catchment. Specifically, given that allochthonous DOC can increase rapidly in lakes during periods of elevated runoff (e.g., during snowmelt or large precipitation events) and prairie wetlands have notably high DOC concentrations, we expected local catchment flow (Q_{LC}) to be coherent with DOC at short timescales. Instead, coherence between Q_{LC} and DOC was very low (0.10) at short timescales (Table B.3) and non-significant. This result likely reflects the generally smaller contribution of the local catchment to flow and intermittency of these sources making signals challenging to ascertain. Local catchment flows, though sometimes large, are infrequent (Figure 3.3) due to the ephemeral nature of these sources and their tendency to dry out in late summer and drier years, while also not flowing for extended periods in the winter. Given lower flow frequency and less reliability, characterizing coherence for this flow input is more challenging, particularly in light of the often lower flow contribution. Large pulses of inflows from the local catchment do still appear important to the lake. As such, the local catchment is likely an important source of allochthonous DOC. Flows into Buffalo Pound Lake (Q_{BP}) were likewise incoherent with DOC at both short and long timescales (Table B.3). Because Q_{BP} combines flows from Lake Diefenbaker and parts of the local catchment, this metric may obscure relationships by

integrating different mechanisms by which the two flow sources impact chemistry (e.g., greater allochthonous inputs from the local catchment).

In addition to flow from Lake Diefenbaker, SO_4^{2-} , TP, Chl *a*, and NH_4^+ were also significantly coherent with DOC at short and/or long timescales. At short timescales (≤ 18 months) DOC lagged behind SO_4^{2-} on average but at long timescales (> 18 months) this relationship was strongly in-phase, suggesting within-year or seasonal DOC and SO_4^{2-} dynamics may differ but their patterns become more synchronous at longer timescales. Total phosphorus, Chl *a*, and NH_4^+ concentrations were strongly in-phase with DOC at short timescales, and TP remained strongly in-phase at long timescales. Possible mechanisms for these relationships include internal production and transformations and synchronous inputs of nutrients and allochthonous DOC from the local catchment, discussed in detail below.

Using SO_4^{2-} , TP, NH_4^+ , Chl *a*, and Q_{LD} as predictors in a GAM describing DOC explained 56% of the deviance in DOC concentrations observed over this 30-year data set, where all predictors were significant except for Chl *a*. This result presents evidence that DOC concentration in Buffalo Pound Lake is strongly linked to its major flow source, Lake Diefenbaker, and in-lake nutrient and solute chemistry. We attempted to incorporate time-lagged relationships between DOC and SO_4^{2-} and Q_{LD} into the GAM approach; however, a feature of wavelet coherence analysis is that phase relationships can only be determined *on-average* over the timescale of interest (J. Walter pers. comm.), and thus specific time-lags (e.g., 6 months, 24 months, etc.) cannot be accurately measured with this approach. The true time-lag relationship between Q_{LD} and DOC also likely varies depending on flow magnitude. To assess concerns over potential collinearity between DOC and TP we ran a GAM with SRP in place of TP but found no discernable differences in model results.

Dissolved organic carbon was not the only chemical variable that underwent dramatic change within Buffalo Pound over the study period. Indeed, 6-fold variation in concentration in SO_4^{2-} was observed. The rapid rise and fall in DOC and SO_4^{2-} concentrations in the 2010s may be linked to both internal and external processes. The majority of SO_4^{2-} fluxes to lakes come from soils and wetlands in the catchment, often in mineral forms or bound in allochthonous organic matter containing oxygen-bound S (e.g., as ester- SO_4 or other organo- SO_4 species) (Couture et al., 2016), helping explain coherence between SO_4^{2-} and DOC. Much like prairie catchments have high DOC, they can also have high SO_4^{2-} , again, due to soil and wetland

sources. Pothole ponds have a wide range of SO_4^{2-} concentrations, with a median of 163 (mean 519) mg L^{-1} , and some ponds reaching concentrations of 5500 mg L^{-1} (L. Dyck unpublished data for ~150 prairie pothole region ponds in 2019) and prairie soils can be similarly high in SO_4^{2-} (Fennell and Bentley, 1998). Annually-measured SO_4^{2-} samples at Lake Diefenbaker from 1990 to 2019 showed median concentrations of 58 mg L^{-1} and maxima $< 90 \text{ mg L}^{-1}$ (unpublished data), values near the low range of SO_4^{2-} seen in Buffalo Pound Lake. The much higher median Ridge Creek SO_4^{2-} (estimated at ~1094 mg L^{-1} ; unpublished data), combined with the below-average inflows from Lake Diefenbaker (and higher Q_{LC}) in the early 2010s mean that catchment SO_4^{2-} sources must have contributed to the higher SO_4^{2-} concentrations seen in Buffalo Pound Lake during the latter part of the observation record. Groundwater may be infusing minerals such as SO_4^{2-} to the lake (BPWTP, 2022) but we lack data to support this SO_4^{2-} source. Extreme flooding across the prairies in 2011 could have created an exceptional ‘fill and spill’ scenario (see Nachshon et al., 2014; Shook and Pomeroy, 2012) where water containing elevated levels of SO_4^{2-} and DOC was transported via runoff from upland ponds to Buffalo Pound Lake. Similar mechanisms were likely important in 2014 and 2015, two years with periods of high precipitation in the region (Water Security Agency, 2018) and above-average catchment inflows, when SO_4^{2-} and DOC concentrations further increased. Prairie soils and lake sediments are rich in gypsum (CaSO_4) and pyrite (FeS_2) deposited during glaciation 10,000 years ago may also play a role. Reoxidation of lake sediments rich in H_2S , CaSO_4 , FeS_2 , and other sulfides can also increase surface water SO_4^{2-} concentrations (Holmer and Storkholm, 2001), and in freshwater sediments, high rates of oxidation of reduced S compounds can shift the sediments from net sinks to sources of SO_4^{2-} (Holmer and Storkholm, 2001), particularly if there are no high SO_4^{2-} groundwater sources to the lake.

Strong in-phase coherence at both short and long timescales between DOC and TP concentrations, as well as the strong linear effect of TP on DOC, suggest that there is synchrony in the processes influencing DOC and TP in Buffalo Pound Lake. As for SO_4^{2-} , prairie ponds can also be important P sources to downstream lakes during periods of elevated catchment flow, particularly because ponds high in SO_4^{2-} tend to have greater sediment P release rates (Jensen et al., 2009). Open-water season TP concentrations measured at ~150 ponds across the prairie region in 2019 revealed mean TP concentrations in excess of 500 $\mu\text{g P L}^{-1}$ (McFarlan, 2021) suggesting potential for notable nutrient inputs during periods of elevated Q_{LC} . Painter et al.

(2022) linked mid-summer algal blooms at Buffalo Pound Lake to large pulses of internal P released from sediments during transient stratification events, noting that these stratification and P release events can occur repeatedly in polymictic lakes like Buffalo Pound Lake (see also North et al., 2015; Orihel et al., 2015). Dissolved iron concentrations below levels of detection ($0.01 \text{ mg Fe L}^{-1}$) at Buffalo Pound Lake in spring and summer months, along with past evidence of internal P loading in the lake (D'Silva, 2017), corroborated these episodes of internal P release, owing to the importance of Fe in P sequestration via formation of ferrous-phosphate minerals.

Chlorophyll *a* concentration, a measure of algal abundance, was not significant in the GAM but showed in-phase coherence with DOC concentrations at short timescales, suggesting a seasonal effect associated with cyanobacterial/algal biomass in the lake. Inefficient conversion of light energy to organic molecules during photosynthesis means that a portion of the organic materials produced by algal cells are released as DOM/DOC to ambient water over the lifetime of the alga (Fogg, 1966; Mykkestad, 1995). Extracellular DOC release, via the overflow model (Fogg, 1983, 1966; Williams, 1990) or the passive diffusion model (Bjørnsen, 1988; Fogg, 1966), has been shown to be an important source of autochthonous DOC, where as much as 5–35% of fixed organic carbon may be release immediately as DOM, often with high proportions of DOC (Carlson and Hansell, 2015). Autochthonous DOM production may increase DOC concentrations by $1\text{--}2 \text{ mg L}^{-1}$ between the Buffalo Pound Lake inflow and outflow in years dominated by flow from Lake Diefenbaker (Chapter 2), consistent with potential contribution from extracellular release.

Observed in-phase coherence between DOC and NH_4^+ at short timescales and significance of NH_4^+ as a predictor of DOC in the GAM may be related to several mechanisms. The lake is sometimes N-limited (Swarbrick et al., 2019), suggesting increased NH_4^+ could support increased productivity, and autochthonous production. This temperate lake is also highly seasonal, with major summer blooms (Painter et al., 2022a, 2022b), followed by long, cold winter periods when the lake is ice-covered and NH_4^+ dynamics undergo rapid change (Cavaliere and Baulch, 2020). The early winter phase is marked by increasing NH_4^+ concentrations associated with decreased autotrophy, oxygen depletion, and organic matter mineralization. We observed several years where DOC concentrations decreased during the early winter period. The late winter phase shows a decline in NH_4^+ likely associated with the spring bloom and the

influence of lake water mixing with surface inflows. Seasonal variation in DOC:DON ratios are also apparent (Figure B.6). Higher C:N occurs under ice cover then decreases beginning around spring ice-off (~100th day of the year), reaching its lowest in late summer concurrent with seasonal maximum Chl *a* concentrations.

3.4.3 Flow management and effective water treatment

Cyclic wet–dry periods in the prairie region are associated with elevated flood risk and severe drought. Examples include the major drought from 1999–2004 and extensive flooding in 2011 and 2014. Flood risk and drought underpin water management concerns in the region, which include balancing the provision of water from Buffalo Pound Lake to meet the needs of more than 270,000 people. Other water management considerations include irrigated agriculture, industrial and natural resource development, discharges from major cities and agriculture, wetland drainage, and water quality (Wheater and Gober, 2013). “Natural” and “managed” flow scenarios associated with wet–dry cycles each present challenges for Buffalo Pound Lake water quality and for the Buffalo Pound Water Treatment Plant (BPWTP). Years with high local catchment flows (natural flow scenario) lead to high DOC and poor water quality that can take years to dissipate, and create added challenges and costs for the BPWTP to maintain safe drinking water standards. For example, during a prolonged drought from 1999–2005 SUVA₂₅₄ values were very low (~0.9–1.6 L mg-C⁻¹ m⁻¹ over this period) but after extensive flooding in 2011 SUVA₂₅₄ exceeded 2.5 L mg-C⁻¹ m⁻¹ and remained above 1.5 L mg-C⁻¹ m⁻¹ into 2019 (Figure B.7). At the same time, managed flow conditions—that arise when the system is dry, and flows from Lake Diefenbaker are important to maintaining water levels in Buffalo Pound Lake—may contribute to worse algal blooms in Buffalo Pound Lake in terms of magnitude (Painter et al., 2022a), and may lead to high autochthonous DOC production in the lake (e.g. Chapter 2). Elevated DOC concentrations and changes in DOC colour and quality can be problematic and pose challenges for drinking water treatment (Williamson et al., 2016). At high DOC levels, water treatment is impaired by costly increases in coagulant loads required for pre-treatment DOM removal (Cooke and Kennedy, 2001) and coliform regrowth in distribution systems (LeChevallier et al., 1996). Untreated DOC can also contribute to poor taste and odour problems (Matilainen et al., 2011). When chlorine reacts with DOC during water treatment, the compounds that comprise DOC can act as precursors for a suite of harmful disinfection

byproducts (DBPs) with potentially carcinogenic and mutagenic properties (Chow et al., 2003), and are thus strictly regulated (Health Canada, 2006, 2008). Disinfection byproduct formation is a major concern for the BPWTP (Williams et al., 2019), particularly when DOC is high and cyanobacteria are abundant in the lake. Under these circumstances, the BPWTP must use a pre-chlorination step to reduce algal growth and prevent rising floc (organic materials that coalesce and resist coagulation) that can impact treatment capacity by accumulating on filtration media (Painter et al., 2022a). Pre-chlorination is typically required in the summer months when algae are abundant in Buffalo Pound Lake (Painter et al., 2022a), and thus makes it difficult for the BPWTP to meet regulatory THM limits in years where DOC is also elevated (BPWTP, 2016).

The variable magnitude, timing, and water quality of flows from Lake Diefenbaker and the local catchment underscore the complexity in developing environmental flow rules for Buffalo Pound Lake. Here, demand for good sourcewater quality is complicated by a number of competing priorities, including hydropower production, flood control, agricultural drainage of wetlands, and irrigation projects. Maintaining stable water levels within the lake to limit valley slumping and erosion is also important (Saskatchewan Environment and Resources Management, 2001). Other water quality concerns include effluent disposal practices on agricultural land, leaking septic tanks from cottages, and pollution from tourism and recreational activities. Buffalo Pound Lake is also critical fish and wildlife habitat, and environmental flow rules, such as the fishway through the dam at the outlet of the lake, should strive to minimize impacts on valuable species when developing strategies to maintain water quality in the lake. A \$4B Lake Diefenbaker irrigation expansion project announced in July 2020 is one example that may impact flow quantity and timing, and the quality of water entering Buffalo Pound Lake. This project, which expects to open up ~200,000 ha of arable land to consistent water supply and facilitate growth in industrial and potash mining operations, may degrade Buffalo Pound Lake water quality by increasing nutrient influxes (e.g., from fertilizers) to the lake. In the Canadian prairies where water quality is often naturally poor in multiple watersheds water treatment plants face multiple challenges (e.g., eutrophication and algal blooms, cyanobacterial toxins, waterborne pathogens; Schindler and Donahue, 2006) in addition to considerable variation in sourcewater DOM quantity and quality. Optimizing treatment operations to effectively remove DOM and limit DBP formation under variable flow scenarios and competing water demands is a

pressing issue for water managers in the region and is a major focus in plans for an upcoming \$233M upgrade to the water treatment plant at Buffalo Pound Lake.

3.5 Conclusions

Flow management, along with climate and hydrological variability, are important controls on DOC concentration in this shallow prairie lake. Flow from upstream mesotrophic reservoir Lake Diefenbaker is a key predictor/driver of DOC concentration over long timescales, though pulses of allochthonous DOC from the local catchment during wet periods can raise DOC concentration in the lake for several years. Total phosphorus and NH_4^+ concentrations are synchronous with DOC in Buffalo Pound Lake and positively correlated, suggesting that internal production/autochthony and the seasonal dynamics of nutrients and organic matter transformations under ice and during the open-water season are important in years where flows are overwhelmingly from Lake Diefenbaker. Irrigated agriculture expansion in the region may increase nutrient inputs to Buffalo Pound Lake and further enhance cultural eutrophication. In turn, autochthonous DOC concentrations in the lake may also increase in concert with greater primary production. Sulfate, which was also highly variable over the 30-year period, was synchronous and positively correlated with DOC, revealing the close link between solutes and DOC sourced from the local catchment, as opposed to Lake Diefenbaker which tends to be lower in SO_4^{2-} , and perhaps suggests there are other sources of SO_4^{2-} and DOC to Buffalo Pound Lake from groundwater. Occasional large pulses of local catchment flow during wet climate phases, along with strict management of water levels in the lake to prevent erosion, have led to large fluctuations in DOC in Buffalo Pound Lake. Our analyses underscore the relationship between DOC and flow source for Buffalo Pound Lake, and show that poor water quality often results from elevated local catchment flow. If the prairies experience higher rainfall totals and less precipitation as snow with a changing climate, episodes of allochthonous inputs of DOC, nutrients, and solutes may become more frequent and further degrade water quality in the lake, making water management and drinking water treatment increasingly difficult.

3.6 Acknowledgements

Research funding for this work was provided by NSERC Discovery Grants to Helen M. Baulch and Colin J. Whitfield, and an NSERC Graduate Scholarship – Master's to Anthony A. P. Baron. Funding was also provided through an academic-industry partnership with the Buffalo

Pound Water Treatment Plant supported by the Mitacs Accelerate program, along with ongoing funding of the Buffalo Pound Water Treatment Plant for operations. Many thanks are owed to Blair Kardash, Laboratory Manager at the Buffalo Pound Water Treatment Plant, for stewardship of treatment plant data, insights on the Buffalo Pound Lake ecosystem, and cooperation throughout the project, as well as the Buffalo Pound Water Treatment Plant for chemical analyses. We also thank John-Mark Davies from the Saskatchewan Water Security Agency (WSA) for sharing perspective and knowledge from many years of working in this watershed, and the WSA for provision of streamflow data. We also wish to thank Jonathon Walter and Lawrence Sheppard for guidance on wavelet analyses. Finally, we acknowledge members of the SaskWatChe and Bigfoot labs for their support and feedback from the inception of this work.

3.7 Author contributions

A.A.P Baron: Conceptualization, Methodology, Software, Formal Analysis, Data Curation, Writing – Original Draft, Writing – Review & Editing, Visualization; **H.M. Baulch:** Conceptualization, Methodology, Investigation, Data Curation, Writing – Review & Editing, Supervision, Project Administration, Funding Acquisition; **C.J. Whitfield:** Conceptualization, Methodology, Investigation, Data Curation, Writing – Review & Editing, Supervision, Project Administration, Funding Acquisition; **A. Nazemi:** Formal Analysis, Data Curation, Writing – Review & Editing.

Chapter 4: General conclusions

4.0 Summary

In the Canadian prairies and globally, freshwater resources are increasingly threatened on multiple fronts by human activities. Among these are cultural eutrophication driven by increasing use of fertilizers for crop growth along with nutrient-rich urban and industrial runoff, climate change induced effects on key hydrological processes (e.g., snowfall amount and timing of snowmelt in the Canadian prairies), water scarcity associated with increasing water demands and intersectoral competition and severe drought, and conversion from natural landscapes to heavily managed agricultural systems (e.g., Gober and Wheeler, 2014). Water treatment challenges arise synergistically from the interactions of these threats in lakes and reservoirs used as drinking water sources.

Effective dissolved organic carbon (DOC) removal and water treatment that minimizes disinfection by-product (DBP) formation are impaired when the quantity, quality, and timing of organic matter fluxes in source waters are changing and unpredictable. Understanding DOC concentration and dissolved organic matter (DOM) quality dynamics, and their drivers of change, is thus imperative as eutrophication, climate change, land-use change, and competing demands for water resources alter DOM quantity and quality in receiving lakes and reservoirs. This study aimed to identify the roles that water sources and in-lake chemical change have on DOC concentration, and investigate DOM quality within Buffalo Pound Lake, with the overarching goal of aiding in water treatment decision-making and watershed management within the region.

There have been numerous attempts to unify the hypotheses of drivers of DOC concentration patterns, and quantitatively and qualitatively describe DOM quality in lakes and reservoirs. Despite these efforts, the molecular complexity and diversity of DOM, and the role of local watershed controls on lake and reservoir DOC make it challenging to describe a unifying theory on the controls of DOC concentration and to compare DOM quality across studies and in different environments.

In Chapter 2 DOC concentration and DOM optical spectroscopy (i.e., DOM quality) measured over four open-water seasons along the length of Buffalo Pound Lake were analyzed. Here we provided evidence for increasing autochthony along the length of the lake driven by primary production and subsequent extracellular DOC release by algae and cyanobacteria. The

four years of study were relatively dry, as indicated by minimal flows from the local catchment; flows into the lake were similar in magnitude to those leaving upstream Lake Diefenbaker. Consistent year-to-year increases in DOC concentration coupled with shifts in fluorescence metrics toward more autochthonous signatures from lake inflow to outflow demonstrated that DOM quality is highly dynamic within the lake during the open-water season, and improved our understanding of the way DOM cycles and transforms in the lake when Lake Diefenbaker is the dominant water source—insights unattainable from DOC concentration alone. Future study of DOC concentration and DOM quality during abnormally wet years—when the local catchment can be an important water source—is needed to provide further insight into how DOM quality changes in the lake under these conditions. During these wet phases, DOM inputs to the lake are presumably more allochthonous, and DOC concentrations are several mg L⁻¹ higher (see Chapter 3). Expanding DOM quality measurements to wet years would be beneficial to the Buffalo Pound Water Treatment Plant (BPWTP), as it is during these wet years that removal of DOC and limiting DBP formation during water treatment are particularly challenging. In the year prior to the beginning of this study (2015), exceptionally wet conditions led to a water crisis for the BPWTP (CTV, 2015). During this crisis managed flow from Lake Diefenbaker was reduced, as runoff from the local catchment presented an elevated flood risk, and resulted in a decline in water quality in the lake, including elevated DOC concentrations. Unusually warm temperatures also contributed to deteriorating water quality, and ultimately limited rates of treatment, contributing to water supply shortages. While drinking water safety was not impacted, improved understanding of the nature of DOM sourced from the local catchment during events such as this would aid the BPWTP in current decision-making strategies, which include strengthening demand management and commissioning dissolved air flotation clarification (BPWTP, 2016).

Year-round DOM quality measurements that include shoulder season and ice-covered periods would further provide a more complete understanding of DOM quality and DOC concentration change throughout Buffalo Pound Lake, as DOM dynamics during snowmelt (Boyer et al., 2000; Meingast et al., 2020; Qiu et al., 2016) and under ice (Guo et al., 2012; Kurek et al., 2022) can be distinct from or influence open-water season DOM quantity and quality. Unfortunately, sampling in shoulder seasons during ice formation and melting presents a safety concern, making it difficult and infeasible to get measurements during these seasons without enhanced technology. Advancements in *in situ* DOM fluorescence sampling

technologies such as field fluorimeters may provide one solution to this problem, but can be costly and currently face several disadvantages compared to benchtop spectrofluorimeters (Carstea et al., 2020).

In Chapter 3, a 30-year data set of DOC concentration, nutrients, and sulfate, along with flow data upstream of Buffalo Pound Lake were used to disentangle the drivers of large fluctuations in DOC concentration in the lake. Here, we focussed on the roles of variable water source, multi-year variability in climate, and the role of nutrients and sulfate on moderating DOC concentration in the reservoir. Using wavelet coherence analyses and generalized additive models we clearly demonstrated the importance of flow source and in-lake water chemistry as factors driving DOC concentration in Buffalo Pound Lake, and linked periods of extreme wet and dry conditions to episodes of rapid change in DOC concentration within the lake. Despite linking DOC concentration to flow source and water chemistry, we found it difficult to develop a mechanistic framework responsible for observed DOC dynamics in Buffalo Pound Lake. Additional monitoring and data, such as a streamflow gauge at the lake outflow would facilitate calculations of DOC, nutrient, and sulfate mass balances and fluxes, and improve capacity to identify water residence time, which we suspect plays a large role in controlling DOC concentration in this system. Under higher flow conditions, Buffalo Pound Lake may behave similar to a slow-moving river, while longer residence times under low flow conditions can yield more typical reservoir behaviour. Similarly, these data could provide insight on the role of groundwater sources of DOC and solutes to the lake, which are currently thought to be important (BPWTP, 2017) but have not been quantified. The 30-year record investigated in this chapter provided an opportunity to study DOC concentration and its drivers through periods of both drought and deluge; however, questions remain about cyclicity in DOC concentrations over longer timescales. For example, in addition to shorter-term changes, we observed large fluctuations in DOC concentration at approximately decadal scales. Revisiting the long-term record in an additional 10, 20, or 30 years would help identify such patterns as cyclic or part of a longer-term trend, similar to those reported for systems in other regions of the Northern Hemisphere.

The investigations carried out in this thesis provide a foundation for DOC forecasting in Buffalo Pound Lake by showing how water source and water chemistry affect DOC concentration, and how DOM quality shifts as water transits through the reservoir during the

open-water season when Lake Diefenbaker is the dominant flow source. Together, the works presented in this thesis will inform drinking water treatment strategies and be of use for watershed management, particularly with respect to decisions made around water diversions and managing flow sources to Buffalo Pound Lake. More broadly, these works add to the scarce literature on the drivers of change and characterization of DOM quantity and quality in shallow lakes on the Canadian prairies, and in regions that have not experienced significant SO_4^{2-} deposition and subsequent reduction in acid rain. In this way our findings contribute to efforts to quantify the role of lakes and reservoirs in the global carbon cycle (e.g., Cole et al., 2007). Some areas of eastern North America and Europe have documented long-term changes in DOC attributed to policy change concerning sulphur dioxide emissions, changes in climate and land-use, natural sea salt deposition cycles, or other climatic, hydrological, or anthropogenic factors. Here we illustrate similar changes in DOC concentration (~ 3-fold change over a decade) tied largely to natural fluctuations in climate and the overarching management of flow through Buffalo Pound Lake.

4.1 Implications for watershed management and forecasting lake and reservoir DOC concentrations

Surface waters across the Canadian prairies are heavily managed, and few streams and rivers experience natural flow regimes. Instead, dams and the creation of reservoirs have stabilized flow regimes to meet water demands for drinking water, hydropower, agriculture, and industry. In reservoirs like Buffalo Pound Lake water levels are increasingly managed to slow erosion, maintain water supplies, and manage flood risks, yet water quality issues associated with stable water levels and managed flow regimes are critically understudied. However, in light of the recent water crisis faced by the BPWTP, growing population, and increasing intersectoral competition, water quality concerns are of increasing interest, particularly as the treatment plant has begun a \$325M upgrade to continue to provide safe drinking water and meet increasing water demands over the next 50 years.

4.2 Impact and opportunities for future work

The work presented in this thesis aimed to answer novel questions about the nature of DOC in Buffalo Pound Lake and the impacts flow management can have on an ecosystem facing multiple pressures ranging from growing demand for water, deteriorating water quality, and an

uncertain climate future. While we have gained important insights into the drivers of long-term DOC and the quality of DOM in this system, which will certainly benefit the BPWTP, there are several opportunities for future work related to DOM quantity and quality in Buffalo Pound Lake and the broader implications of flow management in this system.

One of the challenges we faced was unraveling a mechanistic understanding of DOM behaviour as it relates to changing flow source, and the broader role of pothole ponds, agricultural drainage, groundwater intrusion, and point and non-point sources of pollutants, and nutrients. Related to this, there is opportunity to investigate the trade-offs between water quality and flow management. While our results suggest a beneficial effect of flows from Lake Diefenbaker on water quality, which we attribute to flushing with water of better quality, there are limits to flow management to aid in water treatment owing to upstream channel capacity, lake levels downstream, and competing water demands out of Lake Diefenbaker. Given the challenges to providing drinking water from this eutrophic reservoir, more investigation to the effects of nutrient inputs associated with wetland drainage projects in the watershed would be another valuable area for future research. Data to support such investigations are sparse at present, but will prove to be of interest to those managing water treatment, and water resources more broadly in this system. We expect further extreme conditions (continued blooms, more severe droughts and floods, shorter ice cover durations), and new tools are needed to predict how this system will respond to such events, as they do not currently exist. This is an important outlook for future work because it will allow us to build from what we have learned from this wealthy data set and make predictions of future change, which we have not been able to do here.

References

- Addison, P.S., 2002. *The Illustrated Wavelet Transform Handbook: Introductory Theory and Applications in Science, Engineering, Medicine and Finance*, 2nd ed. CRC Press, Edinburgh, Scotland.
- Aiken, G.R., McKnight, D.M., Thorn, K.A., Thurman, E.M., 1992. Isolation of hydrophilic organic acids from water using nonionic macroporous resins. *Org. Geochem.* 18, 567–573. [https://doi.org/10.1016/0146-6380\(92\)90119-1](https://doi.org/10.1016/0146-6380(92)90119-1)
- Aitkenhead-Peterson, J., McDowell, W., Neff, J., 2003. Sources, Production, and Regulation of Allochthonous Dissolved Organic Matter Inputs to Surface Waters, in: Findlay, S., Sinsabaugh, R. (Eds.), *Aquatic Ecosystems: Interactivity of Dissolved Organic Matter*. Elsevier Science, USA, pp. 25–70.
- Algesten, G., Sobek, S., Bergström, A.-K., Ågren, A., Tranvik, L.J., Jansson, M., 2004. Role of lakes for organic carbon cycling in the boreal zone. *Glob. Chang. Biol.* 10, 141–147. <https://doi.org/dor.org/10.1111/j.1365-2486.2003.00721.x>
- Ali, G., English, C., 2019. Phytoplankton blooms in Lake Winnipeg linked to selective water-gatekeeper connectivity. *Sci. Rep.* 9, 8395. <https://doi.org/10.1038/s41598-019-44717-y>
- Altman, N.S., 1992. An introduction to kernel and nearest-neighbor nonparametric regression. *Am. Stat.* 46, 175–185. <https://doi.org/doi.org/10.1080/00031305.1992.10475879>
- APHA, 2012. *Standard Methods for the Examination of Water and Wastewater*, 22nd ed. American Public Health Association, American Water Works Association, Water Environment Federation.
- Arts, M.T., Robarts, R.D., Kasai, F., Waiser, M.J., Tumber, V.P., Plante, A.J., Rai, H., de Lange, H.J., 2000. The attenuation of ultraviolet radiation in high dissolved organic carbon waters of wetlands and lakes on the northern Great Plains. *Limnol. Oceanogr.* 45, 292–299. <https://doi.org/doi.org/10.4319/lo.2000.45.2.0292>
- Ashworth, D.J., Alloway, B.J., 2007. Complexation of Copper by Sewage Sludge-derived Dissolved Organic Matter: Effects on Soil Sorption Behaviour and Plant Uptake. *Water Air Soil Pollut.* 182, 187–196. <https://doi.org/10.1007/s11270-006-9331-7>
- Baddeley, A., Rubak, E., Turner, R., 2015. *Spatial Point Patterns: Methodology and Applications with R*. Chapman and Hall/CRC Press, London.

- Badr, E.-S.A., Achterberg, E.P., Tappin, A.D., Hill, S.J., Braungardt, C.B., 2003. Determination of dissolved organic nitrogen in natural waters using high-temperature catalytic oxidation. *Trends Anal. Chem.* 22, 819–827. [https://doi.org/10.1016/S0165-9936\(03\)01202-0](https://doi.org/10.1016/S0165-9936(03)01202-0)
- Bastviken, D., Persson, L., Odham, G., Tranvik, L., 2004. Degradation of dissolved organic matter in oxic and anoxic lake water. *Limnol. Oceanogr.* 49, 109–116. <https://doi.org/10.4319/lo.2004.49.1.0109>
- Benjamini, Y., Hochberg, Y., 1995. Controlling the False Discovery Rate: A Practical and Powerful Approach to Multiple Testing. *J. R. Statist. Soc. B.* 57, 289–300.
- Bertilsson, S., Jones, J., 2003. Supply of Dissolved Organic Matter to Aquatic Ecosystems: Autochthonous Sources, in: Findlay, S., Sinsabaugh, R. (Eds.), *Aquatic Ecosystems: Interactivity of Dissolved Organic Matter*. Elsevier Science, USA, pp. 3–24.
- Bjørnsen, P.K., 1988. Phytoplankton exudation of organic matter: why do healthy cells do it? *Limnol. Oceanogr.* 33, 151–154.
- Boyer, E.W., Hornberger, G.M., Bencala, K.E., McKnight, D.M., 2000. Effects of asynchronous snowmelt on flushing of dissolved organic carbon: a mixing model approach. *Hydrol. Process.* 14, 3291–3308. [https://doi.org/10.1002/1099-1085\(20001230\)14:18<3291::AID-HYP202>3.0.CO;2-2](https://doi.org/10.1002/1099-1085(20001230)14:18<3291::AID-HYP202>3.0.CO;2-2)
- BPWTP, 2022. Buffalo Pound Water Treatment Plant Annual Report 2021. 77 p.
- BPWTP, 2021. Buffalo Pound Water Treatment Plant Annual Report 2020. 84 p.
- BPWTP, 2020. Buffalo Pound Water Treatment Plant Annual Report 2019. 72 p.
- BPWTP, 2017. Buffalo Pound Water Treatment Plant Annual Report 2016. 60 p.
- BPWTP, 2016. Buffalo Pound Water Treatment Plant Annual Report 2015. 60 p.
- Brimelow, J., Stewart, R., Hanesiak, J., Kochtubajda, B., Szeto, K., Bonsal, B., 2014. Characterization and assessment of the devastating natural hazards across the Canadian Prairie Provinces from 2009 to 2011. *Nat. Hazards* 73, 761–785. <https://doi.org/10.1007/s11069-014-1107-6>
- Brunet, N.N., Westbrook, C.J., 2012. Wetland drainage in the Canadian prairies: Nutrient, salt and bacteria characteristics. *Agric. Ecosyst. Environ.* 146, 1–12. <https://doi.org/10.1016/j.agee.2011.09.010>

- Buffam, I., Laudon, H., Temnerud, J., Mörth, C., Bishop, K., 2007. Landscape-scale variability of acidity and dissolved organic carbon during spring flood in a boreal stream network. *J. Geophys. Res. Biogeosci.* 112. <https://doi.org/10.1029/2006JG000218>
- Carlson, C.A., Hansell, D.A., 2015. Chapter 3 — DOM Sources, Sinks, Reactivity, and Budgets, in: Carlson, C.A., Hansell, D.A. (Eds.), *Biogeochemistry of Marine Dissolved Organic Matter*. Elsevier.
- Carpenter, K.D., Kraus, T.E.C., Goldman, J.G., Saraceno, J.F., Downing, B.D., Bergamaschi, B.A., McGhee, G., Triplett, T., 2013. Sources and Characteristics of Organic Matter in the Clackamas River, Oregon, Related to the Formation of Disinfection By-Products in Treated Drinking Water. U.S. Geological Survey Scientific Investigations Report 2013—5001, 78 p. <https://doi.org/10.3133/sir20135001>.
- Carstea, E.M., Popa, C.L., Baker, A., Bridgeman, J., 2020. In situ fluorescence measurements of dissolved organic matter: A review. *Sci. Total Environ.* 699, 134361. <https://doi.org/10.1016/j.scitotenv.2019.134361>
- Casas-Ruiz, J.P., Catalán, N., Gómez-Gener, L., von Schiller, D., Obrador, B., Kothawala, D.N., López, P., Sabater, S., Marcé, R., 2017. A tale of pipes and reactors: Controls on the in-stream dynamics of dissolved organic matter in rivers: Controls on in-stream DOM dynamics. *Limnol. Oceanogr.* 62, S85–S94. <https://doi.org/10.1002/lno.10471>
- Casas-Ruiz, J.P., Jakobsson, J., del Giorgio, P.A., 2021. The role of lake morphometry in modulating surface water carbon concentrations in boreal lakes. *Environ. Res. Lett.* 16, 074037. <https://doi.org/10.1088/1748-9326/ac0be3>
- Cavaliere, E., Baulch, H.M., 2020. Winter in two phases: Long-term study of a shallow reservoir in winter. *Limnol. Oceanogr.* 9999, 1–18. <https://doi.org/10.1002/lno.11687>
- Chen, C., Zhang, X., Zhu, L., Liu, J., He, W., Han, H., 2008. Disinfection by-products and their precursors in a water treatment plant in North China: Seasonal changes and fraction analysis. *Sci. Total Environ.* 397, 140–147. <https://doi.org/10.1016/j.scitotenv.2008.02.032>
- Chen, H., Zheng, B., Song, Y., Qin, Y., 2011. Correlation between molecular absorption spectral slope ratios and fluorescence humification indices in characterizing CDOM. *Aquat. Sci.* 73, 103–112. <https://doi.org/10.1007/s00027-010-0164-5>

- Chin, Y., Aiken, G., O'Loughlin, E., 1994. Molecular Weight, Polydispersity, and Spectroscopic Properties of Aquatic Humic Substances. *Environ. Sci. Technol.* 28, 1853–1858.
<https://doi.org/10.1021/es00060a015>
- Chow, A.T., Tanji, K.K., Gao, S., 2003. Production of dissolved organic carbon (DOC) and trihalomethane (THM) precursor from peat soils. *Water Res.* 37, 4475–4485.
[https://doi.org/10.1016/S0043-1354\(03\)00437-8](https://doi.org/10.1016/S0043-1354(03)00437-8)
- Clark, J.M., Bottrell, S.H., Evans, C.D., Monteith, D.T., Bartlett, R., Rose, R., Newton, R.J., Chapman, P.J., 2010. The importance of the relationship between scale and process in understanding long-term DOC dynamics. *Sci. Total Environ.* 408, 2768–2775.
<https://doi.org/10.1016/j.scitotenv.2010.02.046>
- Clark, J.M., Lane, S.N., Chapman, P.J., Adamson, J.K., 2007. Export of dissolved organic carbon from an upland peatland during storm events: Implications for flux estimates. *J. Hydrol.* 347, 438–447. <https://doi.org/10.1016/j.jhydrol.2007.09.030>
- Cohen, J., 1988. *Statistical Power Analysis for the Behavioral Sciences*, 2nd ed. Routledge Academic, New York, MNY.
- Cole, J.J., Prairie, Y.T., Caraco, N.F., McDowell, W.H., Tranvik, L.J., Striegl, R.G., Duarte, C.M., Kortelainen, P., Downing, J.A., Middelburg, J.J., Melack, J., 2007. Plumbing the Global Carbon Cycle: Integrating Inland Waters into the Terrestrial Carbon Budget. *Ecosystems* 10, 172–185. <https://doi.org/10.1007/s10021-006-9013-8>
- Cooke, G.D., Kennedy, R.H., 2001. Managing Drinking Water Supplies. *Lake Reserv. Manag.* 17, 157–174. <https://doi.org/10.1080/07438140109354128>
- Cory, R.M., Kling, G.W., 2018. Interactions between sunlight and microorganisms influence dissolved organic matter degradation along the aquatic continuum. *Limnol. Oceanogr. Lett.* 3, 102–116. <https://doi.org/10.1002/lol2.10060>
- Cory, R.M., McKnight, D.M., 2005. Fluorescence Spectroscopy Reveals Ubiquitous Presence of Oxidized and Reduced Quinones in Dissolved Organic Matter. *Environ. Sci. Technol.* 39, 8142–8149. <https://doi.org/10.1021/es0506962>
- Cory, R.M., McNeill, K., Cotner, J.P., Amado, A., Purcell, J.M., Marshall, A.G., 2010a. Singlet Oxygen in the Coupled Photochemical and Biochemical Oxidation of Dissolved Organic Matter. *Environ. Sci. Technol.* 44, 3683–3689. <https://doi.org/10.1021/es902989y>

- Cory, R.M., Miller, M.P., McKnight, D.M., Guerard, J.J., Miller, P.L., 2010b. Effect of instrument-specific response on the analysis of fulvic acid fluorescence spectra: Evaluating instrument-specific response. *Limnol. Oceanogr. Methods* 8, 67–78. <https://doi.org/10.4319/lom.2010.8.67>
- Couture, R.-M., Fischer, R., Van Cappellen, P., Gobeil, C., 2016. Non-steady state diagenesis of organic and inorganic sulfur in lake sediments. *Geochim. Cosmochim. Acta* 194, 15–33. <https://doi.org/10.1016/j.gca.2016.08.029>
- Couture, S., Houle, D., Gagnon, C., 2011. Increases of dissolved organic carbon in temperate and boreal lakes in Quebec, Canada. *Environ. Sci. Pollut. Res.* 19, 361–371.
- Croue, J.P., Debroux, J.F., Amy, G.L., Aiken, G.R., Leenheer, J.A., 1999. Natural organic matter: structural characteristics and reactive properties., in: Singer, P.C. (Ed.), *Formation and Control of Disinfection By-Products in Drinking Water*. American Water Works Association, Denver, CO, pp. 65–93.
- Deborde, M., von Gunten, U., 2008. Reactions of chlorine with inorganic and organic compounds during water treatment—Kinetics and mechanisms: A critical review. *Water Res.* 42, 13–51. <https://doi.org/10.1016/j.watres.2007.07.025>
- Del Vecchio, R., Blough, N.V., 2002. Photobleaching of chromophoric dissolved organic matter in natural waters: kinetics and modeling. *Mar. Chem.* 78, 231–253. [https://doi.org/10.1016/S0304-4203\(02\)00036-1](https://doi.org/10.1016/S0304-4203(02)00036-1)
- Dillon, P.J., Molot, L.A., 2005. Long-term trends in catchment export and lake retention of dissolved organic carbon, dissolved organic nitrogen, total iron, and total phosphorus: The Dorset, Ontario, study, 1978–1998. *J. Geophys. Res.* 110, G01002. <https://doi.org/10.1029/2004JG000003>
- Dillon, P.J., Molot, L.A., 1997. Effect of landscape form on export of dissolved organic carbon, iron, and phosphorus from forested stream catchments. *Water Resour. Res.* 33, 2591–2600. <https://doi.org/10.1029/97WR01921>
- Dinsmore, K.J., Billett, M.F., Dyson, K.E., 2013. Temperature and precipitation drive temporal variability in aquatic carbon and GHG concentrations and fluxes in a peatland catchment. *Glob. Chang. Biol.* 19, 2133–2148.
- Downing, J.A., Prairie, Y.T., Cole, J.J., Duarte, C.M., Tranvik, L.J., Striegl, R.G., McDowell, W.H., Kortelainen, P., Caraco, N.F., Melack, J.M., Middelburg, J.J., 2006. The global

- abundance and size distribution of lakes, ponds, and impoundments. *Limnol. Oceanogr.* 51, 2388–2397. <https://doi.org/10.4319/lo.2006.51.5.2388>
- D’Silva, L.P., 2017. Biological and physicochemical mechanisms affecting phosphorus and arsenic efflux from prairie reservoir sediment, Buffalo Pound Lake, SK, Canada. Master’s thesis, University of Saskatchewan.
- Eimers, M.C., Buttle, J.M., Watmough, S.A., 2008a. Influence of seasonal changes in runoff and extreme events on dissolved organic carbon trends in wetland- and upland-draining streams. *Can. J. Fish. Aquat. Sci.* 65, 796–808. <https://doi.org/10.1139/f07-194>
- Eimers, M.C., Watmough, S.A., Buttle, J.M., 2008b. Long-term trends in dissolved organic carbon concentration: a cautionary note. *Biogeochemistry* 87, 71–81. <https://doi.org/10.1007/s10533-007-9168-1>
- Elliott, J., 2013. Evaluating the potential contribution of vegetation as a nutrient source in snowmelt runoff. *Can. J. Soil. Sci.* 93, 435–443. <https://doi.org/10.4141/cjss2012-050>
- Elliott, J., Gallén, D., Tucker, A., 2008. Snowmelt Simulations to Determine the Source of Nutrients in Snowmelt Runoff. Environment Canada, Saskatoon, SK. 7pp.
- Evans, C.D., Chapman, P.J., Clark, J.M., Monteith, D.T., Cresser, M.S., 2006. Alternative explanations for rising dissolved organic carbon export from organic soils. *Glob. Chang. Biol.* 12, 2044–2053. <https://doi.org/10.1111/j.1365-2486.2006.01241.x>
- Evans, C.D., Goodale, C.L., Caporn, S.J.M., Dise, N.B., Emmett, B.A., Fernandez, I.J., Field, C.D., Findlay, S.E.G., Lovett, G.M., Meesenburg, H., Moldan, F., Sheppard, L.J., 2008. Does elevated nitrogen deposition or ecosystem recovery from acidification drive increased dissolved organic carbon loss from upland soil? A review of evidence from field nitrogen addition experiments. *Biogeochem.* 91, 13–35. <https://doi.org/10.1007/s10533-008-9256-x>
- Evans, C.D., Monteith, D.T., Cooper, D.M., 2005. Long-term increases in surface water dissolved organic carbon: Observations, possible causes and environmental impacts. *Environ. Pollut.* 137, 55–71. <https://doi.org/10.1016/j.envpol.2004.12.031>
- Exall, K., Vanloon, G., 2000. Using coagulants to remove organic matter. *J. Am. Water Works Assoc.* 92, 93–102.

- Fasching, C., Behounek, B., Singer, G.A., Battin, T.J., 2014. Microbial degradation of terrigenous dissolved organic matter and potential consequences for carbon cycling in brown-water streams. *Sci. Rep.* 4, 4981. <https://doi.org/10.1038/srep04981>
- Fennell, J., Bentley, L.R., 1998. Distribution of sulfate and organic carbon in a prairie till setting: Natural versus industrial sources. *Water Resour. Res.* 34, 1781–1794.
- Finlay, K., Leavitt, P.R., Patoine, A., Patoine, A., Wissel, B., 2010. Magnitudes and controls of organic and inorganic carbon flux through a chain of hard-water lakes on the northern Great Plains. *Limnol. Oceanogr.* 55, 1551–1564. <https://doi.org/10.4319/lo.2010.55.4.1551>
- Finlay, K., Vogt, R., Simpson, G., Leavitt, P., 2019. Seasonality of pCO₂ in a hard-water lake of the northern Great Plains: The legacy effects of climate and limnological conditions over 36 years. *Limnol Oceanogr* 64. <https://doi.org/10.1002/lno.11113>
- Fix, E., Hodges, J.L., 1951. Discriminatory Analysis. Nonparametric Discrimination: Consistency Properties. USAF School of Aviation Medicine, Randolph Field, Texas.
- Fleck, J.A., Gill, G., Bergamaschi, B.A., Kraus, T.E.C., Downing, B.D., Alpers, C.N., 2014. Concurrent photolytic degradation of aqueous methylmercury and dissolved organic matter. *Sci. Total Environ.* 484, 263–275. <https://doi.org/10.1016/j.scitotenv.2013.03.107>
- Fogg, G.E., 1983. The ecological significance of extracellular products of phytoplankton. *Bot. Mar.* 26, 3–14.
- Fogg, G.E., 1966. The extracellular products of algae. *Oceanogr. Mar. Biol. Annu. Rev.* 4, 195–212.
- Fox, J., Weisburg, S., 2019. *An R Companion to Applied Regression, Third Edition.* ed. Sage, Thousand Oaks, CA.
- Fram, M., Fujii, R., Weishaar, J., Bergamaschi, B., Aiken, G., 1999. How DOC Composition May Explain the Poor Correlation Between Specific Trihalomethane Formation Potential and Specific UV Absorbance. *Water-Resources Investigations Report 99–4018B*, Charleston, SC.
- Freeman, C., Fenner, N., Ostle, N.J., Kang, H., Dorrick, D.J., Reynolds, B., Lock, M.A., Sleep, D., Huges, S., Hudson, J., 2004. Export of dissolved organic carbon from peat lands under elevated carbon dioxide levels. *Nature* 430, 195–198.

- Frost, P.C., Larson, J.H., Johnston, C.A., Young, K.C., Maurice, P.A., Lamberti, G.A., Bridgham, S.D., 2006. Landscape predictors of stream dissolved organic matter concentration and physicochemistry in a Lake Superior river watershed. *Aquat. Sci.* 68, 40–51. <https://doi.org/10.1007/s00027-005-0802-5>
- Futter, M.N., Valinia, S., Löfgren, S., Köhler, S.J., Fölster, J., 2014. Long-term trends in water chemistry of acid-sensitive Swedish lakes show slow recovery from historic acidification. *AMBIO* 43, 77–90.
- Gober, P., Wheatler, H.S., 2014. Socio-hydrology and the science–policy interface: a case study of the Saskatchewan River basin. *Hydrol. Earth Syst. Sci.* 18, 1413–1422. <https://doi.org/10.5194/hess-18-1413-2014>
- Godwin, R.B., Martin, F.R.J., 1975. Calculation of Gross and Effective Drainage Areas for the Prairie Provinces, Canadian Hydrology Symposium - 1975 Proceedings, Winnipeg, Manitoba, 5 pp.
- Golea, D.M., Upton, A., Jarvis, P., Moore, G., Sutherland, S., Parsons, S.A., Judd, S.J., 2017. THM and HAA formation from NOM in raw and treated surface waters. *Water Res.* 112, 226–235. <https://doi.org/10.1016/j.watres.2017.01.051>
- Grinsted, A., Moore, J.C., Jevrejeva, S., 2004. Application of the cross wavelet transform and wavelet coherence to geophysical time series. *Nonlinear Process. Geophys.* 11, 561–566. <https://doi.org/10.5194/npg-11-561-2004>
- Gudasz, C., Bastviken, D., Steger, K., Premke, K., Sobek, S., Tranvik, L.J., 2010. Temperature-controlled organic carbon mineralization in lake sediments. *Nature* 466, 478–481. <https://doi.org/10.1038/nature09186>
- Guo, L., Cai, Y., Belzile, C., Macdonald, R.W., 2012. Sources and export fluxes of inorganic and organic carbon and nutrient species from the seasonally ice-covered Yukon River. *Biogeochem.* 107, 187–206. <https://doi.org/10.1007/s10533-010-9545-z>
- Haig, H.A., Hayes, N.M., Simpson, G.L., Yi, Y., Wissel, B., Hodder, K.R., Leavitt, P.R., 2021. Effects of seasonal and interannual variability in water isotopes ($\delta^2\text{H}$, $\delta^{18}\text{O}$) on estimates of water balance in a chain of seven prairie lakes. *J. Hydrol.* X. 10, 100069. <https://doi.org/10.1016/j.hydroa.2020.100069>

- Hall, R., Leavitt, P., Dixit, A., Quinlan, R., Smol, J., 1999. Limnological succession in reservoirs: a paleolimnological comparison of two methods of reservoir formation. *Can. J. Fish. Aquat. Sci.* 56, 1109–1121.
- Hammer, U.T., 1971. Limnological Studies of the Lakes and Streams of the Upper Qu'Appelle River System, Saskatchewan, Canada: I. Chemical and Physical Aspects of the Lakes and Drainage System. *Hydrobiologia* 37, 473–507.
- Hanesiak, J.M., Stewart, R.E., Bonsal, B.R., Harder, P., Lawford, R., Aider, R., Amiro, B.D., Atallah, E., Barr, A.G., Black, T.A., Bullock, P., Brimelow, J.C., Brown, R., Carmichael, H., Derksen, C., Flanagan, L.B., Gachon, P., Greene, H., Gyakum, J., Henson, W., Hogg, E.H., Kochtubajda, B., Leighton, H., Lin, C., Luo, Y., McCaughey, J.H., Meinert, A., Shabbar, A., Snelgrove, K., Szeto, K., Trishchenko, A., van der Kamp, G., Wang, S., Wen, L., Wheaton, E., Wielki, C., Yang, Y., Yirdaw, S., Zha, T., 2011. Characterization and Summary of the 1999–2005 Canadian Prairie Drought. *Atmos. Ocean.* 49, 421–452. <https://doi.org/10.1080/07055900.2011.626757>
- Hansen, A., Fleck, J., Kraus, T., Downing, B., von Dessonneck, T., Bergamaschi, B., 2018. Procedures for Using the Horiba Scientific Aqualog® Fluorometer to Measure Absorbance and Fluorescence from Dissolved Organic Matter: U.S. Geological Survey Open-File Report 2018–1096, 31 p.
- Hansen, A.M., Kraus, T.E.C., Pellerin, B.A., Fleck, J.A., Downing, B.D., Bergamaschi, B.A., 2016. Optical properties of dissolved organic matter (DOM): Effects of biological and photolytic degradation. *Limnol. Oceanogr.* 61, 1015–1032. <https://doi.org/10.1002/lno.10270>
- Health Canada, 2008. Guidelines for Canadian Drinking Water Quality: Guideline Technical Document — Haloacetic Acids. Water, Air and Climate Change Bureau, Healthy Environments and Consumer Safety Branch, Health Canada, Ottawa, Ontario.
- Health Canada, 2006. Guidelines for Canadian Drinking Water Quality: Guideline Technical Document — Trihalomethanes. Water Quality and Health Bureau, Healthy Environments and Consumer Safety Branch, Health Canada, Ottawa, Ontario.
- Heeb, M.B., Criquet, J., Zimmermann-Steffens, S.G., von Gunten, U., 2014. Oxidative treatment of bromide-containing waters: Formation of bromine and its reactions with inorganic and

- organic compounds — A critical review. *Water Res.* 48, 15–42.
<https://doi.org/10.1016/j.watres.2013.08.030>
- Helms, J., Stubbins, A., Ritchie, J., Minor, E., Kieber, D., Mopper, K., 2008. Absorption spectral slopes and slope ratios as indicators of molecular weight, source, and photobleaching of chromophoric dissolved organic matter. *Limnology and Oceanography* 53, 955–969.
<https://doi.org/10.4319/lo.2008.53.3.0955>
- Helms, J.R., Stubbins, A., Perdue, E.M., Green, N.W., Chen, H., Mopper, K., 2013. Photochemical bleaching of oceanic dissolved organic matter and its effect on absorption spectral slope and fluorescence. *Mar. Chem.* 155, 81–91.
<https://doi.org/10.1016/j.marchem.2013.05.015>
- Holmer, M., Storkholm, P., 2001. Sulphate reduction and sulphur cycling in lake sediments: a review: Sulphate cycling in lake sediments. *Freshwater Biology* 46, 431–451.
<https://doi.org/10.1046/j.1365-2427.2001.00687.x>
- Hongve, D., Riise, G., Kristiansen, J.F., 2004. Increased colour and organic acid concentrations in Norwegian forest lakes and drinking water - a result of increased precipitation. *Aquat. Sci.* 66, 231–238.
- Howard, D.W., Hounshell, A.G., Lofton, M.E., Woelmer, W.M., Hanson, P.C., Carey, C.C., 2021. Variability in fluorescent dissolved organic matter concentrations across diel to seasonal time scales is driven by water temperature and meteorology in a eutrophic reservoir. *Aquat. Sci.* 83, 30. <https://doi.org/10.1007/s00027-021-00784-w>
- Hrudey, S., Fawell, J., 2015. 40 years on: what do we know about drinking water disinfection by-products (DBPs) and human health? *Water Supply* 15, 667–674.
<https://doi.org/doi.org/10.2166/ws.2015.036>
- Hruška, J., Krám, P., McDowell, W.H., Oulehle, F., 2009. Increased Dissolved Organic Carbon (DOC) in Central European Streams is driven by reductions in Ionic Strength Rather than Climate Change or decreasing Acidity. *Environ. Sci. Technol.* 43, 4320–4326.
- Hudson, J.J., Dillon, P.J., Somers, K.M., 2003. Long-term patterns in dissolved organic carbon in boreal lakes: the role of incident radiation, precipitation, air temperature, southern oscillation and acid deposition. *Hydrol. Earth Syst. Sci.* 7, 390–398.
<https://doi.org/10.5194/hess-7-390-2003>

- Huguet, A., Vacher, L., Relexans, S., Saubusse, S., Froidefond, J.M., Parlanti, E., 2009. Properties of fluorescent dissolved organic matter in the Gironde Estuary. *Org. Geochem.* 40, 706–719. <https://doi.org/10.1016/j.orggeochem.2009.03.002>
- Jafari, M., Ansari-Pour, N., 2019. Why, When and How to Adjust Your P Values? *Cell J.* 20, 604–607. <https://doi.org/10.22074/cellj.2019.5992>
- Jaffé, R., McKnight, D., Maie, N., Cory, R., McDowell, W.H., Campbell, J.L., 2008. Spatial and temporal variations in DOM composition in ecosystems: The importance of long-term monitoring of optical properties. *J. Geophys. Res. Biogeosci.* 113, G04032. <https://doi.org/10.1029/2008JG000683>
- Jane, S.F., Winslow, L.A., Remucal, C.K., Rose, K.C., 2017. Long-term trends and synchrony in dissolved organic matter characteristics in Wisconsin, USA, lakes: Quality, not quantity, is highly sensitive to climate. *J. Geophys. Res. Biogeosci.* 122, 546–561. <https://doi.org/10.1002/2016JG003630>
- Jeffrey, S., Humphrey, G., 1975. New Spectrophotometric Equations for Determining Chlorophylls a, b, c1, and c2 in Higher Plants, Algae and Natural Phytoplankton. *Biochem. Physiol. Pflanzen* 167, 191–194. [https://doi-org.cyber.usask.ca/10.1016/S0015-3796\(17\)30778-3](https://doi-org.cyber.usask.ca/10.1016/S0015-3796(17)30778-3)
- Jensen, H.S., Nielsen, O.I., Koch, M.S., de Vicente, I., 2009. Phosphorus release with carbonate dissolution coupled to sulfide oxidation in Florida Bay seagrass sediments. *Limnol. Oceanogr.* 54, 1753–1764. <https://doi.org/10.4319/lo.2009.54.5.1753>
- Kalbitz, K., Geyer, W., Geyer, S., 1999. Spectroscopic properties of dissolved humic substances – a reflection of land use history in a fen area. *Biogeochemistry* 47, 219–238. <https://doi.org/10.1007/BF00994924>
- Kalinin, A., Covino, T., McGlynn, B., 2016. The influence of an in-network lake on the timing, form, and magnitude of downstream dissolved organic carbon and nutrient flux. *Water Resour. Res.* 52, 8668–8684. <https://doi.org/10.1002/2016WR019378>
- Kassambara, A., 2021. rstatix: Pipe-Friendly Framework for Basic Statistical Tests. R package version 0.7.0.
- Kehoe, M.J., Chun, K.P., Baulch, H.M., 2015. Who Smells? Forecasting Taste and Odor in a Drinking Water Reservoir. *Environ. Sci. Technol.* 49, 10984–10992. <https://doi.org/10.1021/acs.est.5b00979>

- Kellerman, A.M., Dittmar, T., Kothawala, D.N., Tranvik, L.J., 2014. Chemodiversity of dissolved organic matter in lakes driven by climate and hydrology. *Nat. Commun.* 5, 3804. <https://doi.org/10.1038/ncomms4804>
- Kirk, J.T.O., 1994. *Light and Photosynthesis in Aquatic Ecosystems*, 2nd ed. Cambridge University Press, Cambridge, United Kingdom.
- Klaminder, J., Bindler, R., Laudon, H., Bishop, K., Emteryd, O., Renberg, I., 2006. Flux Rates of Atmospheric Lead Pollution within Soils of a Small Catchment in Northern Sweden and Their Implications for Future Stream Water Quality. *Environ. Sci. Technol.* 40, 4639–4645. <https://doi.org/10.1021/es0520666>
- Kortelainen, P., 1993. Content of Total Organic Carbon in Finnish Lakes and Its Relationship to Catchment Characteristics. *Can. J. Fish. Aquat. Sci.* 50, 1477–1483. <https://doi.org/10.1139/f93-168>
- Kraus, T.E.C., Bergamaschi, B.A., Hernes, P.J., Doctor, D., Kendall, C., Downing, B.D., Losee, R.F., 2011. How reservoirs alter drinking water quality: Organic matter sources, sinks, and transformations. *Lake Reserv. Manag.* 27, 205–219. <https://doi.org/10.1080/07438141.2011.597283>
- Kurek, M.R., Frey, K.E., Guillemette, F., Podgorski, D.C., Townsend-Small, A., Arp, C.D., Kellerman, A.M., Spencer, R.G.M., 2022. Trapped Under Ice: Spatial and Seasonal Dynamics of Dissolved Organic Matter Composition in Tundra Lakes. *J. Geophys. Res. Biogeosci.* 127, e2021JG006578. <https://doi.org/10.1029/2021JG006578>
- Labagh, J.W., Winter, T.C., Adomaitis, V.A., Swanson, G.A., 1987. Hydrology and chemistry of selected prairie wetlands in the Cottonwood Lake area, Stutsman County, North Dakota, 1979-82. Professional Paper 1431. United States Geological Survey. 31 pp.
- Lampert, W., 1978. Release of dissolved organic carbon by grazing zooplankton. *Limnol. Oceanogr.* 23, 831–834. <https://doi.org/10.4319/lo.1978.23.4.0831>
- Larson, J.H., Frost, P.C., Xenopoulos, M.A., Williams, C.J., Morales-Williams, A.M., Vallazza, J.M., Nelson, J.C., Richardson, W.B., 2014. Relationships Between Land Cover and Dissolved Organic Matter Change Along the River to Lake Transition. *Ecosystems* 17, 1413–1425. <https://doi.org/10.1007/s10021-014-9804-2>
- Laudon, H., Berggren, M., Ågren, A., Buffam, I., Bishop, K., Grabs, T., Jansson, M., Köhler, S., 2011. Patterns and Dynamics of Dissolved Organic Carbon (DOC) in Boreal Streams:

- The Role of Processes, Connectivity, and Scaling. *Ecosystems* 14, 880–893.
<https://doi.org/10.1007/s10021-011-9452-8>
- Laudon, H., Kohler, S., Buffam, I., 2004. Seasonal TOC export from seven boreal catchments in northern Sweden. *Aquat. Sci.* 66, 223–230.
- Lavonen, E.E., Gonsior, M., Tranvik, L.J., Schmitt-Kopplin, P., Köhler, S.J., 2013. Selective Chlorination of Natural Organic Matter: Identification of Previously Unknown Disinfection Byproducts. *Environ. Sci. Technol.* 47, 2264–2271.
<https://doi.org/10.1021/es304669p>
- Lawaetz, A.J., Stedmon, C.A., 2009. Fluorescence Intensity Calibration Using the Raman Scatter Peak of Water. *Appl. Spectrosc.* 63, 936–940.
<https://doi.org/10.1366/000370209788964548>
- LeChevallier, M.W., Welch, N.J., Smith, D.B., 1996. Full-scale studies of factors related to coliform regrowth in drinking water. *Appl. Environ. Microbiol.* 62, 2201–2211.
- Lepistö, A., Futter, M.N., Kortelainen, P., 2014. Almost 50 years of monitoring shows that climate, not forestry, controls long-term organic carbon fluxes in a large boreal watershed. *Glob. Chang. Biol.* 20, 1225–1237. <https://doi.org/10.1111/gcb.12491>
- Levene, H., 1960. Robust tests for equality of variances, in: Olkin, I., Hotelling, H. (Eds.), *Contributions to Probability and Statistics: Essays in Honor of Harold Hotelling*. Stanford University Press, pp. 278–292.
- Li, C., Benjamin, M., Korshin, G., 2000. Use of UV Spectroscopy To Characterize the Reaction between NOM and Free Chlorine. *Environ. Sci. Technol.* 34, 2570–2575.
<https://doi.org/10.1021/es990899o>
- Li, X., Mitch, W., 2018. Drinking Water Disinfection Byproducts (DBPs) and Human Health Effects: Multidisciplinary Challenges and Opportunities. *Environ. Sci. Technol.* 52, 1681–1689. <https://doi.org/10.1021/acs.est.7b05440>
- Liao, X., Chen, C., Yuan, B., Wang, J., Zhang, X., 2017. Control of Nitrosamines, THMs, and HAAs in Heavily Impacted Water with O3-BAC. *J. Am. Water Works Assoc.* 109, E215–E225. <https://doi.org/10.5942/jawwa.2017.109.0057>
- Liu, J., Elliott, J.A., Wilson, H.F., Macrae, M.L., Baulch, H.M., Lobb, D.A., 2021. Phosphorus runoff from Canadian agricultural land: A cross-region synthesis of edge-of-field results.

- Agricultural Water Management 255, 107030.
<https://doi.org/10.1016/j.agwat.2021.107030>
- Liu, K., Elliott, J.A., Lobb, D.A., Flaten, D.N., Yarotski, J., 2014. Conversion of Conservation Tillage to Rotational Tillage to Reduce Phosphorus Losses during Snowmelt Runoff in the Canadian Prairies. *J. Environ. Qual.* 43, 1679–1689.
<https://doi.org/10.2134/jeq2013.09.0365>
- Maheux, H., Leavitt, P.R., Jackson, L.J., 2016. Asynchronous onset of eutrophication among shallow prairie lakes of the Northern Great Plains, Alberta, Canada. *Glob. Chang. Biol.* 22, 271–283. <https://doi.org/10.1111/gcb.13076>
- Mash, H., Westerhoff, P.K., Baker, L.A., Nieman, R.A., Nguyen, M.-L., 2004. Dissolved organic matter in Arizona reservoirs: assessment of carbonaceous sources. *Org. Geochem.* 35, 831–843. <https://doi.org/10.1016/j.orggeochem.2004.03.002>
- Matilainen, A., Gjessing, E.T., Lahtinen, T., Hed, L., Bhatnagar, A., Sillanpää, M., 2011. An overview of the methods used in the characterisation of natural organic matter (NOM) in relation to drinking water treatment. *Chemosphere* 83, 1431–1442.
<https://doi.org/10.1016/j.chemosphere.2011.01.018>
- McCormack, A., Erlich, A., 2019. mapcan: Tools for Plotting Canadian Choropleth Maps and Choropleth Alternatives. R package version 0.0.1.
- McDowell, W.H., Likens, G.E., 1988. Origin, Composition, and Flux of Dissolved Organic Carbon in the Hubbard Brook Valley. *Ecol. Monogr.* 58, 177–195.
<https://doi.org/10.2307/2937024>
- McFarlan, L.S., 2021. Where’s the P in prairie potholes? Identifying patterns of phosphorus accumulation in Canadian prairie wetlands. Master’s thesis, University of Saskatchewan.
- McGowan, S., Leavitt, P.R., Hall, R.I., 2005. A Whole-Lake Experiment to Determine the Effects of Winter Droughts on Shallow Lakes. *Ecosystems* 8, 694–708.
<https://doi.org/10.1007/s10021-003-0152-x>
- McKnight, D.M., Boyer, E.W., Westerhoff, P.K., Doran, P.T., Kulbe, T., Andersen, D.T., 2001. Spectrofluorometric characterization of dissolved organic matter for indication of precursor organic material and aromaticity. *Limnol. Oceanogr.* 46, 38–48.
<https://doi.org/10.4319/lo.2001.46.1.0038>

- Meingast, K.M., Kane, E.S., Coble, A.A., Marcarelli, A.M., Toczydlowski, D., 2020. Climate, snowmelt dynamics and atmospheric deposition interact to control dissolved organic carbon export from a northern forest stream over 26 years. *Environ. Res. Lett.* 15, 104034. <https://doi.org/10.1088/1748-9326/ab9c4e>
- Miller, M.P., McKnight, D.M., 2010. Comparison of seasonal changes in fluorescent dissolved organic matter among aquatic lake and stream sites in the Green Lakes Valley. *J. Geophys. Res.* 115, G00F12. <https://doi.org/10.1029/2009JG000985>
- Monteith, D.T., Stoddard, J.L., Evans, C.D., de Wit, H.A., Forsius, M., Høgåsen, T., Wilander, A., Skjelkvåle, B.L., Jeffries, D.S., Vuorenmaa, J., Keller, B., Kopáček, J., Vesely, J., 2007. Dissolved organic carbon trends resulting from changes in atmospheric deposition chemistry. *Nature* 450, 537–540. <https://doi.org/10.1038/nature06316>
- Murphy, K.R., Butler, K.D., Spencer, R.G.M., Stedmon, C.A., Boehme, J.R., Aiken, G.R., 2010. Measurement of Dissolved Organic Matter Fluorescence in Aquatic Environments: An Interlaboratory Comparison. *Environ. Sci. Technol.* 44, 9405–9412. <https://doi.org/10.1021/es102362t>
- Myklestad, S.M., 1995. Release of extracellular products by phytoplankton with special emphasis on polysaccharides. *Sci. Total Environ., Marine Mucilages* 165, 155–164. [https://doi.org/10.1016/0048-9697\(95\)04549-G](https://doi.org/10.1016/0048-9697(95)04549-G)
- Nachshon, U., Ireson, A., van der Kamp, G., Davies, S.R., Wheeler, H.S., 2014. Impacts of climate variability on wetland salinization in the North American prairies. *Hydrol. Earth Syst. Sci.* 18, 1251–1263. <https://doi.org/10.5194/hess-18-1251-2014>
- North, R.L., Johansson, J., Vandergucht, D.M., Doig, L.E., Liber, K., Lindenschmidt, K.-E., Baulch, H., Hudson, J.J., 2015. Evidence for internal phosphorus loading in a large prairie reservoir (Lake Diefenbaker, Saskatchewan). *J. Great Lakes Res.* 41, 91–99. <https://doi.org/10.1016/j.jglr.2015.07.003>
- Obernosterer, I., Reitner, B., Herndl, G.J., 1999. Contrasting effects of solar radiation on dissolved organic matter and its bioavailability to marine bacterioplankton. *Limnol. Oceanogr.* 44, 1645–1654. <https://doi.org/10.4319/lo.1999.44.7.1645>
- Ohno, T., 2002. Fluorescence Inner-Filtering Correction for Determining the Humification Index of Dissolved Organic Matter. *Environ. Sci. Technol.* 36, 742–746. <https://doi.org/10.1021/es0155276>

- Orihel, D.M., Schindler, D.W., Ballard, N.C., Graham, M.D., O'Connell, D.W., Wilson, L.R., Vinebrooke, R.D., 2015. The “nutrient pump:” Iron-poor sediments fuel low nitrogen-to-phosphorus ratios and cyanobacterial blooms in polymictic lakes: Low iron and polymixis fuel blooms. *Limnol. Oceanogr.* 60, 856–871. <https://doi.org/10.1002/lno.10076>
- Osburn, C.L., Wigdahl, C.R., Fritz, S.C., Saros, J.E., 2011. Dissolved organic matter composition and photoreactivity in prairie lakes of the U.S. Great Plains. *Limnol. Oceanogr.* 56, 2371–2390. <https://doi.org/10.4319/lo.2011.56.6.2371>
- Pace, M.L., Cole, J.J., 2002. Synchronous variation of dissolved organic carbon and color in lakes. *Limnol. Oceanogr.* 47, 333–342. <https://doi.org/10.4319/lo.2002.47.2.0333>
- Pagano, T., Bida, M., Kenny, J., 2014. Trends in Levels of Allochthonous Dissolved Organic Carbon in Natural Water: A Review of Potential Mechanisms under a Changing Climate. *Water* 6, 2862–2897. <https://doi.org/10.3390/w6102862>
- Painter, K.J., Venkiteswaran, J.J., Baulch, H., 2022a. Blooms and flows: Effects of variable hydrology and management on reservoir water quality (preprint). *Environmental Sciences*. <https://doi.org/10.1002/essoar.10512334.2>
- Painter, K.J., Venkiteswaran, J.J., Simon, D.F., Vo Duy, S., Sauvé, S., Baulch, H.M., 2022b. Early and late cyanobacterial bloomers in a shallow, eutrophic lake. *Environ. Sci. Process. Impacts* 24, 1212–1227. <https://doi.org/10.1039/D2EM00078D>
- Parlanti, E., Wörz, K., Geoffroy, L., Lamotte, M., 2000. Dissolved organic matter fluorescence spectroscopy as a tool to estimate biological activity in a coastal zone submitted to anthropogenic inputs. *Org. Geochem.* 31, 1765–1781. [https://doi.org/10.1016/S0146-6380\(00\)00124-8](https://doi.org/10.1016/S0146-6380(00)00124-8)
- Pärn, J., Mander, Ü., 2012. Increased organic carbon concentrations in Estonian rivers in the period 1992-2007 as affected by deepening droughts. *Biogeochem.* 108, 351–358.
- Pedersen, T.L., 2020. patchwork: The Composer of Plots. R package version 1.1.1. <https://CRAN.R-project.org/package=patchwork>.
- Pham, S.V., Leavitt, P.R., McGowan, S., Wissel, B., Wassenaar, L.I., 2009. Spatial and temporal variability of prairie lake hydrology as revealed using stable isotopes of hydrogen and oxygen. *Limnol. Oceanogr.* 54, 101–118. <https://doi.org/10.4319/lo.2009.54.1.0101>

- Piirsoo, K., Viik, M., Kõiv, T., Käiro, K., Laas, A., Nõges, T., Pall, P., Selberg, A., Toomsalu, L., Vilbaste, S., 2012. Characteristics of dissolved organic matter in the inflows and in the outflow of Lake Võrtsjärv, Estonia. *J. Hydrol.* 475, 306–313.
<https://doi.org/10.1016/j.jhydrol.2012.10.015>
- Pomeroy, J.W., Gray, D.M., Brown, T., Hedstrom, N.R., Quinton, W.L., Granger, R.J., Carey, S.K., 2007. The cold regions hydrological model: a platform for basing process representation and model structure on physical evidence. *Hydrol. Process.* 21, 2650–2667. <https://doi.org/10.1002/hyp.6787>
- Porcal, P., Koprivnjak, J.-F., Molot, L.A., Dillon, P.J., 2009. Humic substances—part 7: the biogeochemistry of dissolved organic carbon and its interactions with climate change. *Environ. Sci. Pollut. Res.* 16, 714–726. <https://doi.org/10.1007/s11356-009-0176-7>
- Prairie, Y.T., 2008. Carbocentric limnology: looking back, looking forward. *Can. J. Fish. Aquat. Sci.* 65, 543–548. <https://doi.org/10.1139/f08-011>
- Pyra, N., Wood, S.N., 2016. A note on basis dimension selection in generalized additive modelling. *arXiv*. [https://doi.org/A note on basis dimension selection in generalized additive modelling](https://doi.org/A%20note%20on%20basis%20dimension%20selection%20in%20generalized%20additive%20modelling)
- Qiu, L., Cui, H., Wu, J., Wang, B., Zhao, Y., Li, J., Jia, L., Wei, Z., 2016. Snowmelt-driven changes in dissolved organic matter and bacterioplankton communities in the Heilongjiang watershed of China. *Sci. Total Environ.* 556, 242–251.
<https://doi.org/10.1016/j.scitotenv.2016.02.199>
- R Core Team, 2022. *R: A Language and Environment for Statistical Computing*.
- Randtke, S., 1999. Chapter 12: By-Product Precursor Removal by Coagulation and Precipitative Softening, in: Singer, P. (Ed.), *Formation and Control of Disinfection By-Products in Drinking Water*. American Water Works Association, Denver, CO, pp. 237–258.
- Ravichandran, M., 2004. Interactions between mercury and dissolved organic matter—a review. *Chemosphere* 55, 319–331. <https://doi.org/10.1016/j.chemosphere.2003.11.011>
- Reckhow, D.A., Singer, P.C., Malcolm, R.L., 1990. Chlorination of humic materials: byproduct formation and chemical interpretations. *Environ. Sci. Technol.* 24, 1655–1664.
<https://doi.org/10.1021/es00081a005>

- Reuman, D.C., Anderson, T.L., Walter, J.A., Zhao, L., Sheppard, L.W., 2021. *wsyn: Wavelet Approaches to Studies of Synchrony in Ecology and Other Fields*. R package version 1.0.4.
- Rodríguez-Cardona, B.M., Wymore, A.S., Argerich, A., Barnes, R.T., Bernal, S., Brookshire, E.N.J., Coble, A.A., Dodds, W.K., Fazekas, H.M., Helton, A.M., Johnes, P.J., Johnson, S.L., Jones, J.B., Kaushal, S.S., Kortelainen, P., López-Lloreda, C., Spencer, R.G.M., McDowell, W.H., 2022. Shifting stoichiometry: Long-term trends in stream-dissolved organic matter reveal altered C:N ratios due to history of atmospheric acid deposition. *Glob. Chang. Biol.* 28, 98–114. <https://doi.org/10.1111/gcb.15965>
- Rodríguez-Murillo, J.C., Zobrist, J., Filella, M., 2015. Temporal trends in organic carbon content in the main Swiss rivers, 1974–2010. *Sci. Total Environ.* 502, 206–217. <https://doi.org/10.1016/j.scitotenv.2014.08.096>
- Romera-Castillo, C.R., Sarmiento, H., Álvarez-Salgado, X.A., Gasol, J.M., Marraséa, C., 2010. Production of chromophoric dissolved organic matter by marine phytoplankton. *Limnol. Oceanogr.* 55, 446–454. <https://doi.org/10.4319/lo.2010.55.1.0446>
- Rostad, C.E., Leenheer, J.A., Daniel, S.R., 1997. Organic Carbon and Nitrogen Content Associated with Colloids and Suspended Particulates from the Mississippi River and Some of Its Tributaries. *Environ. Sci. Technol.* 31, 3218–3225. <https://doi.org/10.1021/es970196b>
- Royston, P., 1995. Remark AS R94: A Remark on Algorithm AS 181: The W-test for Normality. *J. Appl. Stat.* 44, 547. <https://doi.org/10.2307/2986146>
- Sakia, R.M., 1992. The Box-Cox Transformation Technique: A Review. *J. R. Stat. Soc. Ser. D. Stat.* 41, 169–178. <https://doi.org/10.2307/2348250>
- Saskatchewan Environment and Resources Management, 2001. Buffalo Pound Lake Land Use and Resource Management Plan. 28 pp.
- Schiff, S.L., Aravena, R., Trumbore, S.E., Hinton, M.J., Elgood, R., Dillon, P.J., 1997. Export of DOC from forested catchments on the Precambrian Shield of Central Ontario: Clues from ¹³C and ¹⁴C. *Biogeochemistry* 36, 43–65.
- Schindler, D.W., Donahue, W.F., 2006. An impending water crisis in Canada's western prairie provinces. *Proc. Natl. Acad. Sci. U.S.A.* 103, 7210–7216. <https://doi.org/10.1073/pnas.0601568103>

- Schlesinger, W., Bernhardt, E., 2013. *Biogeochemistry*, 3rd ed. Elsevier, Academic Press, Waltham, MA.
- Schreiber, T., Schmitz, A., 2000. Surrogate time series. *Phys. D: Nonlinear Phenom.* 142, 346–382. [https://doi.org/10.1016/S0167-2789\(00\)00043-9](https://doi.org/10.1016/S0167-2789(00)00043-9)
- Shapiro, S.S., Wilk, M.B., 1965. An analysis of variance test for normality (complete samples). *Biometrika* 52, 591–611. <https://doi.org/10.1093/biomet/52.3-4.591>
- Sheppard, L., Reid, P., Reuman, D., 2017. Rapid surrogate testing of wavelet coherences. *Nonlinear Biomed. Phys.* 5, 1. <https://doi.org/10.1051/epjnbp/2017000>
- Sheppard, L.W., Bell, J.R., Harrington, R., Reuman, D.C., 2016. Changes in large-scale climate alter spatial synchrony of aphid pests. *Nat. Clim. Chang.* 6, 610–613. <https://doi.org/10.1038/nclimate2881>
- Sheppard, L.W., Defriez, E.J., Reid, P.C., Reuman, D.C., 2019. Synchrony is more than its top-down and climatic parts: interacting Moran effects on phytoplankton in British seas. *PLoS Comput. Biol.* 15, e1006744. <https://doi.org/10.1371/journal.pcbi.1006744>
- Shook, K., Pomeroy, J., 2012. Changes in the hydrological character of rainfall on the Canadian prairies. *Hydrol. Process.* 26, 1752–1766. <https://doi.org/10.1002/hyp.9383>
- Simpson, G.L., 2021. *gratia: Graceful 'ggplot'-Based Graphics and Other Function for GAMs Fitted Using "mgcv"*. R package version 0.6.0.
- Simpson, G.L., 2018. Modelling Palaeoecological Time Series Using Generalised Additive Models. *Front. Ecol. Evol.* 6, 21. <https://doi.org/10.3389/fevo.2018.00149>
- Sobek, S., Tranvik, L.J., Prairie, Y.T., Kortelainen, P., Cole, J.J., 2007. Patterns and regulation of dissolved organic carbon: An analysis of 7,500 widely distributed lakes. *Limnol. Oceanogr.* 52, 1208–1219. <https://doi.org/10.4319/lo.2007.52.3.1208>
- Statistics Canada, 2011. *Water File - Lakes and Rivers (polygons) - 2011 Census*.
- Statistics Canada, 2006. *Water File - Rivers (lines) - 2006 Census*.
- Stepanauskas, R., Moran, M.A., Bergamaschi, B.A., Hollibaugh, J.T., 2005. Sources, bioavailability, and photoreactivity of dissolved organic carbon in the Sacramento–San Joaquin River Delta. *Biogeochemistry* 74, 131–149. <https://doi.org/10.1007/s10533-004-3361-2>

- Striegl, R., Aiken, G., Dornblaser, M., Raymod, P., Wickland, K., 2005. A decrease in discharge-normalized DOC export by the Yukon River during summer through autumn. *Geophys. Res. Lett.* 32. <https://doi.org/doi:10.1029/2005GL024413>
- Student, 1908. The probable error of a mean. *Biometrika* 1–25.
- Swarbrick, V.J., Simpson, G.L., Glibert, P.M., Leavitt, P.R., 2019. Differential stimulation and suppression of phytoplankton growth by ammonium enrichment in eutrophic hardwater lakes over 16 years. *Limnol. Oceanogr.* 64. <https://doi.org/10.1002/lno.11093>
- Temnerud, J., Hytteborn, J.K., Futter, M.N., Köhler, S.J., 2014. Evaluating common drivers for color, iron and organic carbon in Swedish watercourses. *AMBIO* 43, 30–44. <https://doi.org/10.1007/s13280-014-0560-5>
- Thurman, E., 1985. *Organic geochemistry of natural waters*. Kluwer Academic Publishers Group, Dordrecht.
- Tittel, J., Kamjunke, N., 2004. Metabolism of dissolved organic carbon by planktonic bacteria and mixotrophic algae in lake neutralisation experiments. *Freshw. Biol.* 49, 1062–1071. <https://doi.org/10.1111/j.1365-2427.2004.01241.x>
- Traina, S.J., Novak, J., Smeck, N.E., 1990. An Ultraviolet Absorbance Method of Estimating the Percent Aromatic Carbon Content of Humic Acids. *Journal of Environmental Quality* 19, 151–153. <https://doi.org/10.2134/jeq1990.00472425001900010023x>
- Tranvik, L.J., Downing, J.A., Cotner, J.B., Loiselle, S.A., Striegl, R.G., Ballatore, T.J., Dillon, P., Finlay, K., Fortino, K., Knoll, L.B., Kortelainen, P.L., Kutser, T., Larsen, Soren., Laurion, I., Leech, D.M., McCallister, S.L., McKnight, D.M., Melack, J.M., Overholt, E., Porter, J.A., Prairie, Y., Renwick, W.H., Roland, F., Sherman, B.S., Schindler, D.W., Sobek, S., Tremblay, A., Vanni, M.J., Verschoor, A.M., von Wachenfeldt, E., Weyhenmeyer, G.A., 2009. Lakes and reservoirs as regulators of carbon cycling and climate. *Limnol. Oceanogr.* 54, 2298–2314. https://doi.org/10.4319/lno.2009.54.6_part_2.2298
- Tweedie, M.C.K., 1984. An index which distinguishes between some important exponential families. In *Statistics: Applications and New Directions*. Proceedings of the Indian Statistical Institute Golden Jubilee International Conference. Eds. J. K. Ghosh and J. Roy. pp., 579-604. Calcutta: Indian Statistical Institute.

- Vogt, R.J., Sharma, S., Leavitt, P.R., 2018. Direct and interactive effects of climate, meteorology, river hydrology, and lake characteristics on water quality in productive lakes of the Canadian Prairies. *Can. J. Fish. Aquat. Sci.* 75, 47–59.
<https://doi.org/10.1139/cjfas-2016-0520>
- Wagner, E.D., Plewa, M.J., 2017. CHO cell cytotoxicity and genotoxicity analyses of disinfection by-products: An updated review. *Journal of Environmental Sciences, water treatment and disinfection by-products* 58, 64–76.
<https://doi.org/10.1016/j.jes.2017.04.021>
- Waiser, M.J., 2006. Relationship between hydrological characteristics and dissolved organic carbon concentration and mass in northern prairie wetlands using a conservative tracer approach. *J. Geophys. Res. Biogeosci.* 111, G02024.
<https://doi.org/10.1029/2005JG000088>
- Waiser, M.J., Robarts, R.D., 2000. Changes in composition and reactivity of allochthonous DOM in a prairie saline lake. *Limnol. Oceanogr.* 45, 763–774.
<https://doi.org/10.4319/lo.2000.45.4.0763>
- Walter, J.A., Fleck, R., Kastens, J.H., Pace, M.L., Wilkinson, G.M., 2021. Temporal Coherence Between Lake and Landscape Primary Productivity. *Ecosystems* 24, 502–515.
<https://doi.org/10.1007/s10021-020-00531-6>
- Wang, X., Zhang, H., Zhang, Y., Shi, Q., Wang, J., Yu, J., Yang, M., 2017. New Insights into Trihalomethane and Haloacetic Acid Formation Potentials: Correlation with the Molecular Composition of Natural Organic Matter in Source Water [WWW Document]. ACS Publications. <https://doi.org/10.1021/acs.est.6b04817>
- Water Security Agency, 2018. Qu'Appelle Nutrient Mass Balance: 2013–2016. Water Quality & Habitat Assessment Services. 215 pp.
- Weishaar, J.L., Aiken, G.R., Bergamaschi, B.A., Fram, M.S., Fujii, R., Mopper, K., 2003. Evaluation of Specific Ultraviolet Absorbance as an Indicator of the Chemical Composition and Reactivity of Dissolved Organic Carbon. *Environ. Sci. Technol.* 37, 4702–4708. <https://doi.org/10.1021/es030360x>
- Westerhoff, P., Aiken, G., Amy, G., Debroux, J., 1999. Relationships between the structure of natural organic matter and its reactivity towards molecular ozone and hydroxyl radicals. *Water Res.* 33, 2265–2276. [https://doi.org/10.1016/S0043-1354\(98\)00447-3](https://doi.org/10.1016/S0043-1354(98)00447-3)

- Wetzel, R., 2001a. Light in Inland Waters, in: *Limnology: Lake and River Ecosystems*. Elsevier, Academic Press, pp. 49–69.
- Wetzel, R., 2001b. Detritus: Organic Carbon Cycling and Ecosystem Metabolism, in: *Limnology: Lake and River Ecosystems*. Elsevier, Academic Press, pp. 731–783.
- Weyhenmeyer, G.A., Karlsson, J., 2009. Nonlinear response of dissolved organic carbon concentrations in boreal lakes to increasing temperatures. *Limnol. Oceanogr.* 54, 2513–2519. https://doi.org/10.4319/lo.2009.54.6_part_2.2513
- Wheater, H., Gober, P., 2013. Water security in the Canadian Prairies: science and management challenges. *Phil. Trans. R. Soc. A.* 371, 20120409. <https://doi.org/10.1098/rsta.2012.0409>
- Wickham, H., 2016. *ggplot2: Elegant Graphics for Data Analysis*. Springer-Verlag.
- Williams, C.J., Conrad, D., Kothawala, D.N., Baulch, H.M., 2019. Selective removal of dissolved organic matter affects the production and speciation of disinfection byproducts. *Sci. Total Environ.* 652, 75–84. <https://doi.org/10.1016/j.scitotenv.2018.10.184>
- Williams, C.J., Frost, P.C., Morales-Williams, A.M., Larson, J.H., Richardson, W.B., Chiandet, A.S., Xenopoulos, M.A., 2016. Human activities cause distinct dissolved organic matter composition across freshwater ecosystems. *Glob. Chang. Biol.* 22, 613–626. <https://doi.org/10.1111/gcb.13094>
- Williams, C.J., Yamashita, Y., Wilson, H.F., Jaffé, R., Xenopoulos, M.A., 2010. Unraveling the role of land use and microbial activity in shaping dissolved organic matter characteristics in stream ecosystems. *Limnol. Oceanogr.* 55, 1159–1171. <https://doi.org/10.4319/lo.2010.55.3.1159>
- Williams, P.J.L.B., 1990. The importance of losses during microbial growth: commentary on the physiology, measurement and ecology of the release of dissolved organic material. *Mar. Microb. Food Webs* 4, 175–206.
- Williamson, C.E., Overholt, E.P., Pilla, R.M., Leach, T.H., Brentrup, J.A., Knoll, L.B., Mette, E.M., Moeller, R.E., 2016. Ecological consequences of long-term browning in lakes. *Sci. Rep.* 5, 18666. <https://doi.org/10.1038/srep18666>
- Wilson, H.F., Xenopoulos, M.A., 2009. Effects of agricultural land use on the composition of fluvial dissolved organic matter. *Nat. Geosci.* 2, 37–41. <https://doi.org/10.1038/ngeo391>

- Wilson, H.F., Xenopoulos, M.A., 2008. Ecosystem and Seasonal Control of Stream Dissolved Organic Carbon Along a Gradient of Land Use. *Ecosystems* 11, 555–568.
<https://doi.org/10.1007/s10021-008-9142-3>
- Winterdahl, M., Erlandsson, M., Futter, M.N., Weyhenmeyer, G.A., Bishop, K., 2014. Intra-annual variability of organic carbon concentrations in running waters: Drivers along a climatic gradient: Intra-annual variability of stream DOC. *Global Biogeochem. Cy.* 28, 451–464. <https://doi.org/10.1002/2013GB004770>
- Wood, S.N., 2017. *Generalized Additive Models: An Introduction with R*, 2nd ed. CRC Press, Boca Raton.
- Wood, S.N., 2011. Fast stable restricted maximum likelihood and marginal likelihood estimation of semiparametric generalized linear models: Estimation of Semiparametric Generalized Linear Models. *J. R. Stat. Soc. Series B Stat. Methodol.* 73, 3–36.
<https://doi.org/10.1111/j.1467-9868.2010.00749.x>
- Worrall, F., Burt, T., Adamson, J., 2006. Long-term changes in hydrological pathways in an upland peat catchment—recovery from severe drought? *J. Hydrol.* 321, 5–20.
<https://doi.org/10.1016/j.jhydrol.2005.06.043>
- Xenopoulos, M.A., Lodge, D.M., Frentress, J., Kreps, T.A., Bridgham, S.D., Grossman, E., Jackson, C.J., 2003. Regional comparisons of watershed determinants of dissolved organic carbon in temperate lakes from the Upper Great Lakes region and selected regions globally. *Limnol. Oceanogr.* 48, 2321–2334.
<https://doi.org/10.4319/lo.2003.48.6.2321>
- Yallop, A.R., Clutterbuck, B., 2009. Land management as a factor controlling dissolved organic carbon release from upland peat soils 1: Spatial variation in DOC productivity. *Sci. Total Environ.* 407, 3808–3813.
- Yang, L., Kim, D., Uzun, H., Karanfil, T., Hur, J., 2015. Assessing trihalomethanes (THMs) and N-nitrosodimethylamine (NDMA) formation potentials in drinking water treatment plants using fluorescence spectroscopy and parallel factor analysis. *Chemosphere* 121, 84–91.
<https://doi.org/10.1016/j.chemosphere.2014.11.033>
- Zhang, Y., van Dijk, M.A., Liu, M., Zhu, G., Qin, B., 2009. The contribution of phytoplankton degradation to chromophoric dissolved organic matter (CDOM) in eutrophic shallow

lakes: Field and experimental evidence. *Water Res.* 43, 4685–4697.

<https://doi.org/10.1016/j.watres.2009.07.024>

Zsolnay, H.F., Baigar, E., Jimenez, M., Steinweg, B., Saccomandi, F., 1999. Differentiating with fluorescence spectroscopy the sources of dissolved organic matter in soils subjected to drying. *Chemosphere* 38, 45–50.

Appendix A: Supplementary information Chapter 2 (The importance of autochthonous DOM production in Buffalo Pound Lake, Saskatchewan across a series of dry years)

In addition to the Chapter 2 main text we provide here several tables and figures to provide additional context and describe supporting analyses. Included in section A.1 of this supplementary information text are specific details about the timing and frequency of field sampling (Table A.1), rationale for reducing 11 sampling sites to 8 locations used in statistical analyses (see Section A.1.1, Table A.2, and Figures A.1 and A.2), and summary statistics for all water quality and dissolved organic matter (DOM) quantity and quality parameters (Table A.3). Section A.2 includes additional metrics derived from excitation and emission scans using fluorescence spectroscopy. Here, several figures support the analyses and findings presented in the main text, including absorbances at four wavelengths (Figure A.3), a spectral slope and spectral slope ratio (Figure A.4), four spectral peak ratios that describe DOM composition (Figure A.5), and several fluorescence peaks normalized to dissolved organic carbon (DOC) concentration used to infer humic-like (Figure A.6) and fresh-like (Figure A.7) DOM characteristics. These metrics are described in detail in Table 2.2. Section A.3 details individual-year linear modelling results between distance along Buffalo Pound Lake and DOC and TDN concentrations, and several DOM absorbance and fluorescence metrics (Figure A.8, Table A.4), which support the aggregated linear modelling results shown in the main text.

A.1 Sampling and site information, and summary statistics

Table A.1. Field sampling dates and complete sampling days from 2016–2019 at locations along the length of Buffalo Pound Lake during the open water seasons from 2016–2019. Note that the locations reported in this table are compressed from 11 *sites* to a maximum of 8 *locations* based on findings of homogeneity as described below and in Table A.2 and Figures A.1 and A.2).

Year	Sampling dates	Complete sampling days	Locations x days
2016	April 12, April 19, September 22	3	24
2017	March 21, May 15, June 12, July 11, August 9, September 12	6	46*
2018	March 20, May 23, June 19, July 17, August 21, September 27	6	46*
2019	April 22, May 28, June 27, July 22, August 15, September 23	6	48

*Total number of samples reported excludes samples from 2017 and 2018 that did not meet QA/QC standards (two in both years showed evidence of contamination).

A.1.1 Testing for site similarities with ANOVA and Student's t-test

Sites near the inflow to Buffalo Pound Lake and upstream of the causeway are geographically located close together relative to the width and length of the lake. Inflow East, Inflow Centre, and Inflow West are 1.50, 1.70, and 1.94 km respectively from the approximate location of the lake inflow. Upstream Causeway Centre and Upstream Causeway East are 3.68 and 3.83 km from the approximate location of the lake inflow. Statistical tests were used to test the null hypothesis of no difference in the means of select parameters among the sites at Inflow (analysis of variance, ANOVA) and Upstream Causeway (Student's t-test) sites. Parameters were selected to represent metrics of dissolved organic matter (DOM) quantity (dissolved organic carbon (DOC) concentration), absorbance (DOC-specific ultraviolet absorbance at 254 nm (SUVA₂₅₄), and fluorescence (freshness index [β : α ratio] and humification index [HIX]). Non-significant results (no statistical difference in mean values among sites) of these tests indicates redundancy, suggesting these groups of sites thus can be averaged to represent one site (Lake Inflow for the inflow sites and Upstream Causeway for the sites upstream the causeway). Prior to analyses, data were assessed for adherence to assumptions of the analyses. Normally distributed data is a central assumption of ANOVA and Student's t-tests. Visual inspection of quantile–quantile plots indicated most parameters were approximately normally distributed; however, Shapiro-Wilk tests revealed that some parameters deviated from the normal distribution ($W < 0.05$). In cases where $W < 0.05$ tests were run using both untransformed and log-transformation data to see if results were affected. Both tests are sensitive to extreme outliers, and it is recommended to remove values that exceed 3 times the inter-quartile range below the 1st quartile or above the 3rd quartile. No parameter values were extreme outliers for any site. A third assumption is equal variance among groups, and this was assessed via Levene's test for homogeneity of variance. The three groups of inflow measurements and two groups of upstream causeway measurements fulfilled this assumption ($p > 0.05$).

Results from the ANOVA and Student's t-test showed no significant differences in the means of the inflow sites or the sites upstream of the causeway for all parameters ($p > 0.1$ for DOC concentration, SUVA₂₅₄, β : α , and HIX) (Table A.2, Figures A.1 and A.2). These results suggest that averaging the values for these groups of sites will not affect overall patterns in DOM quality and quantity patterns observed in Buffalo Pound Lake. Results reported in the main text

are thus derived from averages of the three inflow sites and two causeway sites, and geographic coordinates are represented as the mean location of each cluster of sites.

Table A.2. Results from ANOVA and Student’s t-test runs for each parameter and site grouping. Test runs that used log-transformed data are not shown; instead *p*-values for untransformed data are reported (consistent with results below, log-transformation did not produce a significant test result in any case).

Sites	Parameter	Test	Statistic	<i>p</i>-value	<i>n</i>
Inflow East, Inflow Centre, Inflow West	DOC concentration	ANOVA	$F(2, 52) = 0.126$	0.882	55
	SUVA ₂₅₄	ANOVA	$F(2, 52) = 0.002$	0.998	55
	$\beta:\alpha$ ratio	ANOVA	$F(2, 52) = 0.064$	0.938	55
	HIX	ANOVA	$F(2, 52) = 0.088$	0.916	55
Upstream Causeway Centre, Upstream Causeway East	DOC concentration	Student’s t-test	$t(36.1) = -0.0134$	0.989	39
	SUVA ₂₅₄	Student’s t-test	$t(36.4) = 0.370$	0.713	39
	$\beta:\alpha$ ratio	Student’s t-test	$t(36.7) = -1.550$	0.130	39
	HIX	Student’s t-test	$t(35.6) = 0.396$	0.694	39

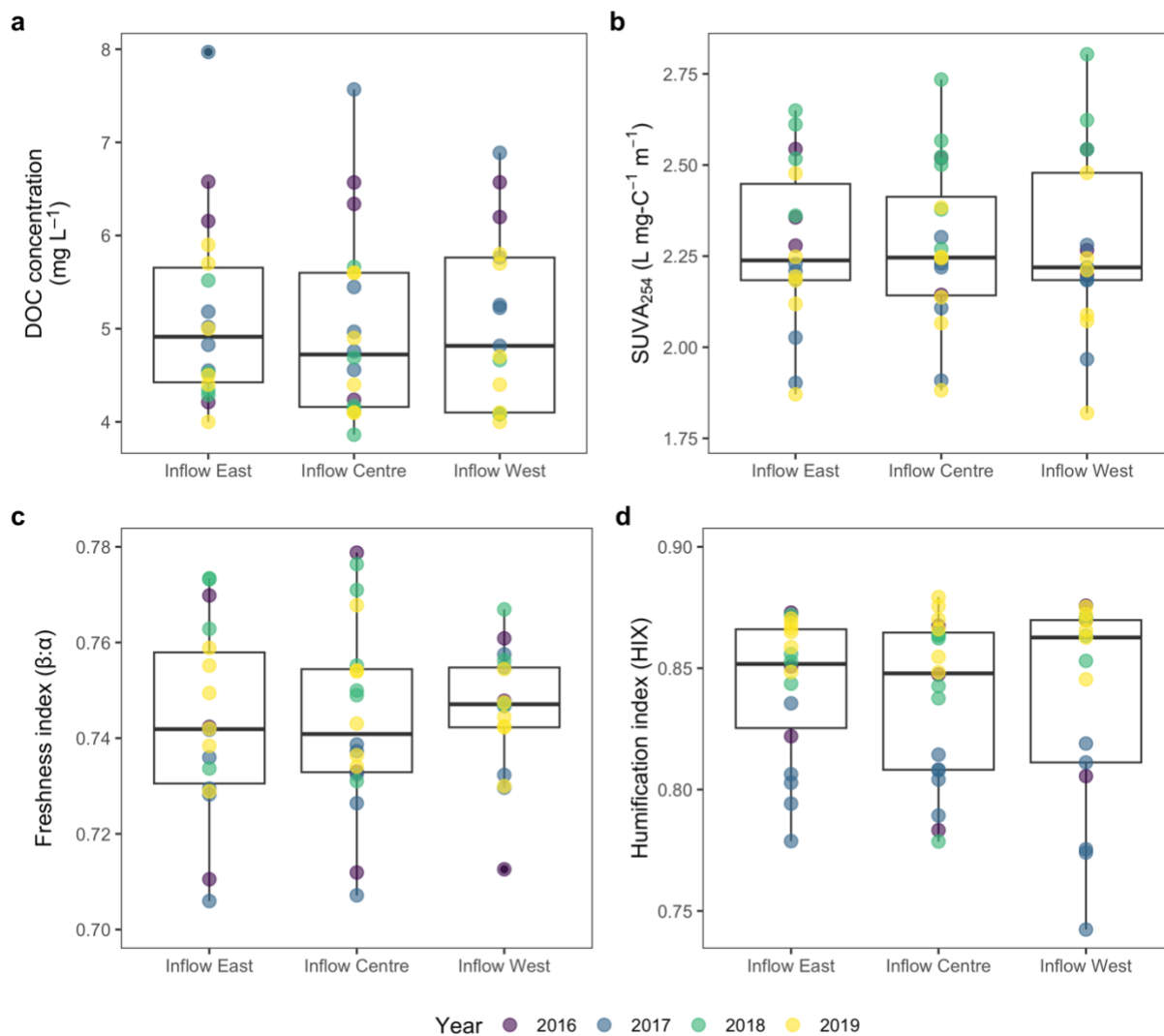


Figure A.1. Sites near the Buffalo Pound Lake inflow that were tested for similarities in (a) DOC concentration, (b) an absorbance metric (SUVA₂₅₄), and (c–d) fluorescence indexes (β:α and HIX). Coloured points are individual samples collected during sampling events from 2016–2019.

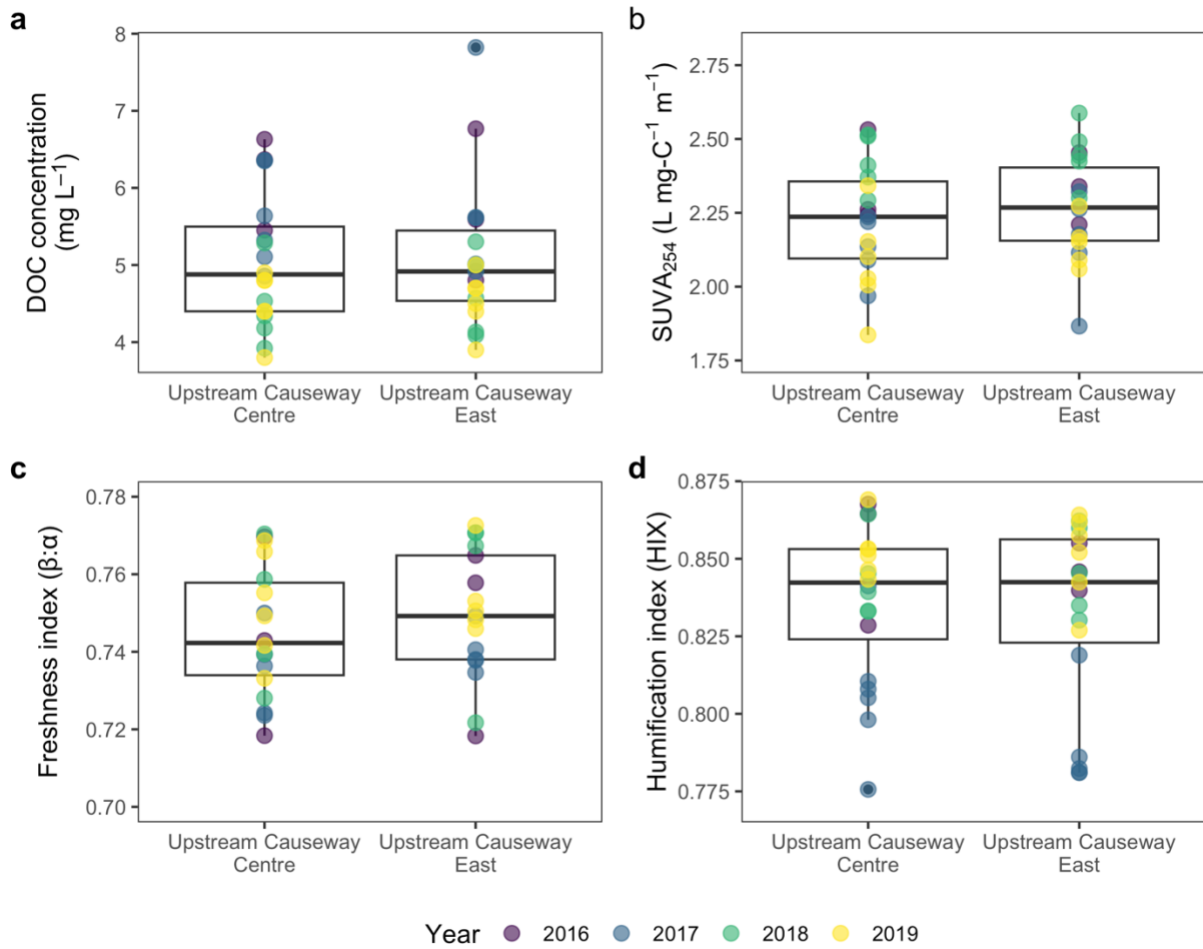


Figure A.2. Sites upstream of the causeway on Buffalo Pound Lake that were tested for similarities in (a) DOC concentration, (b) an absorbance metric (SUVA_{254}), and (c–d) fluorescence indexes ($\beta:\alpha$ and HIX). Coloured points are individual samples collected during sampling events from 2016–2019.

Table A.3. Summary statistics for water quality, DOC concentration, and DOM absorbance and fluorescence parameters. Abbreviations: Q1 – first quartile; Q3 – third quartile.

Parameter	Unit	<i>N</i>	Min	Median	Q1	Q3	Max
Turbidity	NTU	146	0.4	4.3	2.4	10.8	76.7
Chl <i>a</i>	$\mu\text{g L}^{-1}$	147	2.2	12.4	7.3	25.0	141.5
k_T	m^{-1}	131	0.45	1.23	0.90	1.77	4.35
Z_{SD}	m	134	0.2	1.0	0.7	1.5	3.6
TDN	mg L^{-1}	86	0.224	0.411	0.349	0.451	0.640
DOC	mg L^{-1}	165	3.70	5.30	4.77	6.35	8.13
SUVA ₂₅₄	$\text{L mg-C}^{-1} \text{m}^{-1}$	161	1.44	2.05	1.86	2.24	3.00
FI	—	161	1.49	1.57	1.55	1.59	1.66
HIX	—	161	0.730	0.833	0.810	0.851	0.888
$\beta:\alpha$	—	161	0.656	0.774	0.755	0.790	0.849
$S_{275-295}$	nm^{-1}	161	0.016	0.023	0.022	0.024	0.026
$S_{350-400}$	nm^{-1}	161	0.016	0.020	0.019	0.021	0.023
S_R	—	161	1.01	1.18	1.12	1.24	1.45
A_{254}	m^{-1}	161	7.98	11.13	9.76	11.93	19.06
A_{280}	m^{-1}	161	5.35	7.30	6.60	8.02	14.07
A_{350}	m^{-1}	161	1.08	1.65	1.46	1.86	4.49
A_{440}	m^{-1}	161	0.15	0.33	0.26	0.39	1.11
SpA	RU L mg-C^{-1}	160	0.106	0.173	0.148	0.197	0.273
SpB	RU L mg-C^{-1}	160	0.021	0.038	0.032	0.046	0.075
SpC	RU L mg-C^{-1}	160	0.058	0.093	0.078	0.107	0.143
SpD	RU L mg-C^{-1}	160	0.023	0.037	0.031	0.041	0.055
SpE	RU L mg-C^{-1}	160	0.007	0.011	0.009	0.013	0.017
SpM	RU L mg-C^{-1}	160	0.065	0.103	0.090	0.118	0.158
SpN	RU L mg-C^{-1}	160	0.047	0.068	0.058	0.077	0.098
SpT	RU L mg-C^{-1}	160	0.033	0.057	0.050	0.065	0.099
Peak ratio (C:T)	—	161	0.99	1.64	1.49	1.86	2.73
Peak ratio (A:T)	—	161	1.78	3.03	2.68	3.53	5.13
Peak ratio (C:A)	—	161	0.416	0.537	0.524	0.551	0.635
Peak ratio (C:M)	—	161	0.707	0.901	0.887	0.913	0.978

A.2 Additional DOM absorbance and fluorescence metrics

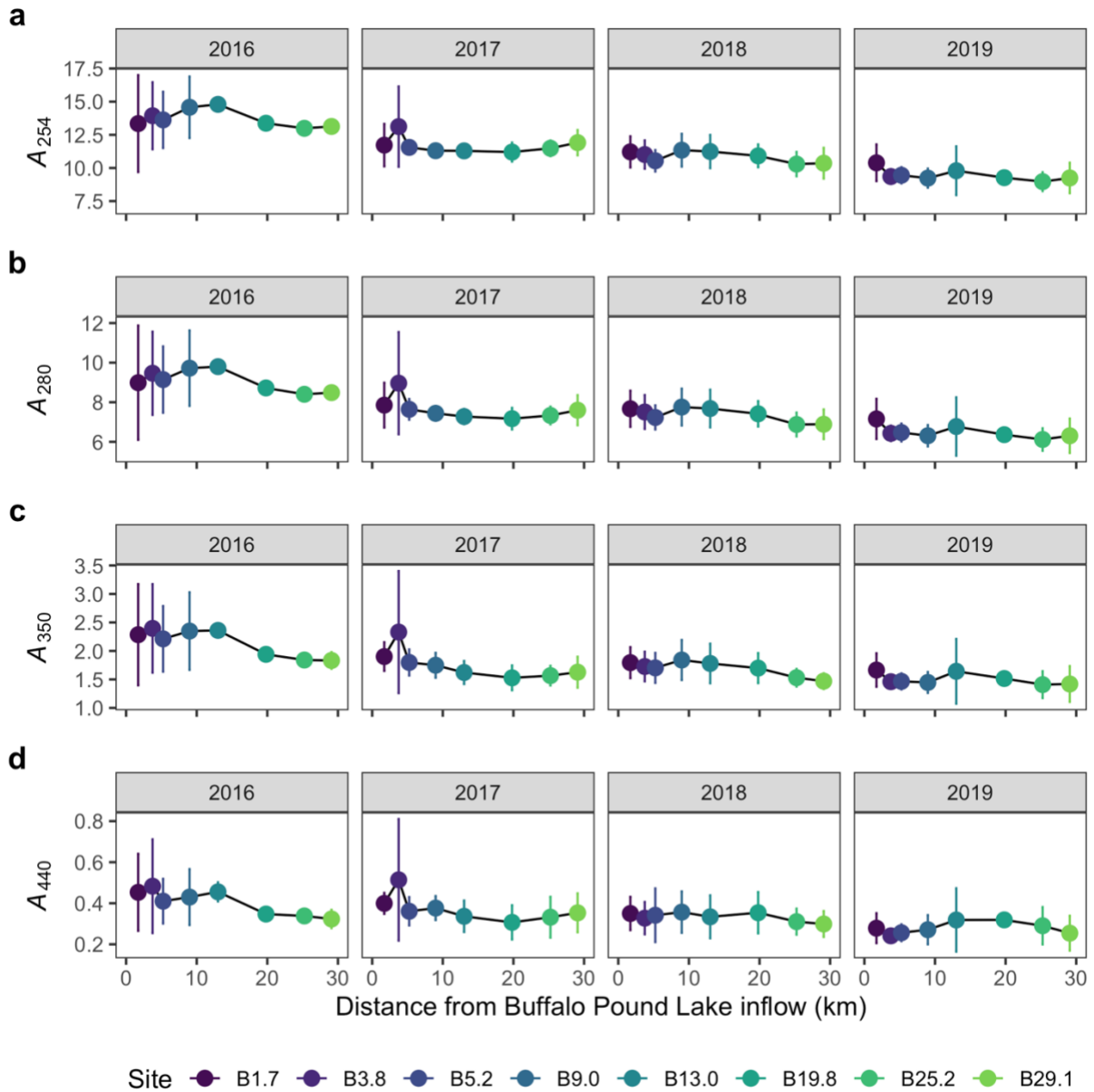


Figure A.3. (a–d) Absorbance (m^{-1}) of bulk water samples at 254, 280, 350, and 440 nm wavelengths measured at 8 locations along Buffalo Pound Lake from 2016–2019. Points are mean values and error bars represent the standard deviation of mean values ($N = 3\text{--}6$). Samples from the lake had high absorbance in the lower UV range (a, b) and much lower absorbance at near-visible and visible wavelengths (c, d).

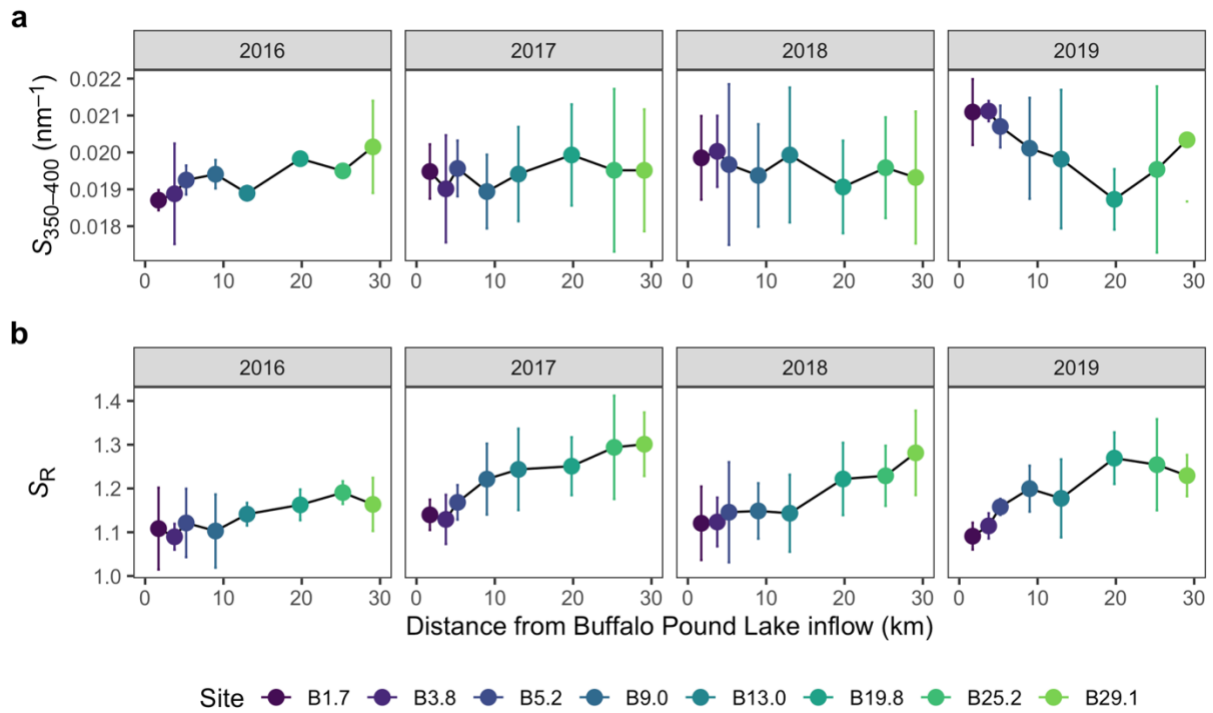


Figure A.4. (a) Spectral slope $S_{350-400}$ and (b) slope ratio S_R ($S_{275-295}:S_{350-400}$) measured at 8 locations along Buffalo Pound Lake from 2016–2019. Points are mean values and error bars represent the standard deviation of mean values ($N = 3-6$). Less intense absorbance near-visible wavelengths (Figure A.3) affected $S_{350-400}$ measurements, as evidenced by the large range in mean \pm one standard deviation values (a).

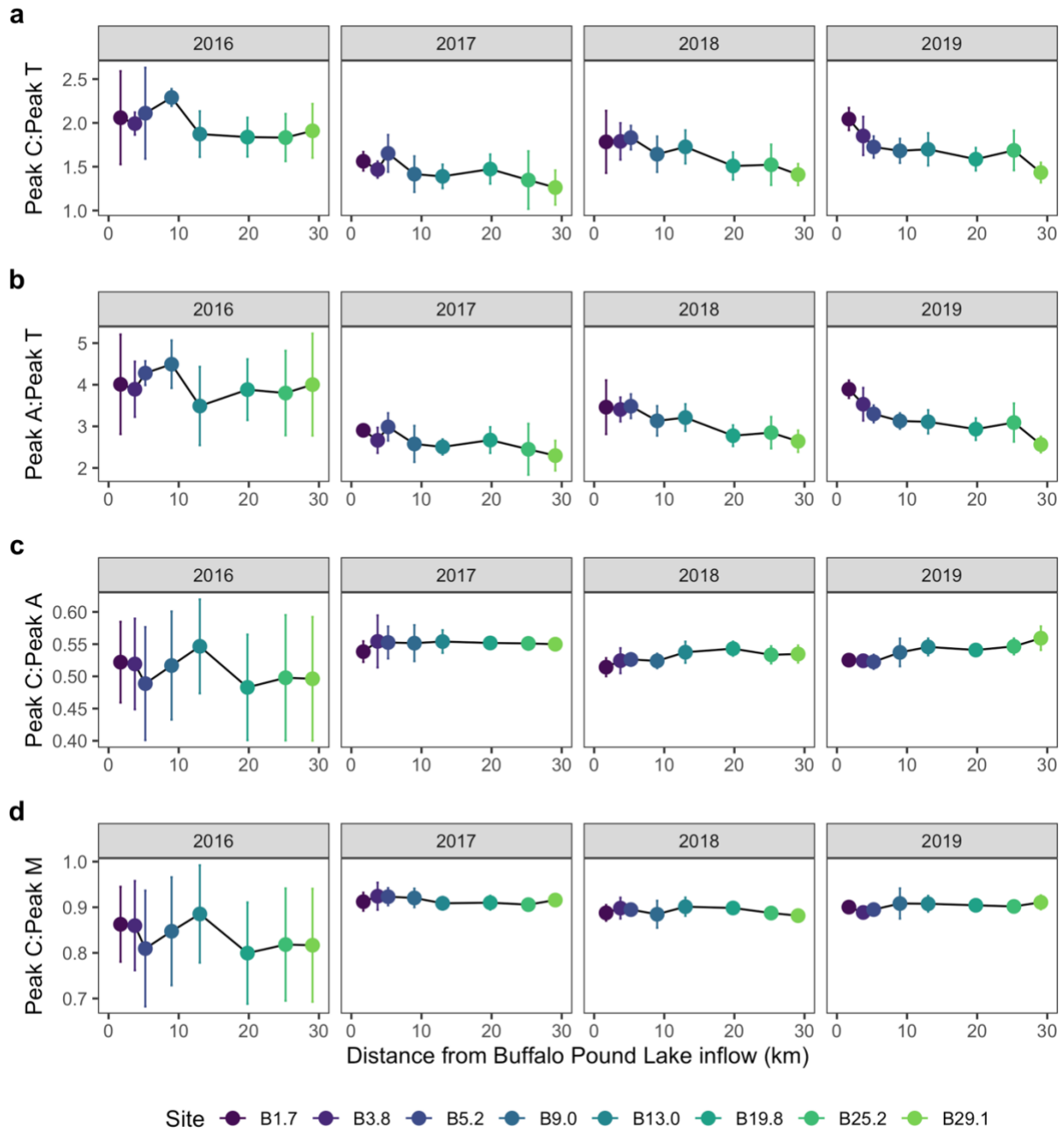


Figure A.5. (a–d) Spectral peak ratios (C:T, A:T, C:A, and C:M) measured at 8 locations along Buffalo Pound Lake from 2016–2019. Points are mean values and error bars represent the standard deviation of mean values ($N = 3–6$).

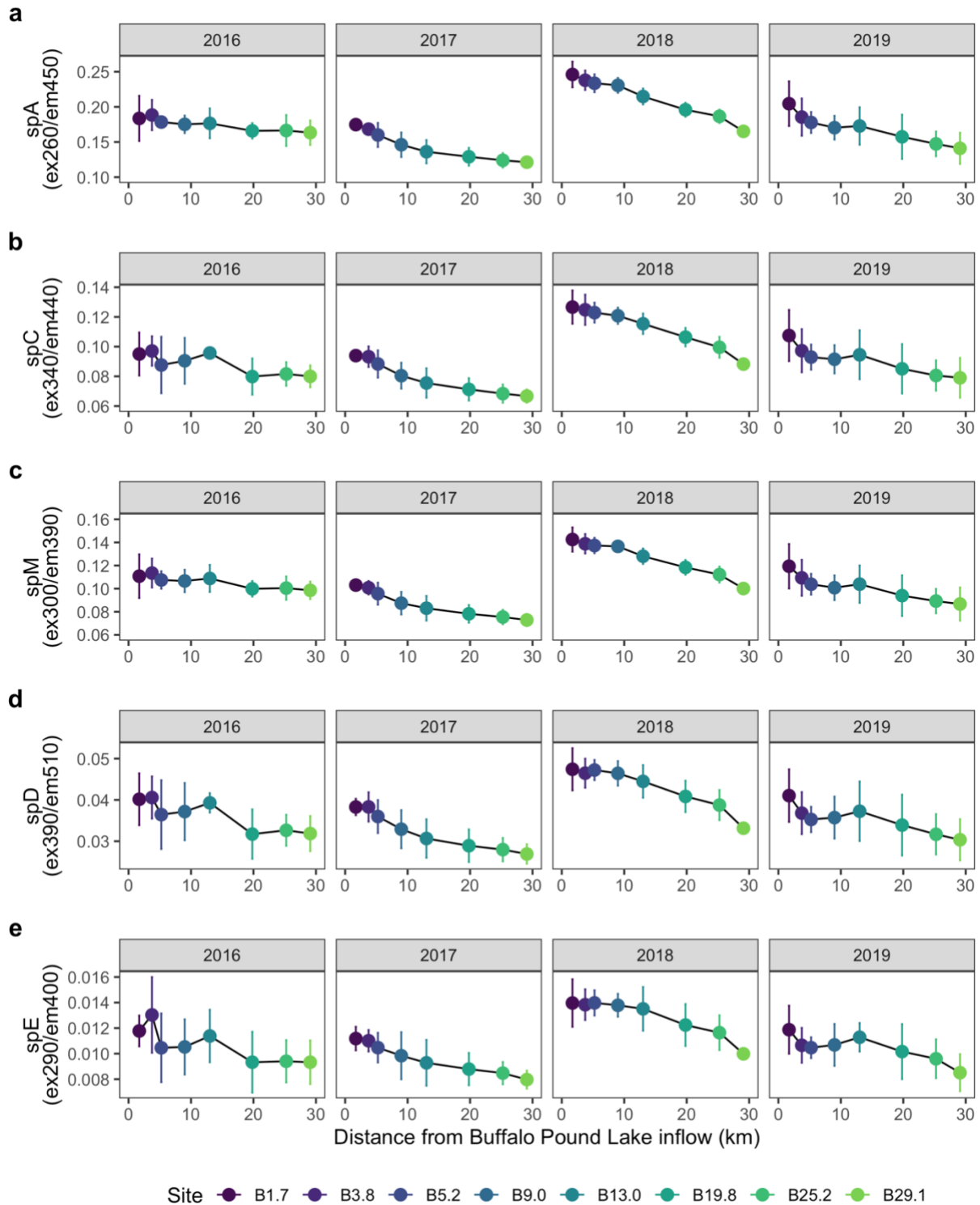


Figure A.6. (a–e) DOC-normalized (specific) humic-like fluorescence peaks (spA, spC, spM, spD, and spE) measured at 8 locations along Buffalo Pound Lake from 2016–2019. Units are in RU L mg-C⁻¹. Points are mean values and error bars represent the standard deviation of mean values ($N = 3–6$). Humic-like peaks were strongly correlated with one another ($R^2 = 0.89–0.99$, $p < 0.00001$ for 10 pairs correlation pairs). In y-axis labels ex refers to excitation wavelength and em refers to emission wavelength.

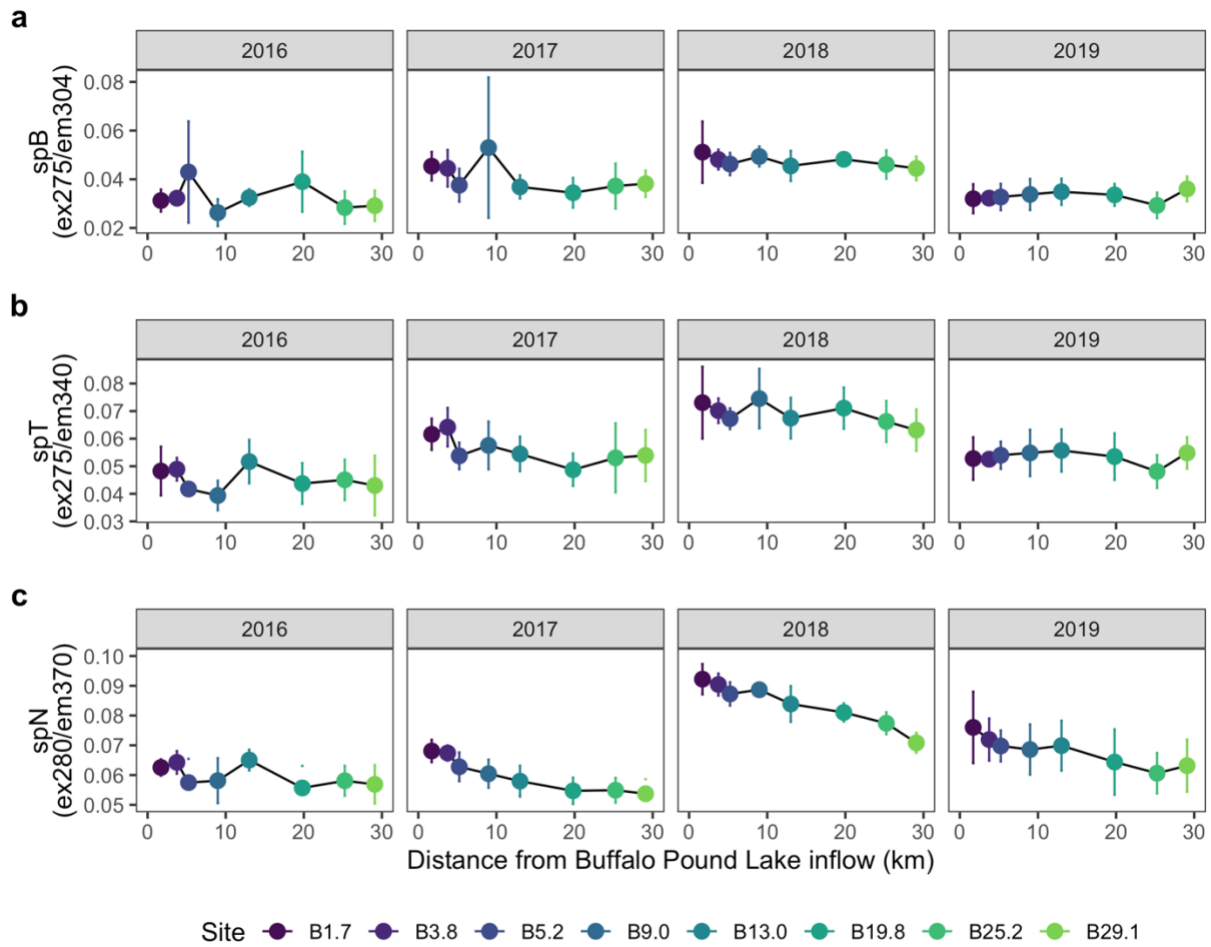


Figure A.7. (a–c) DOC-normalized (specific) fresh-like fluorescence peaks (spB, spT, and spN) measured at 8 locations along Buffalo Pound Lake from 2016–2019. Units are in RU L mg-C⁻¹. Points are mean values and error bars represent the standard deviation of mean values ($N = 3–6$). Fresh-like specific peaks had weak to strong correlations. Peaks spB and spN were weakly correlated ($R^2 = 0.33$, $p = 3.3 \times 10^{-4}$), whereas correlations were stronger between spT and spB ($R^2 = 0.64$, $p = 2.5 \times 10^{-8}$), and spT and spN ($R^2 = 0.72$, $p = 6.7 \times 10^{-10}$). In y-axis labels ex refers to excitation wavelength and em refers to emission wavelength.

A.3 Linear modelling

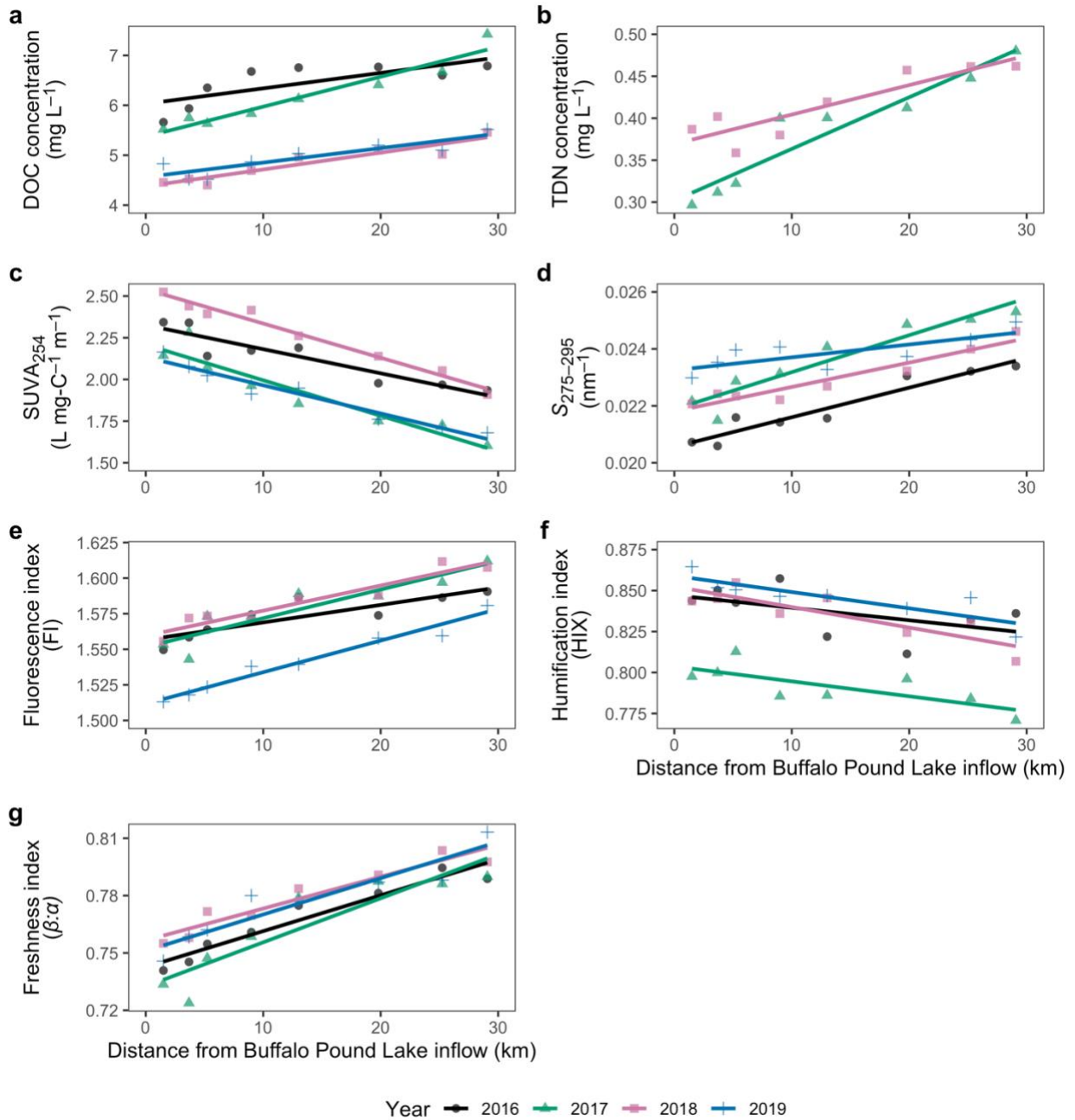


Figure A.8. (a) Dissolved organic carbon concentration, (b) TDN concentration, (c) SUVA₂₅₄, (d) S₂₇₅₋₂₉₅, (e) FI, (f) HIX, and (g) β:α measured at 8 locations along Buffalo Pound Lake from 2016–2019. Points are mean values at each site in an individual year ($N = 3-6$). Lines are fitted linear model trend lines ($R^2 = 0.16-0.97$, $p < 0.0001$).

Table A.4. Equations, R^2 , and false discovery rate adjusted (Benjamini and Hochberg, 1995) p -values between DOM quantity and quality parameters and distance along Buffalo Pound Lake for individual years shown in Figure A.8.

Parameter	Year	Equation	R^2	p -value
DOC concentration	2016	$y = 0.031x + 6.03$	0.488	5.38×10^{-8}
	2017	$y = 0.0599x + 5.37$	0.920	4.71×10^{-9}
	2018	$y = 0.0290x + 4.56$	0.875	2.27×10^{-9}
	2019	$y = 0.031x + 4.56$	0.748	8.54×10^{-9}
TDN concentration	2017	$y = 0.00616x + 0.302$	0.891	4.72×10^{-7}
	2018	$y = 0.00351x + 0.369$	0.770	6.75×10^{-8}
SUVA ₂₅₄	2016	$y = -0.0145x + 2.33$	0.834	1.65×10^{-9}
	2017	$y = -0.0213x + 2.21$	0.883	6.97×10^{-9}
	2018	$y = -0.0205x + 2.54$	0.970	3.05×10^{-11}
	2019	$y = -0.0169x + 2.13$	0.936	3.04×10^{-10}
$S_{275-295}$	2016	$y = 0.000104x + 0.0206$	0.906	6.96×10^{-11}
	2017	$y = 0.00013x + 0.0219$	0.882	3.87×10^{-10}
	2018	$y = 0.0000856x + 0.0218$	0.906	1.51×10^{-11}
	2019	$y = 0.0000451x + 0.0233$	0.499	1.42×10^{-10}
FI	2016	$y = 0.00123x + 1.56$	0.706	5.79×10^{-14}
	2017	$y = 0.00201x + 1.55$	0.816	1.93×10^{-13}
	2018	$y = 0.00177x + 1.56$	0.890	1.50×10^{-14}
	2019	$y = 0.00222x + 1.51$	0.963	3.49×10^{-15}
HIX	2016	$y = -0.000764x + 0.847$	0.158	5.88×10^{-11}
	2017	$y = -0.000912x + 0.804$	0.476	7.21×10^{-12}
	2018	$y = -0.00125x + 0.852$	0.732	3.08×10^{-12}
	2019	$y = -0.000995x + 0.859$	0.667	9.55×10^{-13}
$\beta:\alpha$	2016	$y = 0.00188x + 0.743$	0.930	7.00×10^{-13}
	2017	$y = 0.0023x + 0.733$	0.831	4.98×10^{-11}
	2018	$y = 0.00167x + 0.757$	0.915	5.65×10^{-13}
	2019	$y = 0.00190x + 0.751$	0.877	4.45×10^{-12}

Appendix B: Supplementary information Chapter 3 (Extreme variation in DOC and the importance of climate and flow source for Buffalo Pound Lake, Saskatchewan)

In this supplementary information section we include several tables and figures to support the Chapter 3 main text. Table B.1 provides the locations, station numbers, and complete flow record details for the four gauging stations used in our analyses, and the estimated period for the ungauged portion of the Buffalo Pound Lake catchment. Figures B.1 and B.2 are pedagogical examples to provide background on wavelet coherence and phase analyses. In Table B.2 summary statistics for all streamflow and water chemistry parameters are presented. Figures B.3 and B.4 show continuous wavelet transforms and phase relationships at short (≤ 18 -month) and long (> 18 -month) timescales for all parameters respectively. Table B.3 includes strength of coherence relationships and significance among all parameters and dissolved organic carbon (DOC) concentration. Figure B.5 shows four model diagnostics of the GAM fitted to DOC concentration presented in the main text (Figure 3.6). Figure B.6 and B.7 show long-term patterns of DOC:DON and SUVA₂₅₄ respectively.

Table B.1. Site names, abbreviations, Water Security Agency gauging station numbers, geographic coordinates, and gauged and estimated flow records for five contributing streams and areas above Buffalo Pound Lake.

Site name	Symbol	Station number	Coordinates	Flow record
Lake Diefenbaker outflow	Q_{LD}	SK05JG006	50.97°N, 106.39°W	Gauged 1972–2019
Ridge Creek	Q_{RC}	SK05JG013	50.95°N, 106.32°W	Gauged 1972–2019
Iskwao Creek	Q_{IC}	SK05JG014	50.97°N, 105.95°W	Gauged 1972–2006 (warm season); estimated 1990–2006 (cold season) and 2007–2019
Buffalo Pound Lake inflow	Q_{BP}	SK05JG004	50.78°N, 105.82°W	Complete records 1968–1994 and 2016–2019; estimated 1995–2015
Ungauged	Q_U	—	—	Estimated 1993–2019

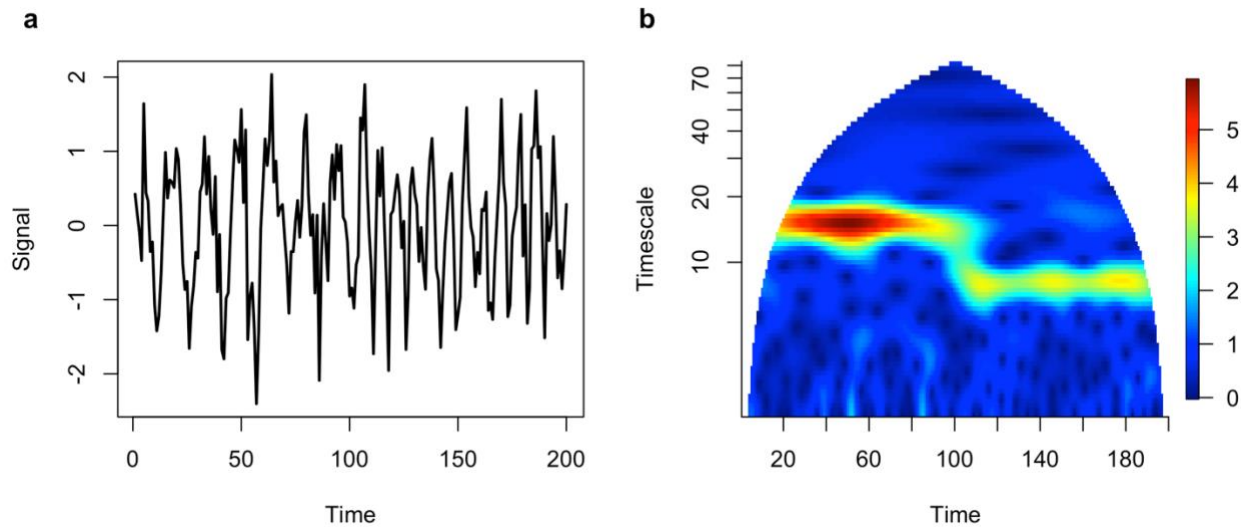


Figure B.1. A hypothetical time series (a) and its wavelet transform as a function of time and timescale (b), adapted from Reuman et al. (2021). The time series in (a) is constructed from three components: 1) a sine wave of amplitude 1 and period 15 that operates for time $t = 1, \dots, T$ but disappears at $t > 100$; 2) a sine wave of amplitude 1 and period 8 that operates for $t = 101, \dots, 200$ but is absent for $t \leq 100$; and 3) normally distributed white noise of mean 0 and standard deviation 0.5. The wavelet transform (b) is a complex-valued function of time $t = 1, \dots, 200$ and timescale σ . The magnitude of the wavelet transform $|W_\sigma(t)|$, presented as the z -axis in (b), is an estimate of the strength of the oscillations in $x(t)$ at time t occurring at timescale σ (Addison, 2002; Reuman et al, 2021). The wavelet transform is based on a convolution of a wavelet function with the time series (Reuman et al., 2021). Because of this, times and timescales where the overlap of the wavelet transform with the time series is insufficient and unreliable are omitted. The ‘rocket ship nose cone’ plot results from omission of these regions (i.e., at times closer the edges of the time series). At long timescales more values are omitted because long-timescale wavelets extend over the end of the time series further in the convolution computation.

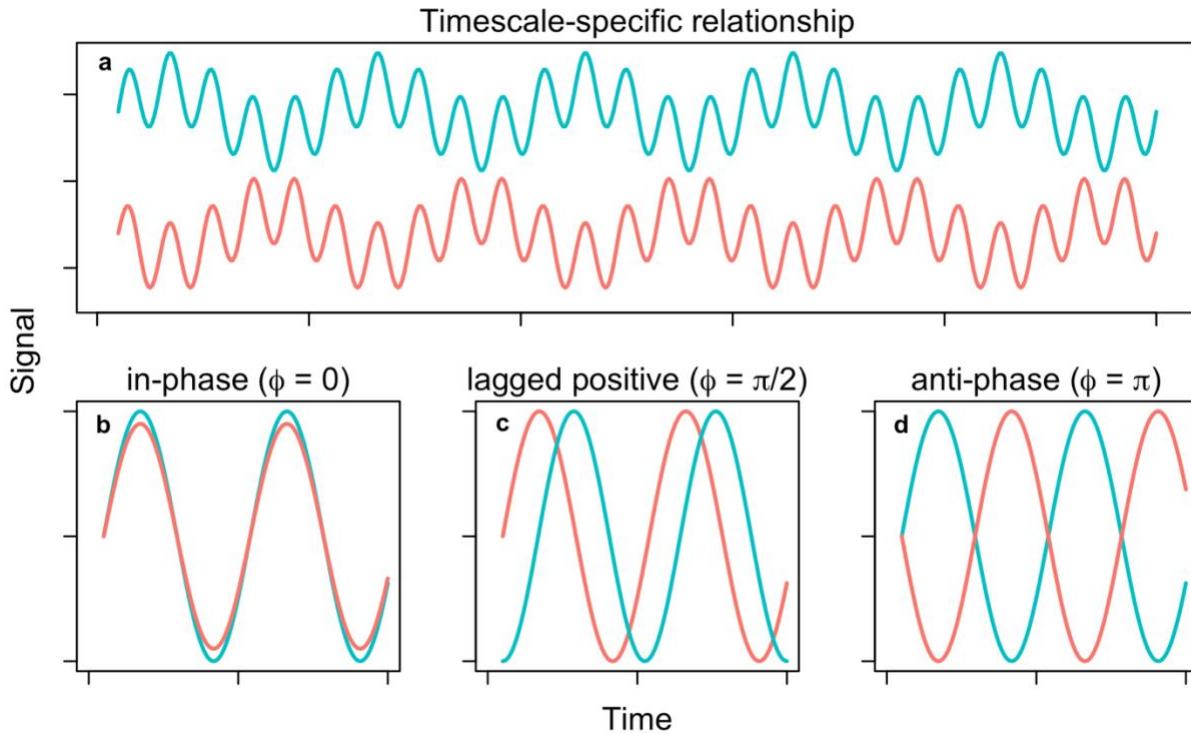


Figure B.2. Illustration adapted from Walter et al. (2021) of timescale-specific relationships between two variables (**a**) and different phase relationships (**b–d**). In (**a**) the two variables are perfectly positively correlated on short timescales and perfectly negatively related at long timescales, a relationship masked through standard correlation methods. In (**b**) fluctuations are in-phase ($\phi = 0$), corresponding to positive correlation. In (**c**) fluctuations are temporally lagged positive, with the pink signal peaking ahead of the blue signal ($\phi = \pi/2$); a time-lagged negative relationship would show the blue signal peaking ahead of the pink signal ($\phi = -\pi/2$). In (**d**) fluctuations are anti-phase ($\phi = \pi$), corresponding to negative correlation.

Table B.2. Summary statistics for DOC concentration and eight environmental predictors (1990–2019). The real number of observed values N is reported here; where $N < 360$ missing values were imputed using $k = 1$ nearest neighbour regression (Altman, 1992; Fix and Hodges, 1951). Abbreviations: Q1 – first quartile; Q3 – third quartile; LOQ – limit of quantification.

Parameter	Unit	N	Min	Median	Q1	Q3	Max
DOC	mg C L ⁻¹	360	3.3	6.3	5.5	7.9	12.4
SO ₄ ²⁻	mg S L ⁻¹	359	56.8	117.4	95.7	156.4	339.8
TP	μg P L ⁻¹	351	14	63	48	85	232
SRP	μg P L ⁻¹	350	< LOQ	10	6	18	99
Chl <i>a</i>	μg L ⁻¹	355	< LOQ	16	9	27	151
NO ₃ ⁻	mg N L ⁻¹	358	< LOQ	0.04	0	0.11	1.54
NH ₄ ⁺	mg N L ⁻¹	348	< LOQ	0.08	0.03	0.13	0.45
Q_{LD}	m ³ s ⁻¹	360	0	2.2	1.5	4.1	12.4
Q_{BP}	m ³ s ⁻¹	360	0.1	2.6	1.6	4.7	18.9
Q_{LC}	m ³ s ⁻¹	360	0	0	0	0.2	8.3

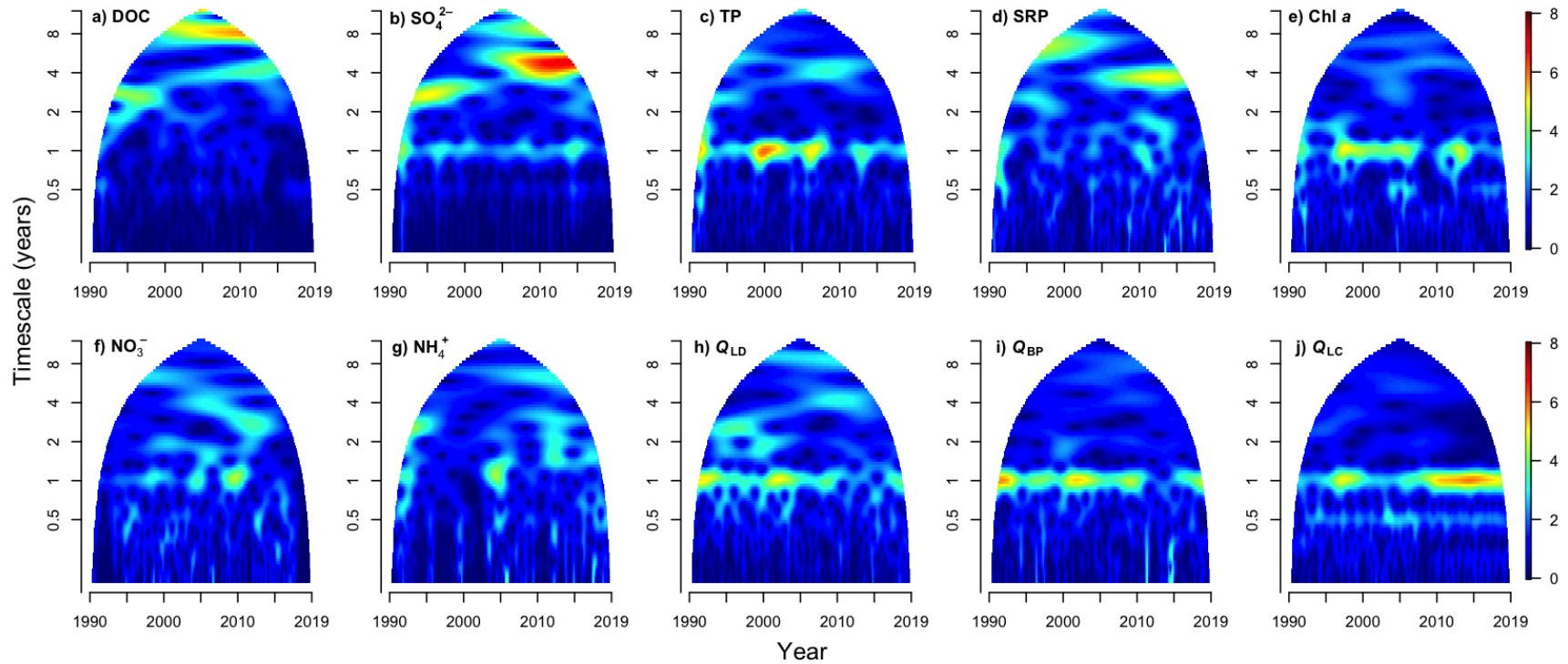


Figure B.3. (a–j) Wavelet transforms of DOC, TP, SRP, SO_4^{2-} , Chl *a*, NO_3^- , NH_4^+ , Q_{LD} , Q_{LC} , and Q_{BP} showing the magnitude of the transform (*z*-axis, colour bar) against time (*x*-axis) and timescale (*y*-axis). Note the *y*-axis is log-transformed. The wavelet transform is based on a convolution of a wavelet function with the time series (Reuman et al., 2021). Because of this, times and timescales where the overlap of the wavelet transform with the time series is insufficient and unreliable are omitted. The ‘rocket ship nose cone’ plot results from omission of these regions (i.e., at times closer to the edges of the time series). At long timescales more values are omitted because long-timescale wavelets extend over the end of the time series further in the convolution computation.

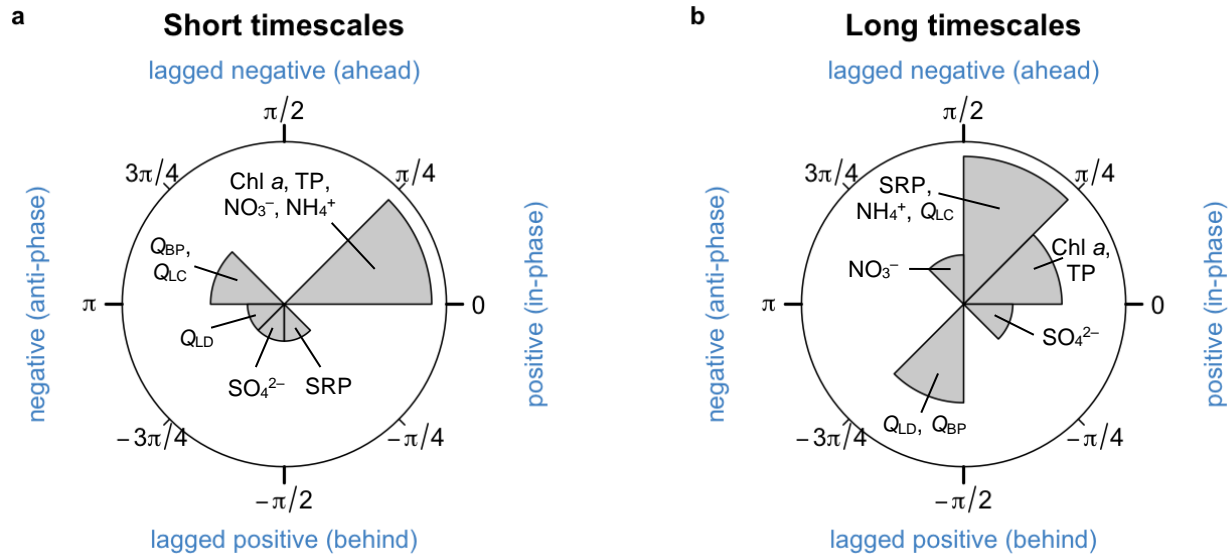


Figure B.4. Distributions of phase differences at (a) short (≤ 18 -month) and (b) long (> 18 -month) timescales for all environmental predictors and DOC concentration. Note: Figure 3.5 in the main text presents only the environmental predictors that were significantly coherent with DOC. Radius length is proportional to the frequency of each type of relationship observed (lagged, in-phase, anti-phase), where longer radii indicate higher frequency (as in (a)). Lagged negative refers to peaks in DOC leading ahead of peaks in a predictor; lagged positive refers to peaks in DOC lagging behind peaks in a predictor. In-phase relationships are analogous to positive correlation, whereas anti-phase relationships are analogous to negative correlation.

Table B.3. Coherences between DOC concentration and nine environmental predictors at short (2- to 18-month timescales) and long (19- to 120-month) timescales. Significant relationships are bolded and denoted by *** ($p < 0.001$), ** ($p < 0.01$), and * ($p < 0.05$). Relationships marginally non-significant ($p < 0.1$) are italicized and denoted by †.

Environmental predictor	Short timescales	Long timescales
SO ₄ ²⁻	0.21*	0.67**
TP	0.36**	0.57*
SRP	0.08	0.54
Chl <i>a</i>	0.50***	0.34
NO ₃ ⁻	0.15	0.15
NH ₄ ⁺	0.27**	0.05
<i>Q</i> _{LD}	0.10	0.74**
<i>Q</i> _{BP}	0.12	<i>0.66</i> †
<i>Q</i> _{LC}	0.10	0.52

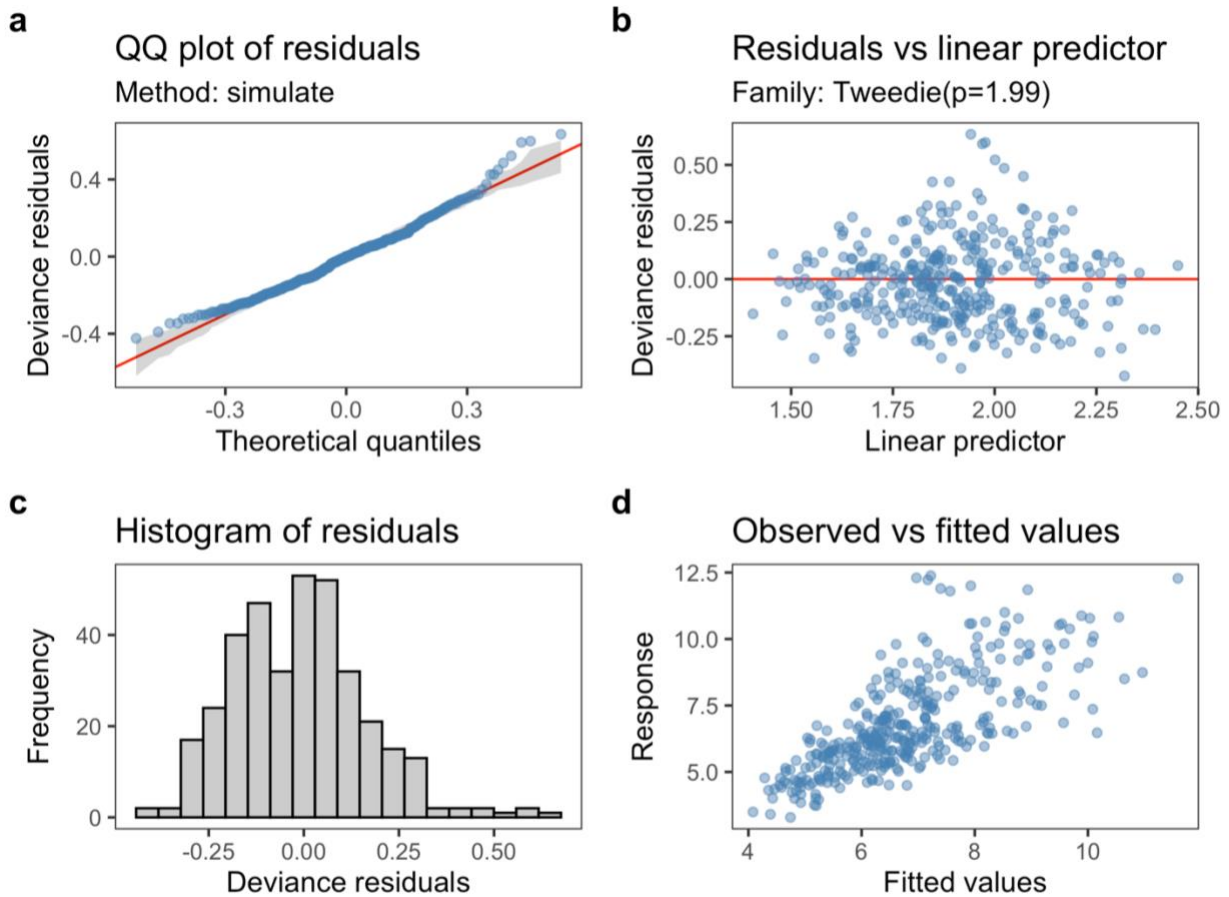


Figure B.5. Model diagnostics of the GAM of DOC concentration with SO_4^{2-} , TP, Chl *a*, NH_4^+ , and Q_{LD} (Figure 3.6 in main text). **(a)** QQ plot of residuals showing some deviation from normality, which is likely affected by the few extreme high and low DOC concentrations in the 30-year record. **(b)** Residuals vs linear predictor plot. While there is not a strong pattern in this plot (evidence of relatively good fit), there are several points at the tails of ‘Linear predictor’ and the higher end of ‘Deviance residuals’ that suggest relatively high and low DOC concentrations were poorly estimated by this model. **(c)** Histogram of residuals. Residuals are approximately normally distributed with a few extreme values at the tails. **(d)**. Observed vs fitted values showing the fit between measured (y-axis) and modeled (x-axis) DOC concentrations. At DOC concentrations $< \sim 8 \text{ mg L}^{-1}$ the GAM provides a good fit to the data; however, at concentrations $> \sim 8 \text{ mg L}^{-1}$ there is often considerable variation between observed and estimated DOC concentrations. At these higher concentrations the coherent environmental predictor covariates struggled to explain variation in DOC.

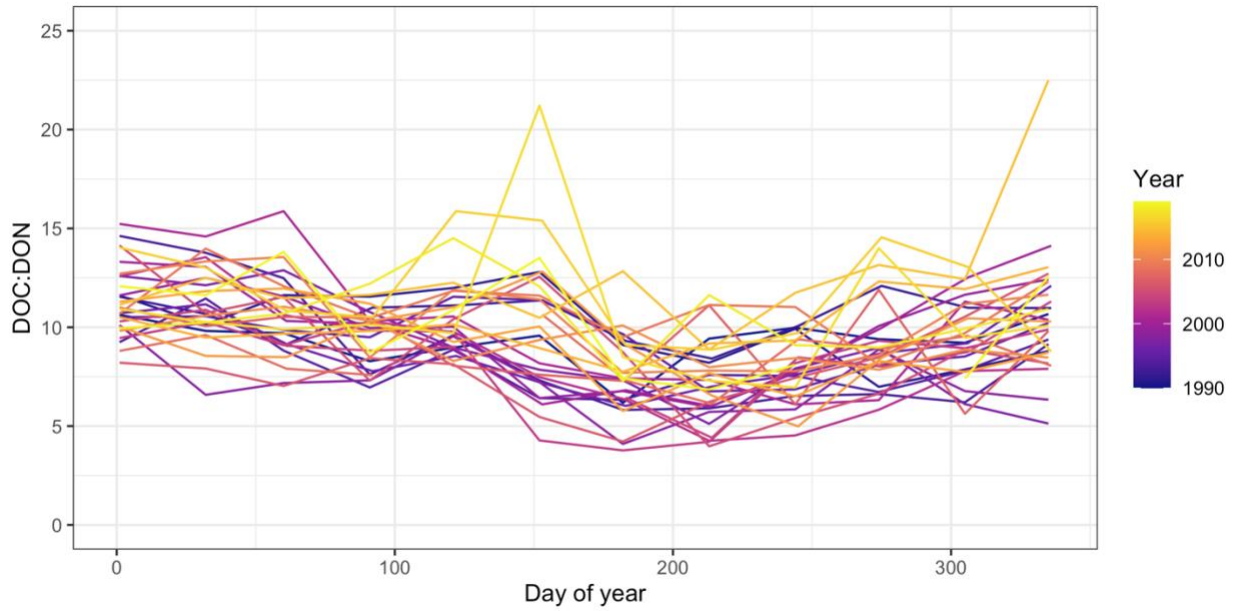


Figure B.6. Intraannual variation in DOC:DON at Buffalo Pound Lake between 1990 and 2019.

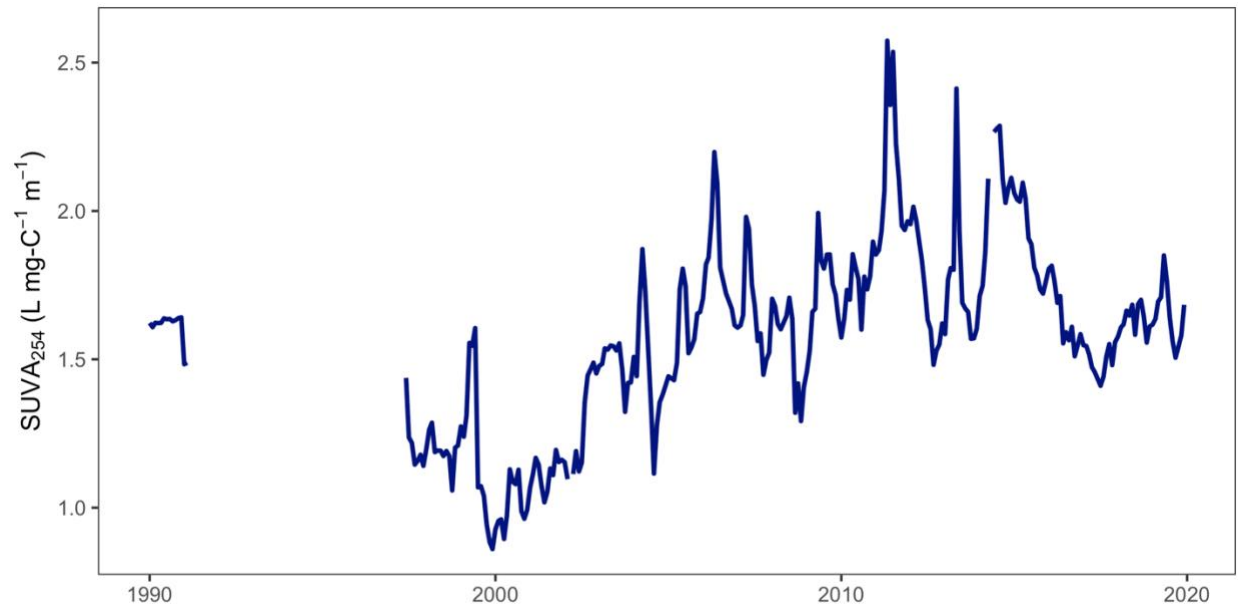


Figure B.7. Buffalo Pound Lake ultraviolet absorbance at 254 nm (A_{254}) normalized to DOC concentration ($SUVA_{254}$) from 1990 to early 1991 and late 1997 to 2019, calculated as A_{254} divided by DOC concentration.